



Hokianga Harbour Hydrodynamic Study

Hydrodynamic Study of WasteWater Discharges

Report prepared for Far North District Council

March 2020

Document History

Versions

Version	Revision Date	Summary	Reviewed by
0.1	04/12/19	Initial document created	Berthot
0.2	16/12/19	Draft for internal review	Zyngfogel/Cussioli
0.3	18/12/19	Draft for client review	Berthot
0.4	10/01/20	Draft for internal review	Berthot
0.5	23/01/20	Draft for internal review	Zyngfogel/Goward-Brown
0.6	23/01/20	Draft for Client review	Berthot
0.7	11/03/20	Draft for Client review	Berthot

Distribution

Version	Date	Distribution
1.0	16/09/2020	Far North District Council

Document ID:

MetOcean Solutions is a Division of Meteorological Services of New Zealand Ltd, MetraWeather (Australia) Pty Ltd [ACN 126 850 904], MetraWeather (UK) Ltd [No. 04833498] and MetraWeather (Thailand) Ltd [No. 0105558115059] are wholly owned subsidiaries of Meteorological Service of New Zealand Ltd (MetService).

The information contained in this report, including all intellectual property rights in it, is confidential and belongs to Meteorological Service of New Zealand Ltd. It may be used by the persons to which it is provided for the stated purpose for which it is provided and must not be disclosed to any third person without the prior written approval of Meteorological Service of New Zealand Ltd. Meteorological Service of New Zealand Ltd reserves all legal rights and remedies in relation to any infringement of its rights in respect of this report.

Executive Summary

Far North District Council (FNDC) currently discharges wastewater from four municipal WasteWater Treatment Plants (WWTP) into the Hokianga Harbour and its tributaries (Figure 1). FNDC are in the process of renewing these resource consents. In the community, there is growing concern over the health of the harbour and FNDC requires information about the effects of these discharges in the receiving environment, and/or identify simple ways to minimise the effects.

FNDC has commissioned MetOcean Solutions (MOS) to undertake a hydrodynamic modelling study of the wastewater discharges. The release of pollutants in the oceanic environment through an outfall is a process that is generally continuous over time, but often subject to significant fluctuations in released quantities. The fate of these pollutants can be assessed based on hydrodynamic modelling of historical conditions, thereby allowing estimations of the expected general spatial dispersion.

For this work MOS has partnered with the Cawthron Institute to undertake a data collection campaign; Water level and currents within Hokianga Harbour were measured in order to calibrate and validate the hydrodynamic model. This study will be used to support the required Quantitative microbial Risk Assessment (QMRA).

In addition, the council has a mandate to accelerate the development of a long-term plan for the existing Hokianga ferry and therefore require the acquisition of sub-bottom geophysical survey data in order to ascertain the viability of alternative route options and northern landing locations. For the survey work MetOcean Solutions has partnered with Scantec Ltd; Survey results are presented in a separate report (Appendix A:).



Figure 1: Hokianga Harbour Location (top) - Municipal Wastewater Treatment Plant Discharges in the Catchment of the Hokianga Harbour (bottom).

Field data collection:

A field measurement campaign was undertaken by Cawthron Institute to assist with the characterisation of the hydrodynamic regime within Hokianga Harbour and provide the necessary field data for calibration and validation of the hydrodynamic model. The campaign focused on four locations between the harbour entrance and the Narrows (Figure 2). The measurement period extended from July 2019 to August 2019 and included measurements of water elevation and current velocities.

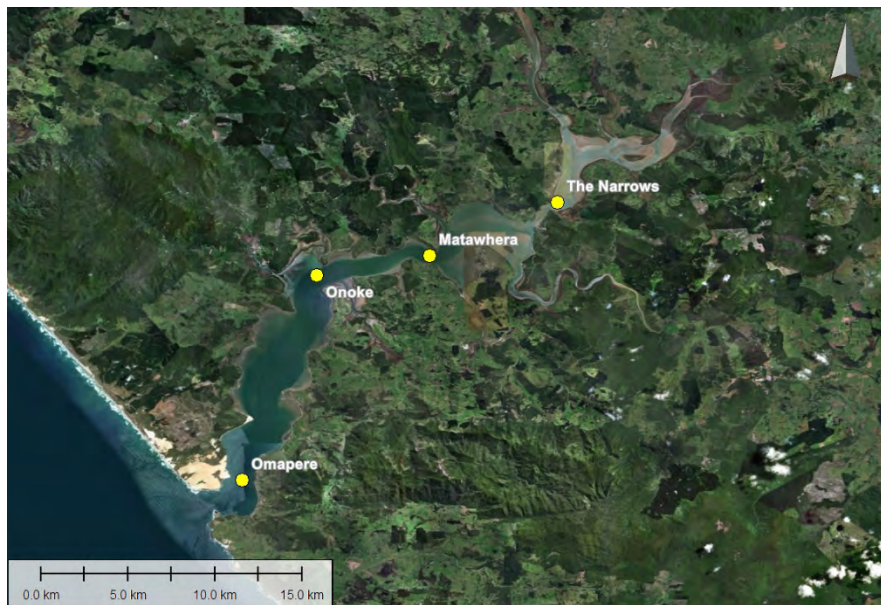


Figure 2: Instruments locations within Hokianga Harbour.

Hydrodynamic Modelling :

A SCHISM hydrodynamic model of Hokianga Harbour was setup for this study. The model resolution was optimised to ensure replication of the salient hydrodynamic processes. The resolution ranged from 90 m at the offshore boundary to 15 m within Hokianga Harbour and near the discharge locations. The model bathymetry was prepared based on the best available datasets for the region. The model was forced by tidal conditions (extracted from MOS greater NZ SCHISM model) and temperature/salinity (HYCOM model) at the offshore boundary, atmospheric data (wind and heat exchange extracted from MOS existing atmospheric models) and river discharges (Discharge report from NIWA for the Waima river (Wairoro-Penakitere-Taheke-Waima River), Waihou River, Orira River and Mangamuka River) forced at the boundary.

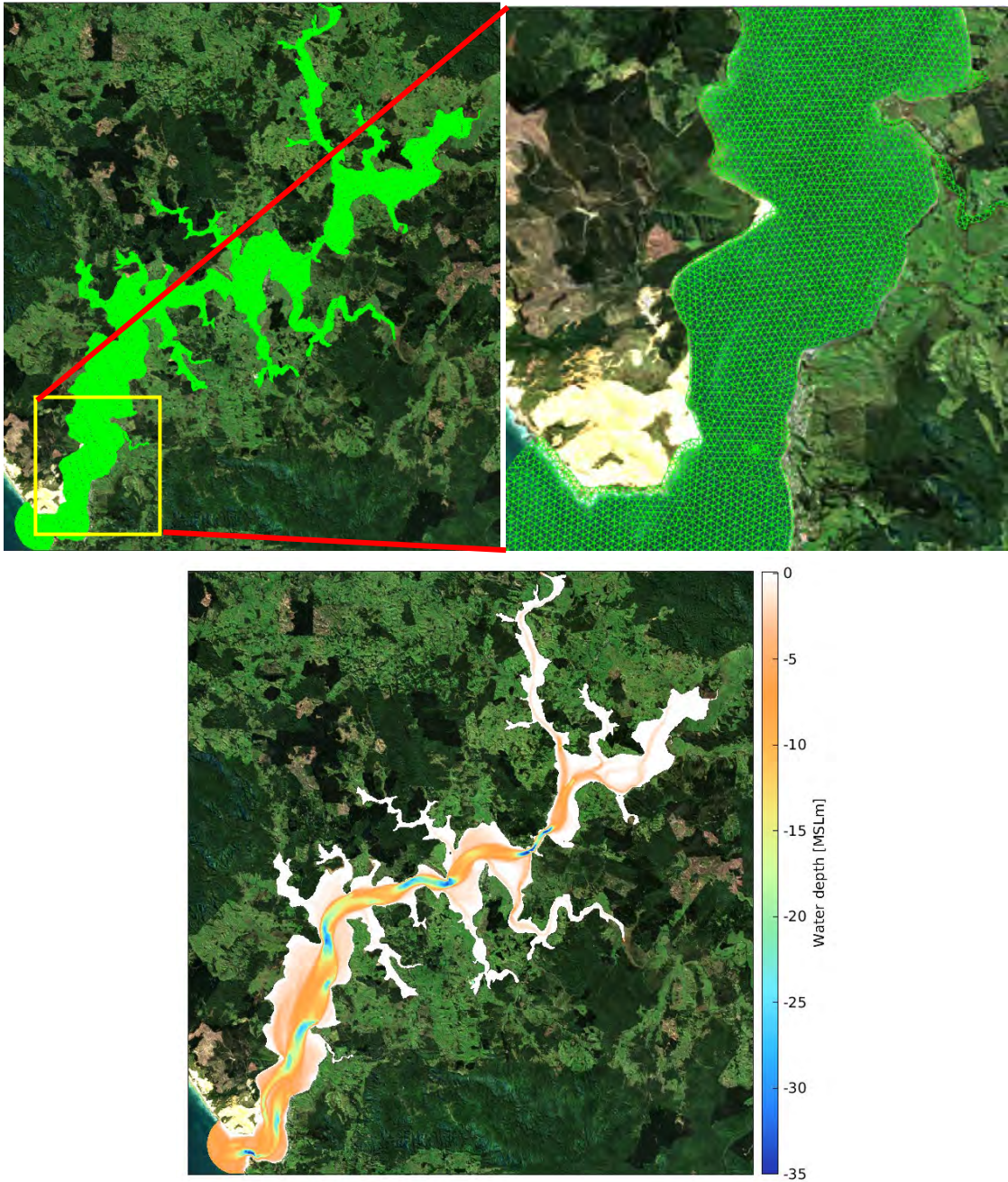


Figure 3: Hydrodynamic model: Bathymetry of model domain showing water depth (left) and triangular model (Center is the whole domain and right show the grid refinement around the Opononi discharge location).

The model was calibrated and validated using the water level and current collected by Cawthron within Hokianga Harbour. Comparisons between the measured and modelled data show that the model successfully reproduces the propagation of the tidal wave inside the harbour, with good agreement in terms of water level, current and temperature patterns.

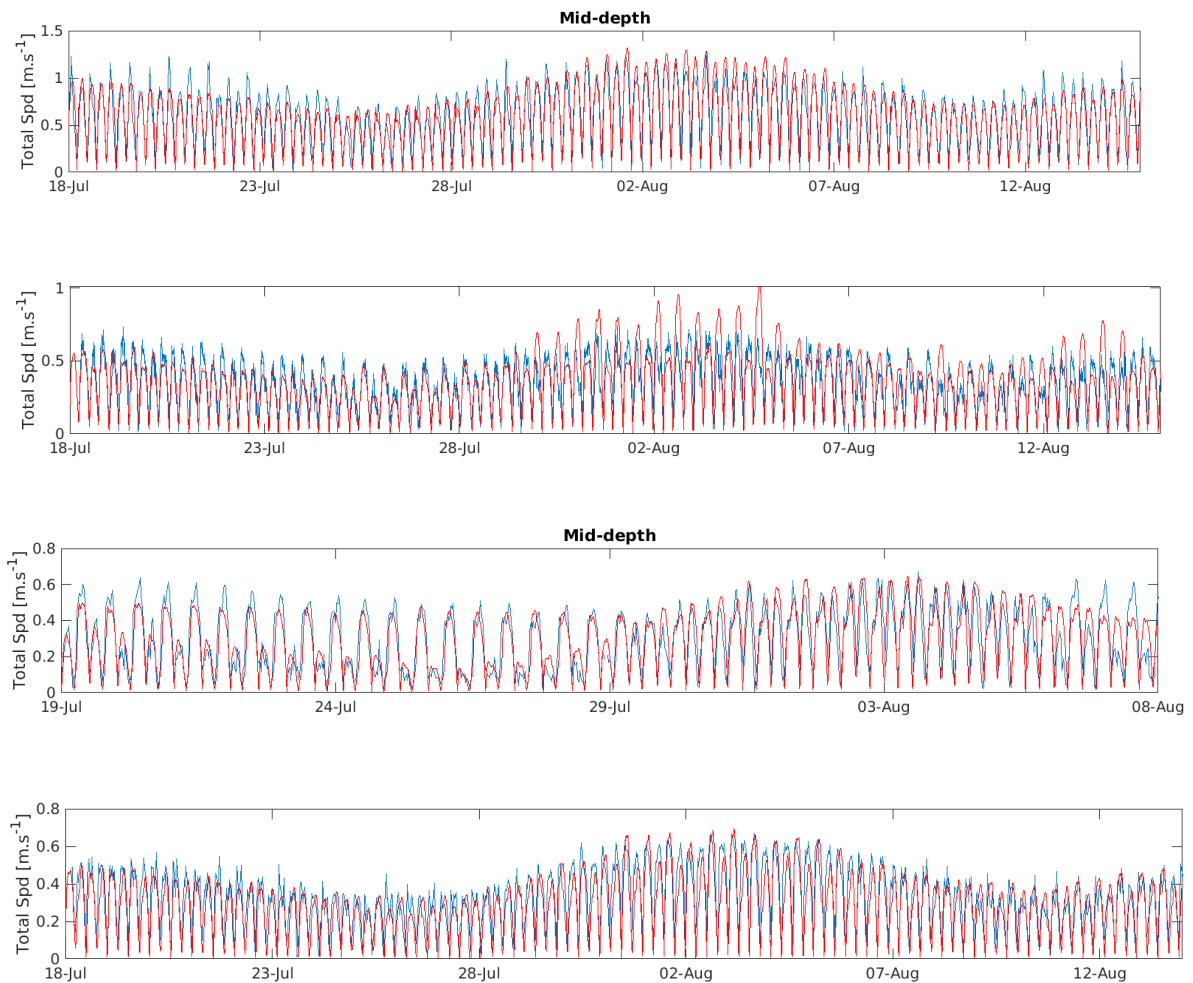


Figure 4: Measured (blue) and modelled (red) current speeds at Omapere ADCP Onoke FSI, Matawhera ADCP The Narrows FSI sites, from July 2019 to August 2019

WWTP Discharge Simulations

In order to model the four WWTP discharges a review of the discharge rate timeseries data was undertaken and a year representative of the variability in the discharge rate as well as a maximum at the proposed resource consent was adopted for each of these four discharges.

Different passive tracers (i.e. a neutrally buoyant pollutant with no decay) were used for each WWTP discharge. A nominated concentration value of 1 mg/L was used so that dilution can be calculated at various distance from the source. Specific contaminant concentration levels can then be determined using concentration ratios and the expected or measured discharge value.

In the present study, the approach consisted of running year-long simulations within two contrasting historical contexts (El Nino / La Niña/El Niño episodes). This allows robust probabilistic estimates of the plume dispersion and dilution patterns to be determined and thus provide some guidance on expected concentration levels associated with the Hokianga Harbour WWTP discharges.

The year-long simulations were extended by two days, and the discharge rate increased to the highest discharge recorded, in order to assess the impact of an extreme isolated event. The model simulations results were processed in term of dilution factors which were determined by dividing the tracer concentration at any grid point to the discharged concentration. A dilution factor of 1:1000 indicates a contaminant concentration at that location 1000 time smaller than discharged. Specific contaminant concentration levels at environmental receptors will be determined by consultants doing the QMRA, using concentration ratios and the expected or measured discharged value.

Results are presented in terms of 50th and 95th percentiles dilution factor maps and timeseries of dilutions factors at selected locations.

The 50th percentile maps present the dilutions factors expected to be exceeded 50% of the time.

The 95th percentile maps present the dilution factors expected to be exceeded 5% of the time (or not exceeded 95% of the time).

Timeseries of tracer concentration were also extracted at selected locations within Hokianga Harbour and dilution factors were calculated and provided to the consultants undertaking the QMRA.

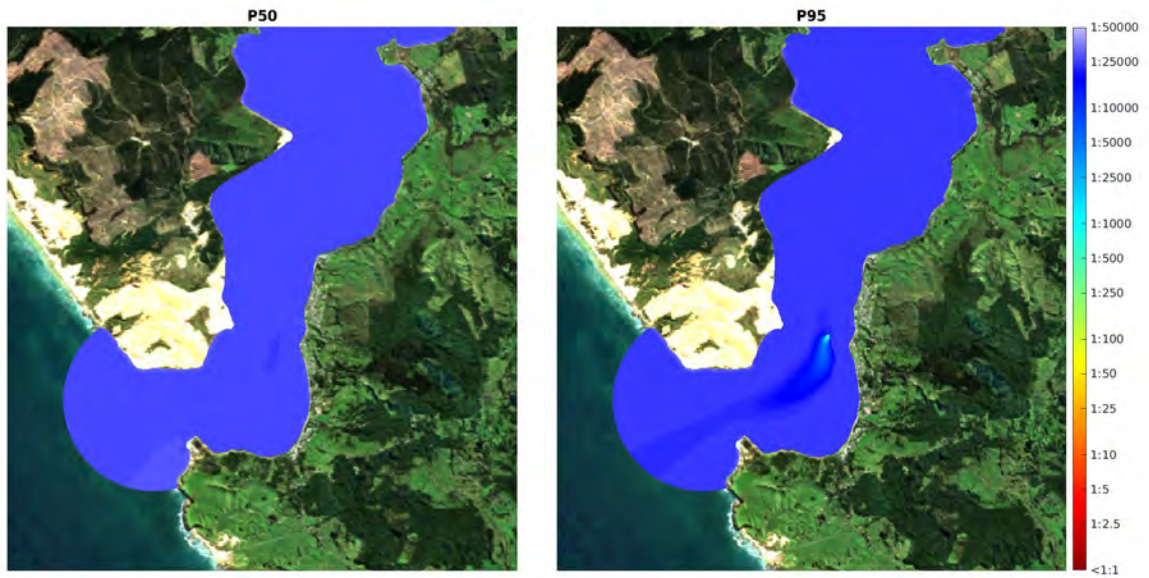


Figure 5:50th Percentile and 95th Percentile Dilution factor for Opononi WWTP during El Nino year (note P50 is less than

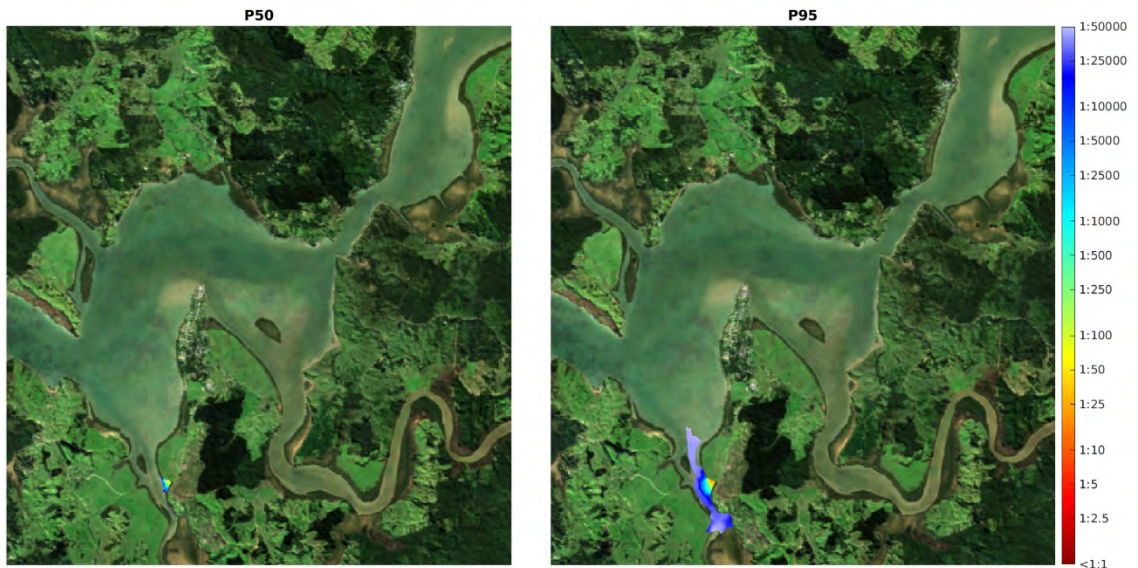


Figure 6:50th Percentile and 95th Percentile Dilution factor for Rawene WWTP during El Nino year.





Figure 7: 50th Percentile and 95th Percentile Dilution factor for Kohukohu WWTP during El Nino year.

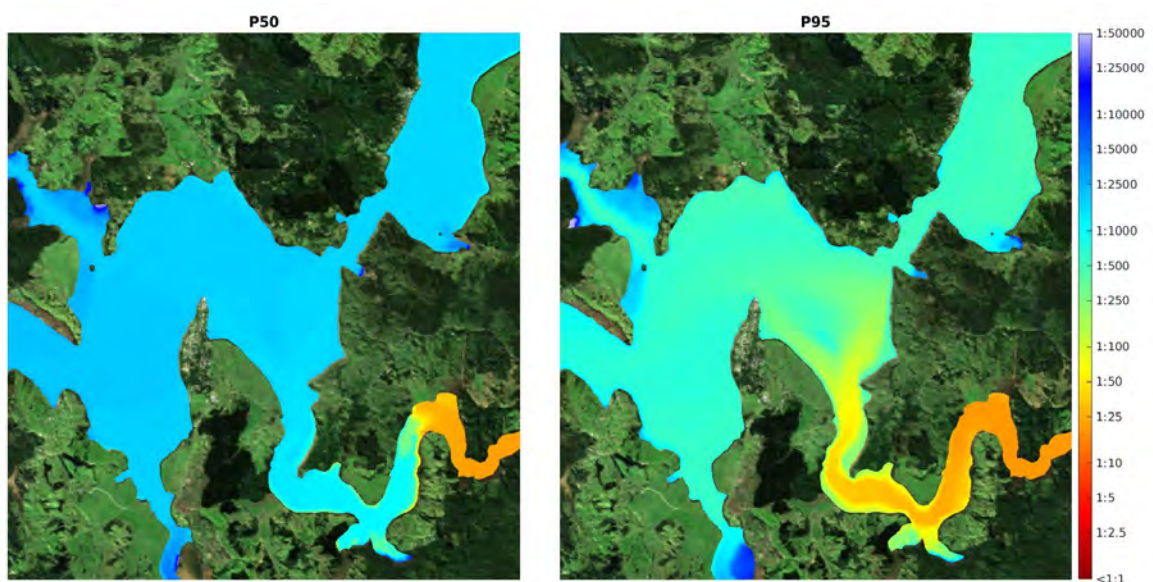


Figure 8: 50th Percentile and 95th Percentile Dilution factor for Kaikohe WWTP during El Nino year.

Results shows that each WWTP discharges present very different plume extents due to their location within the harbour and the actual discharge volumes. Some of the key features for each discharge are:

- The Opononi WWTP discharge present an elongated plume stretching toward the entrance of Hokianga harbour. Dilution factors for the 50th percentile are as high as 1 in 5000 within 100 m of the discharge.

- The Rawene WWTP discharge plume is mostly contained within the Omanaia River and dilution factors for the 50th percentile are about 1 in 5000 at 100 m from the discharge location
- The Kohukohu WWTP discharge plume is mostly confined to the vicinity of the discharge location with a dilution factor of 1 in 50,000 at approx. 50 m for the 50th percentile.
- The Kaikohe WWTP discharge plume present dilution factors of 1 in 25 within the Waima River as far as downstream as the last bend before Motukiore Road. Dilution is about 1 in 1000 to 1 in 2500 within the harbour.

Contents

1. Introduction	11
2. Field Measurement Campaign	13
2.1.1 Instrumentation and Deployment.....	13
2.1.2 Data Processing.....	15
2.1.3 Water Level Measurements	15
2.1.4 Current Measurements	18
3. Sub-Bottom Surveys – Scantec Ltd	23
4. Numerical Modelling	24
4.1 Methodology	24
4.2 Hydrodynamic Model.....	25
4.2.1 Model description.....	25
4.2.2 Model domain and bathymetry.....	26
4.2.3 Vertical discretisation.....	31
4.2.4 Vertical mixing / turbulence closure	33
4.2.5 Submerged Aquatic Vegetation.....	33
4.3 Boundary Conditions and Forcing.....	34
4.3.1 Atmospherics Forcing	34
4.3.2 Open Boundary and Tidal Forcing.....	34
4.3.3 River Discharges	36
4.3.4 Temperature and Salinity	37
4.3.5 WWTP Discharges	38
5. Results	43
5.1 Model validation.....	43
5.1.1 Elevation.....	43
5.1.2 Velocities	48
5.1.3 Temperature and salinity.....	57
5.2 Model results	60

5.3	WWTP Discharge Simulations	64
5.3.1	50 th Percentile and 95 th Percentile Maps	64
5.3.2	Time Series of dilution	75
5.3.3	Discussion.....	81
6.	Conclusions	83
7.	References.....	85
Appendix A: Sub-bottom Profile Survey, Rawene, Hokianga Harbour (Scantec Ltd)		
	86	

List of Figures

Figure 1:Hokianga Harbour Location (top) - Municipal Wastewater Treatment Plant Discharges in the Catchment of the Hokianga Harbour (bottom).....	3
Figure 2:Instruments locations within Hokianga Harbour.....	4
Figure 3:Hydrodynamic model: Bathymetry of model domain showing water depth (left) and triangular model (Center is the whole domain and right show the grid refinement around the Opononi discharge location).....	5
Figure 4:Measured (blue) and modelled (red) current speeds at Omapere ADCP Onoke FSI , Matawhera ADCP The Narrows FSI sites, from July 2019 to August 2019	6
Figure 5:50 th Percentile and 95 th Percentile Dilution factor for Opononi WWTP during El Nino year (note P50 is less than.....	0
Figure 6:50 th Percentile and 95 th Percentile Dilution factor for Rawene WWTP during El Nino year.	0
Figure 7:50 th Percentile and 95 th Percentile Dilution factor for Kohukohu WWTP during El Nino year.	1
Figure 8:50 th Percentile and 95 th Percentile Dilution factor for Kaikohe WWTP during El Nino year.	1
Figure 1.1: Hokianga Harbour Location (top) - Municipal Wastewater Treatment Plant Discharges in the Catchment of the Hokianga Harbour (bottom).....	12
Figure 2.1 Instruments locations within Hokianga Harbour.	14
Figure 2.2 Water level at Omapere, calculated from measured pressure using an RBR Solo pressure sensor.	16
Figure 2.3 Water level at Onoke, calculated from measured pressure using an RBR Solo pressure sensor.....	16
Figure 2.4 Water level at Matawhera, calculated from measured pressure using an RBR Solo pressure sensor.	17
Figure 2.5 Water level at The Narrows, calculated from measured pressure using an RBR Solo pressure sensor.	17
Figure 2.6 Current speed and direction at Omapere, recorded by seabed mounted ADCP. Figure shows a subset of the period recorded for clearer visualization.	19

Figure 2.7	Current speed and direction at Onoke, recorded by an FSI current meter. .	20
Figure 2.8	Current speed and direction at Matawhera, recorded by seabed mounted ADCP. Figure shows a subset of the period recorded for clearer visualization.	21
Figure 2.9	Current speed and direction at The Narrows, recorded by an FSI current meter.....	22
Figure 4.1:	Hydrographic Survey for Hokianga Harbour completed by LINZ in 2015 near the WWTP (Top left: Opononi, Top right: Kohokohu, Bottom left: Rawene, Bottom right: Kaikohe).....	27
Figure 4.2:	Compilation of all bathymetric data used to prepare the hydrodynamic model bathymetry of Hokianga Harbour.....	28
Figure 4.3	Triangular model mesh defined for the Hokianga Harbour. Left is the whole domain and right show the grid refinement around the Opononi discharge location.	29
Figure 4.4	Bathymetry of model domain showing the water depth in m below mean sea level. Left is the whole domain and right is a zoom over the Opononi discharge location.	30
Figure 4.5	Map of Hokianga harbour showing the number of vertical level used in the model (left) and the cross section represented by the black line is shown on the right picture. Note the vertical resolution is increased near the surface to resolve the fresh water forcing.	32
Figure 4.6	Aerial photography of Hokianga Harbour showing in red the mangrove habitat used in the SCHISM model.....	33
Figure 4.7	Extent of the NZ scale finite element domain used to derive tidal constituents at the Hokianga harbour entrance.	35
Figure 4.8	Time series of the IB calculated from the mean sea level pressure from WRF model (top). Timeseries of the wave setup calculated from the wave height at the offshore boundary using the equation from Goda 1985.(middle). Comparison of the residual elevation from IB and wave setup with the residual elevation measured at Opononi.	35
Figure 4.9	Timeseries of the Waihou and Waima river flow used during the validation period of the model.	36
Figure 4.10	Aerial photography showing in red the four rivers included in the model ...	37

Figure 4.11 Timeseries of river temperature, measured at Waiapa river, used for all the rivers in the Hokianga Harbour model between 2010 and 2018.....	38
Figure 4.12 Discharge timeseries (blue) and council limits (red) from the four locations	41
Figure 4.13 Discharge timeseries (blue) and council limits (red) from the four locations selected for use in the modelling.....	41
Figure 4.14 Modelled timeseries of discharge rate (in m ³ /day) from the four discharge locations. Note Opononi was only released during the first four hour of the ebb tide.....	42
Figure 5.1 Timeseries of water elevation measured at the four sites (blue) and modelled (red) between July 2019 and August 2019. Note: the two FSIs have moved positioned during the measurement period.....	46
Figure 5.2 Timeseries of residual water elevation measured at Opononi sites (blue) and modelled (red) between July 2019 and August 2019	47
Figure 5.3 Measured (blue) and modelled (red) total near-surface (top), mid-depth (middle), and near-bottom (bottom), current speeds at Omapere ADCP site from July 2019 to August 2019.	49
Figure 5.4 Measured (blue) and modelled (red) total near-surface (top), mid-depth (middle), and near-bottom (bottom), current direction at Omapere ADCP site from July 2019 to August 2019	50
Figure 5.5 Measured (blue) and modelled (red) total near-surface (top), mid-depth (middle), and near-bottom (bottom), Residual velocities at Omapere ADCP site from July 2019 to August 2019. Note the current were rotated to be aligned with the main channel.	51
Figure 5.6 Measured (blue) and modelled (red) total mid-depth current speeds (top) and direction (bottom) at Onoke FSI site from July 2019 to August 2019	52
Figure 5.7 Measured (blue) and modelled (red) total near-surface (top), mid-depth (middle), and near-bottom (bottom), current speed at Matawhera ADCP site from July 2019 to August 2019	53
Figure 5.8 Measured (blue) and modelled (red) total near-surface (top), mid-depth (middle), and near-bottom (bottom), current direction at Matawhera ADCP site from July 2019 to August 2019	54
Figure 5.9 Measured (blue) and modelled (red) total near-surface (top), mid-depth (middle), and near-bottom (bottom), Residual velocities at Matawhera ADCP site from July 2019 to August 2019. Note the current were rotated to be aligned with the main channel	55

Figure 5.10 Measured (blue) and modelled (red) total mid-depth current speeds (top) and direction (bottom) at The Narrows FSI site from July 2019 to August 2019 .	56
Figure 5.11 Comparison of bottom temperature measured (blue) and modelled (red) at all sites by the FSI and ADCP sensors during July 2019 to August 2019.	58
Figure 5.12 Comparison of bottom temperature measured (blue) and modelled (red) at Onoke and The Narrows sites by the FSI sensors during July 2019 to August 2019.....	59
Figure 5.13 Aerial image from Hokianga harbour showing the peak surface (left) and bottom (right) velocities during the flood tide (top) and ebb tide (bottom)..	61
Figure 5.14 Aerial image zoom over Matawhera showing the peak surface (left) and bottom (right) velocities during the flood tide (top) and ebb tide (bottom)..	62
Figure 5.15 Aerial image from Hokianga harbour showing the surface (left) and bottom (right) temperature (top) and salinity (bottom) in July 2015.	63
Figure 5.16 50 th Percentile and 95 th Percentile Dilution factor (top), tracer concentration in mg/L (bottom) for Opononi WWTP during El Nino year.....	65
Figure 5.17 50 th Percentile and 95 th Percentile Dilution factor (top), tracer concentration in mg/L (bottom) for Opononi WWTP during La Nina year.....	66
Figure 5.18 50 th Percentile and 95 th Percentile Dilution factor (top), tracer concentration in mg/L (bottom) for Rawene WWTP during El Nino year.	67
Figure 5.19 50 th Percentile and 95 th Percentile Dilution factor (top), tracer concentration in mg/L (bottom) for Rawene WWTP during La Nina year.	68
Figure 5.20 50 th Percentile and 95 th Percentile Dilution factor (top), tracer concentration in mg/L (bottom) for Kohukohu WWTP during El Nino year.....	69
Figure 5.21 50 th Percentile and 95 th Percentile Dilution factor (top), tracer concentration in mg/L (bottom) for Kohukohu WWTP during La Nina year.	70
Figure 5.22 50 th Percentile and 95 th Percentile Dilution factor (top), tracer concentration in mg/L (bottom) for Kaikohe WWTP during El Nino year.....	71
Figure 5.23 50 th Percentile and 95 th Percentile Dilution factor (top), tracer concentration in mg/L (bottom) for Kaikohe WWTP during La Nina year.	72
Figure 5.24 50 th Percentile and 95 th Percentile Dilution factor (top), tracer concentration in mg/L (bottom) for the four WWTPs combined during El Nino year.	73
Figure 5.25 50 th Percentile and 95 th Percentile Dilution factor (top), tracer concentration in mg/L (bottom) for the four WWTPs combined during La Nina year.	74

Figure 5.26	Location for tracer concentration timeseries extraction and analysis.....	75
Figure 5.27	Timeseries of tracer concentration in mg/L (based on a 1mg/L concentration at the discharge point) at location P1 for each WWTP discharge for the El Nino and La Nina year simulations.....	76
Figure 5.28	Timeseries of tracer concentration in mg/L (based on a 1mg/L concentration at the discharge point) at location P2 for each WWTP discharge for the El Nino and La Nina year simulations.	77
Figure 5.29	Timeseries of tracer concentration in mg/L (based on a 1mg/L concentration at the discharge point) at location P3 for each WWTP discharge for the El Nino and La Nina year simulations.....	78
Figure 5.30	Timeseries of tracer concentration in mg/L (based on a 1mg/L concentration at the discharge point) at location CR1 for each WWTP discharge for the El Nino and La Nina year simulations.....	79
Figure 5.31	Timeseries of tracer concentration in mg/L (based on a 1mg/L concentration at the discharge point) at location CR4 for each WWTP discharge for the El Nino and La Nina year simulations.....	80

List of Tables

Table 2.1	Latitude, longitude, depth and instruments deployed at each mooring location.	14
Table 4.1	Factor used for each of the river in order to account for the run off in Hokianga harbour.....	36
Table 5.1	Comparison of measured and modelled amplitude and phase for the M2 constituent at all sites.....	43
Table 5.2	Comparison of measured and modelled amplitude and phase for the S2 constituent at all sites.....	44
Table 5.3	Comparison of measured and modelled amplitude and phase for the N2 constituent at all sites.....	44
Table 5.4	Comparison of measured and modelled amplitude and phase for the K2 constituent at all sites.....	44
Table 5.5	Comparison of measured and modelled amplitude and phase for the K1 constituent at all sites.....	45

Table 5.6 Comparison of measured and modelled amplitude and phase for the L2 constituent at all sites.....45

1.Introduction

Far North District Council (FNDC) currently discharges wastewater from four municipal wastewater treatment plants (WWTP) into the Hokianga Harbour or its tributaries (Figure 1.1). FNDC are in the process of renewing two of these resource consents. In the community, there is growing concern over the health of the harbour and FNDC requires information about the effects of these discharges in the receiving environment, and/or identify simple ways to minimise the effects.

FNDC has commissioned MetOcean Solutions (MOS) to undertake a hydrodynamic modelling study of the wastewater discharge. In order to support the modelling, MOS has partnered with Cawthron Institute to undertake a data collection campaign which includes the measurement of water level and currents within Hokianga Harbour.

In addition, the Council has a mandate to accelerate the development of a long-term plan for the existing Hokianga ferry for which they require the acquisition of sub-bottom geophysical surveys to ascertain the viability of alternative route options and northern landing locations. For the survey work, MetOcean Solutions has partnered with Scantec Ltd; Results from the survey will be presented in a separate report in Appendix A:

This report is structured as follows: an introduction to the study background and rationale is provided in Section 1, while a summary of the available measured data are provided in Section 2. Methods applied, including numerical model definitions are presented in Section 3. Model validation and Results are given in Section 4 and Section 5 respectively. Conclusions are presented in Section 6 and References cited within the text are provided in Section 7.



Figure 1.1: Hokianga Harbour Location (top) - Municipal Wastewater Treatment Plant Discharges in the Catchment of the Hokianga Harbour (bottom).

2. Field Measurement Campaign

A field measurement campaign was undertaken by the Cawthron Institute to assist with the characterisation of the hydrodynamic regime within Hokianga Harbour and provide the necessary field data for calibration and validation of the hydrodynamic model. The campaign focused on four locations between the harbour entrance and the Narrows (Figure 2.1).

2.1.1 Instrumentation and Deployment

The measurement period extended from July 2019 to August 2019 and included measurements of water elevation and current velocities. Measurements were undertaken using a range of instruments spread between the Hokianga Harbour entrance and the Narrows (Figure 2.1); coordinates of the deployment sites are provided in Table 2.1. Further details on instrument deployment and measured data are provided in the following sections.

The data collection campaign consisted of the collection of water level and ocean current information via four separate moorings in ~5 to 26m (CD) water depths throughout the Hokianga Harbour for 30 days. Two of the moorings included bottom mounted ADCPs with the other two featuring mid-water mounted FSI current meters. All moorings included pressure sensors. Detailed equipment description follows:

- Two sea-bed mounted ADCP instruments to record water level and current velocity profiles.
- Two FSI current meters deployed at mid-water on individual moorings, recording current velocities at a single point.
- Four RBR Solo pressure sensors (supplied by MetOcean Solutions) deployed on individual moorings, recording water levels.

Figure 2.1 shows the locations of the instruments deployed

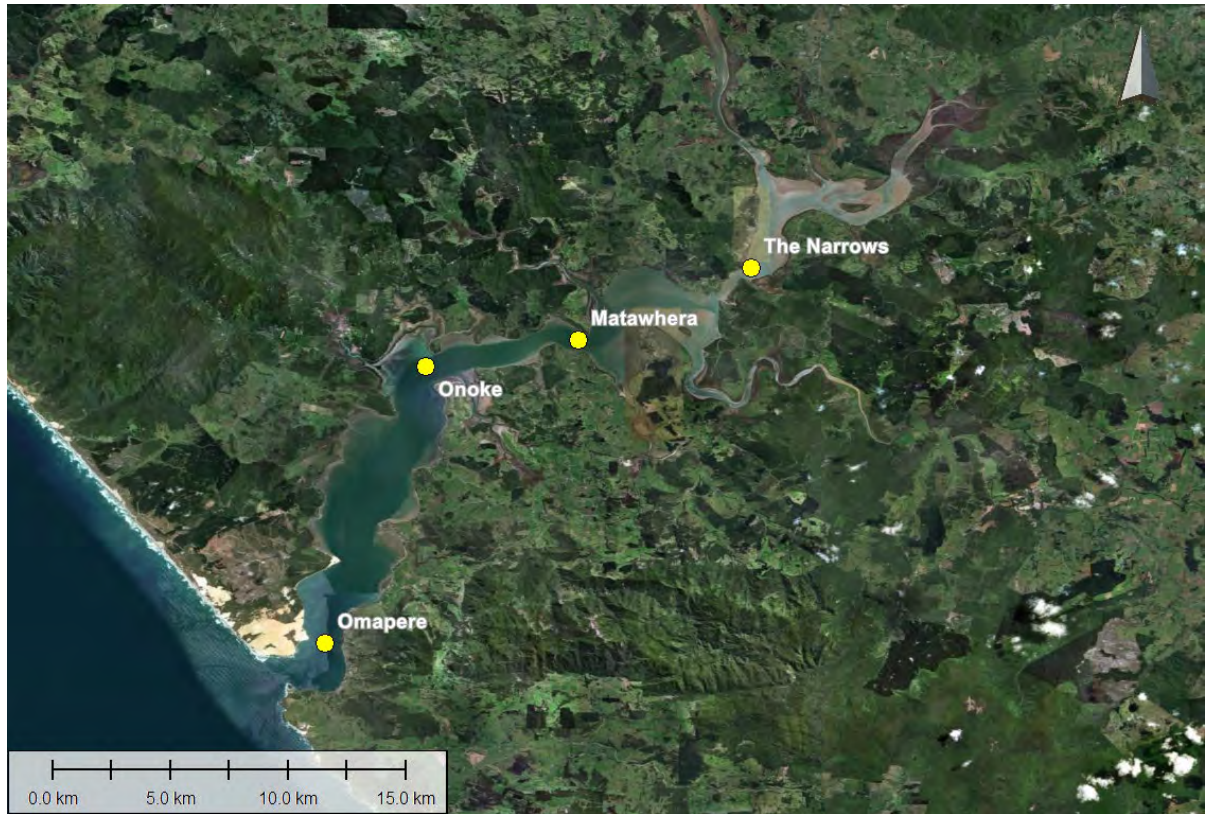


Figure 2.1 Instruments locations within Hokianga Harbour.

Table 2.1 Latitude, longitude, depth and instruments deployed at each mooring location.

Location	Instrument	Latitude/ Longitude	Depth Deployment
Omapere	ADCP	35°31.080'S	16.5 m
	RBR Solo	173°22.850'E	
Onoke	FSI	35°24.739'S	9 m
	RBR Solo	173°25.152'E	
Matawhera	ADCP	-35°24.152'S	25.6 m
	RBR Solo	173°28.652'E	
The Narrows	FSI	-35°22.473'S	5.5 m
	RBR Solo	173°32.673'E	

2.1.2 Data Processing

Data recorded by the pressure sensors were processed in Matlab. The data was checked and any unusable data, such as that collected during the deployment and retrieval of the instrument were removed; Pressure data was converted to water level and saved at 1-minute intervals. Similarly, any data recorded during the deployment and retrieval of the FSI current meters were removed from the dataset. Current magnitude and direction were calculated from U and V velocities and saved at 1-minute intervals.

Native files from the ADCPs were first processed using WinADCP (v 1.14) and various variables (e.g. velocities, depth, pitch, roll, amp, echo) were exported to be processed in Matlab. The instrument was configured with 29 bins (Omapere) and 35 bins (Matawhera), for both ADCPs the bin size was 1.0 m. The blanking depth was 0.50 m for the ADCP deployed at Matawhera and 0.88 m for the Omapere ADCP. In Matlab, bad data was flagged and removed based on threshold values. Bins above the maximum height of the surface layer were removed and the depth was corrected to account for the instrument height of 0.5m.

2.1.3 Water Level Measurements

The pressure sensors recorded during the entire time of deployment and captured well the tidal elevation, including spring and neap cycles (Figure 2.2 to Figure 2.5). Semi-diurnal tides are predominant in this area, with tidal amplitudes displaying variation in elevation between subsequent spring and neap cycles, resulting in some differences in the tidal current magnitudes both within, and between, spring-neap cycles (see next section – Current Measurements).

The deployments at Onoke and The Narrows presented a shift in the pressure data at around the 1st and the 4th of August, respectively. The shift resulted in an increase of 0.5 m in level, from 9 m to 9.5 m at Onoke (Figure 2.3) and from 5.5 to 6 m at The Narrows (Figure 2.5). The dates coincide with the start and the middle of the spring tide. According to data from the field campaign, the instruments did not alter position significantly between deployment and retrieval, therefore, the shift could be a result of the instrument frame sliding slightly along the bed sand/or the anchor weights sinking into the soft sediment.

Tidal amplitude variations (around the mean) for the period of the field campaign were: 3.4 m for Omapere, 4.9 for Onoke, and 3.6 m for Matawhera and The Narrows. Higher amplitudes at Onoke and The Narrows are results of the shift in data described above.

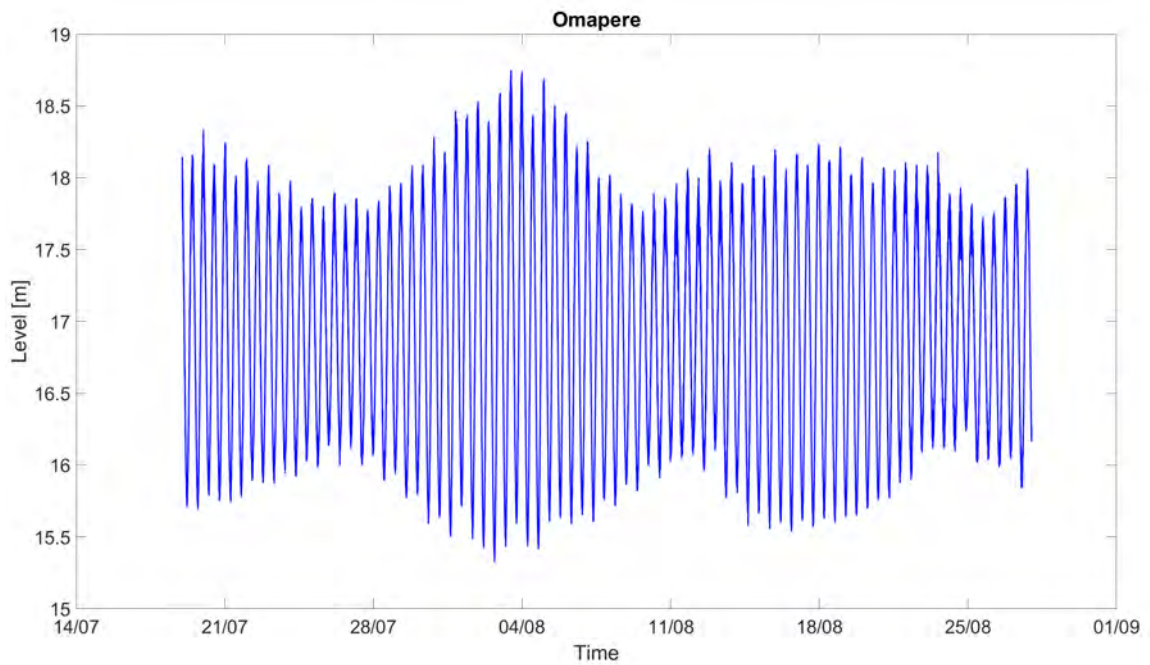


Figure 2.2 Water level at Omapere, calculated from measured pressure using an RBR Solo pressure sensor.

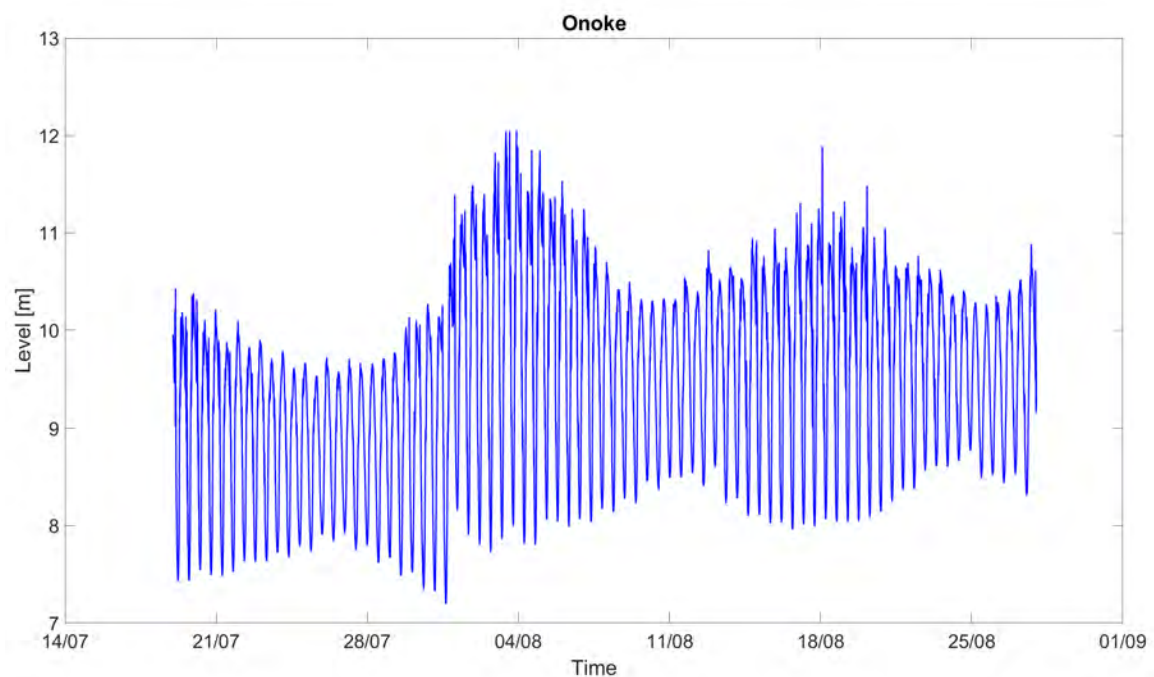


Figure 2.3 Water level at Onoke, calculated from measured pressure using an RBR Solo pressure sensor.

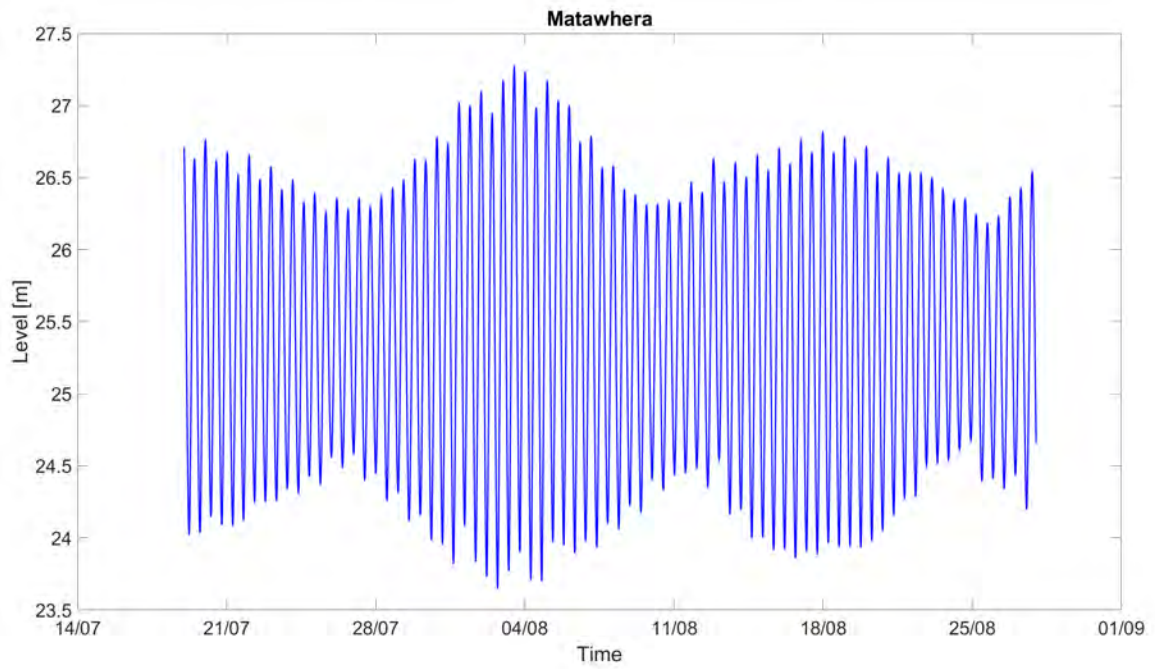


Figure 2.4 Water level at Matawhera, calculated from measured pressure using an RBR Solo pressure sensor.

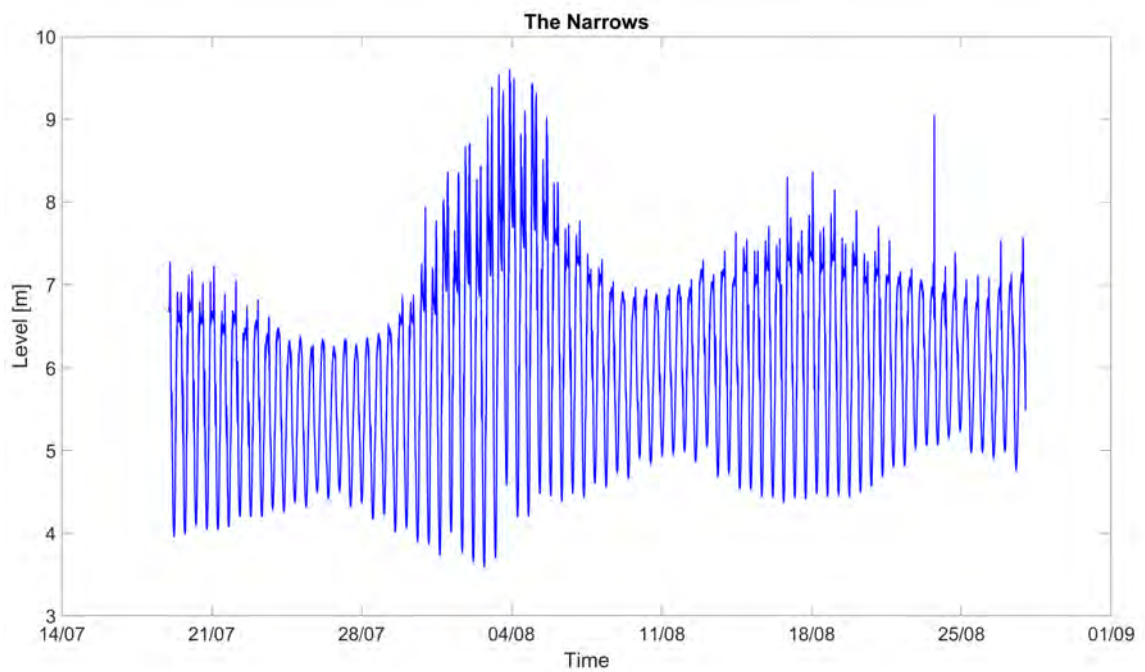


Figure 2.5 Water level at The Narrows, calculated from measured pressure using an RBR Solo pressure sensor.

2.1.4 Current Measurements

Current measurements were carried out using an ADCP at Omapere and Matawhera while an FSI was deployed at Onoke and The Narrows.

The ADCP and FSI current magnitude and direction are presented in Figure 2.6 to Figure 2.9.

For clearer visualisation, a one-week subset of current speed and direction at Omapere is shown in Figure 2.6. Directions of current flow measured at the entrance of the Harbour remained mostly aligned with the N-S axis of the channel throughout the period. Current reversals and magnitudes show a close correlation with tidal elevations, with faster currents at the beginning of the period shown in the subset, which correspond to the end of a spring tide, and slower currents in the following days leading to a neap tide. This indicates the dominant effect of the tide in this area. Mean current speeds over the campaign were 0.5 m s^{-1} and peak speed was 1.4 m s^{-1} .

At Onoke, current direction showed a N-NNE and SW pattern (Figure 2.7) indicating that currents flowing along the west margin of the channel are affected by the significant change in orientation of the main channel from N-S to almost E-W. Mean speed at this location during the field campaign was 0.3 m s^{-1} and the highest speed recorded was 0.7 m s^{-1} .

In contrast, currents at Matawhera typically flowed along the main channel axis, to the east-southeast during flood and to the west-northwest during ebb (Figure 2.8). Mean and maximum speed were 0.3 m s^{-1} and 0.8 m s^{-1} , respectively. The data shows a significant variability in current speed through the water column, with ebb current (WNW) stronger near the surface and flood current (ESE) stronger below mid depth level. This indicates the influence of the freshwater river flowing out to the ocean which tended to reduce the surface current. This pattern mainly occurs in July when the river discharges were much stronger than in August and stratification was likely significant. This is also shown in the validation plots later in this report (Section 5.1.2) with a stronger ebb and weaker flood during the first part of the data collection period.

This pattern is not as pronounced near the entrance where the water is expected to be mixed.

The Narrows was the most upstream, and shallowest, mooring deployment. Flow is predominantly affected by the orientation of the main channel, which can be seen in Figure 2.9 by the predominance of N and WSW current direction. Average and peak current speeds at this location were 0.3 m s^{-1} and 0.8 m s^{-1} respectively, very similar to the values recorded at Onoke and Matawhera.

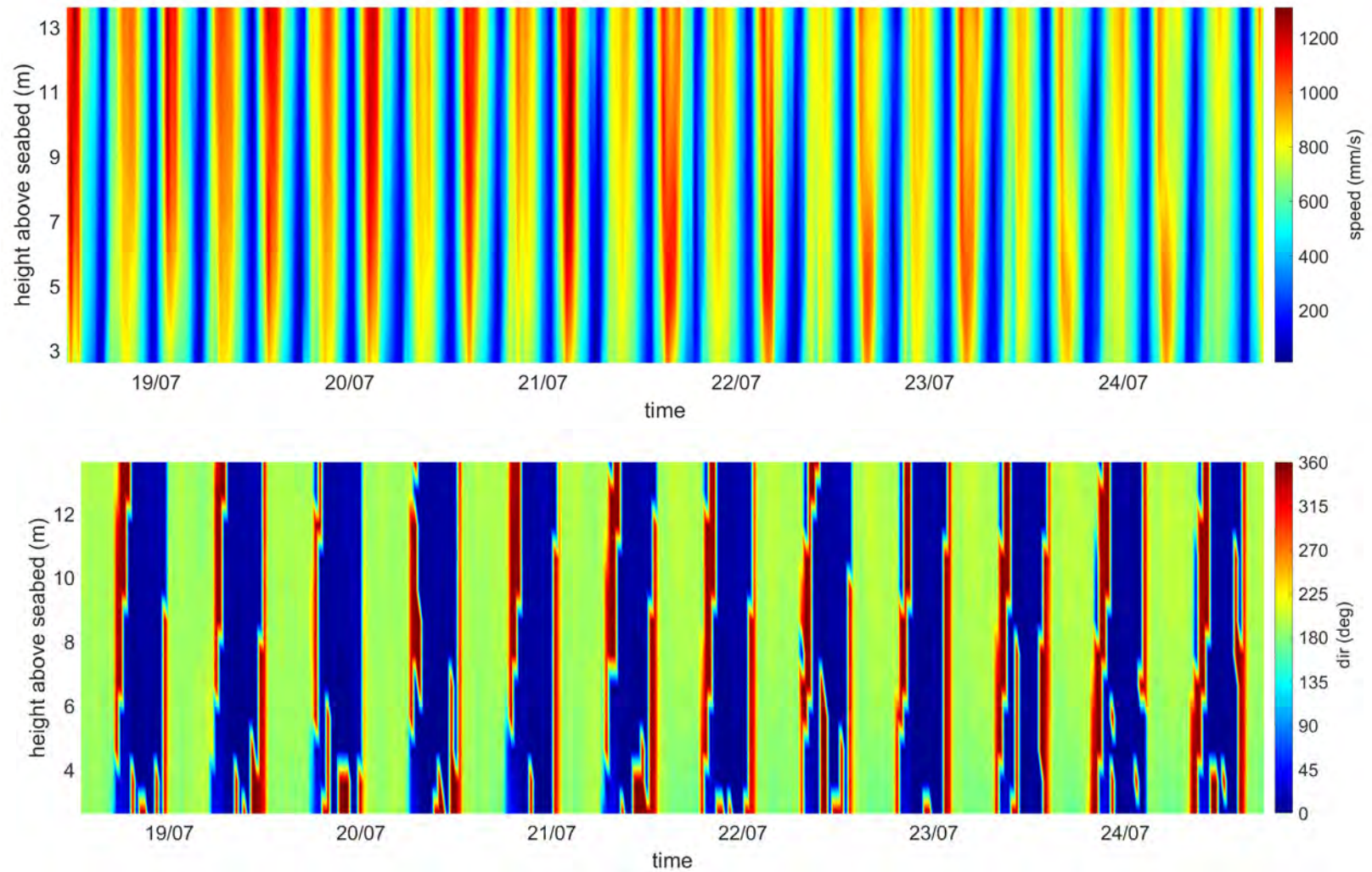


Figure 2.6 Current speed and direction at Omapere, recorded by seabed mounted ADCP. Figure shows a subset of the period recorded for clearer visualization.

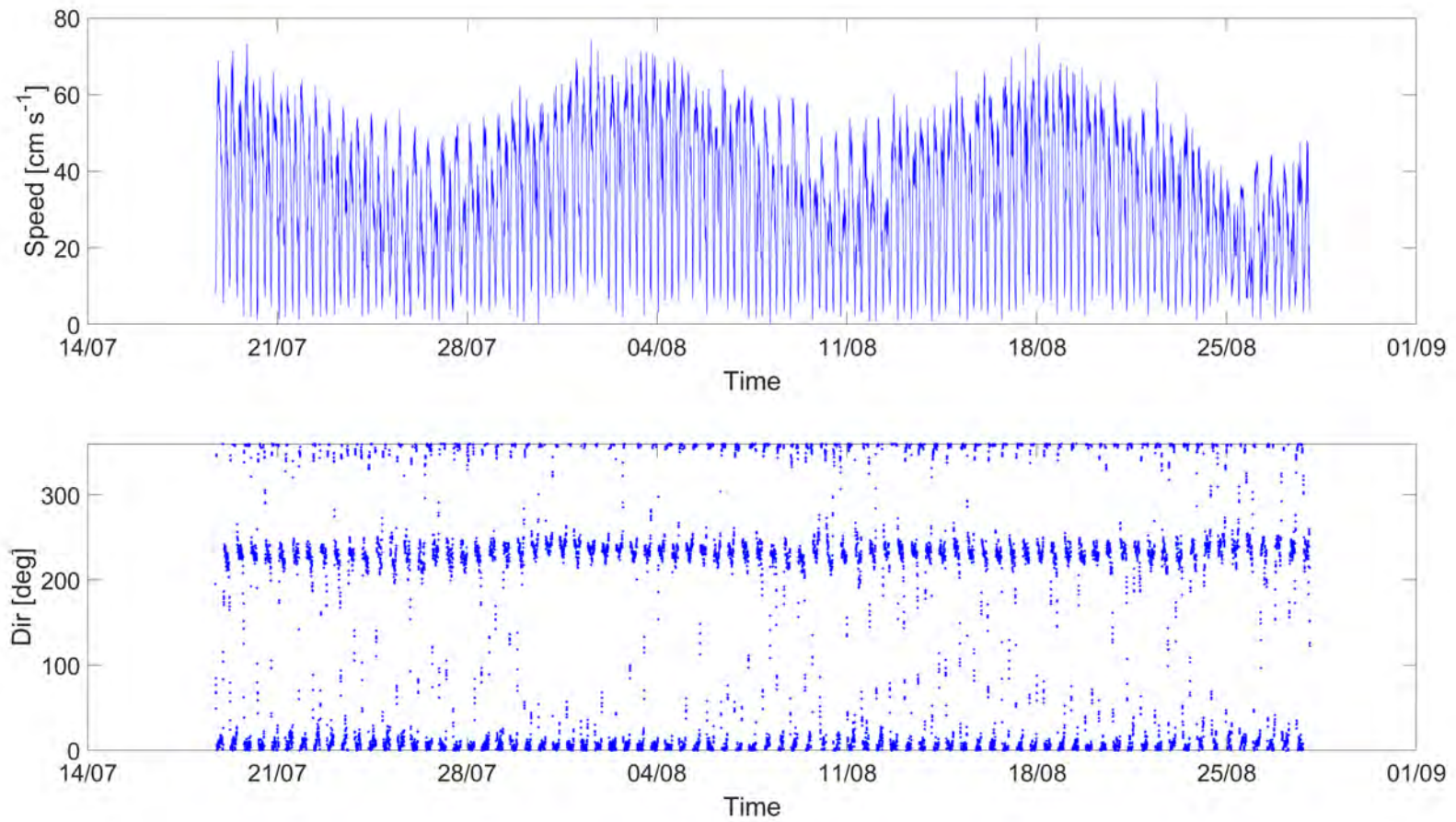


Figure 2.7 Current speed and direction at Onoke, recorded by an FSI current meter.

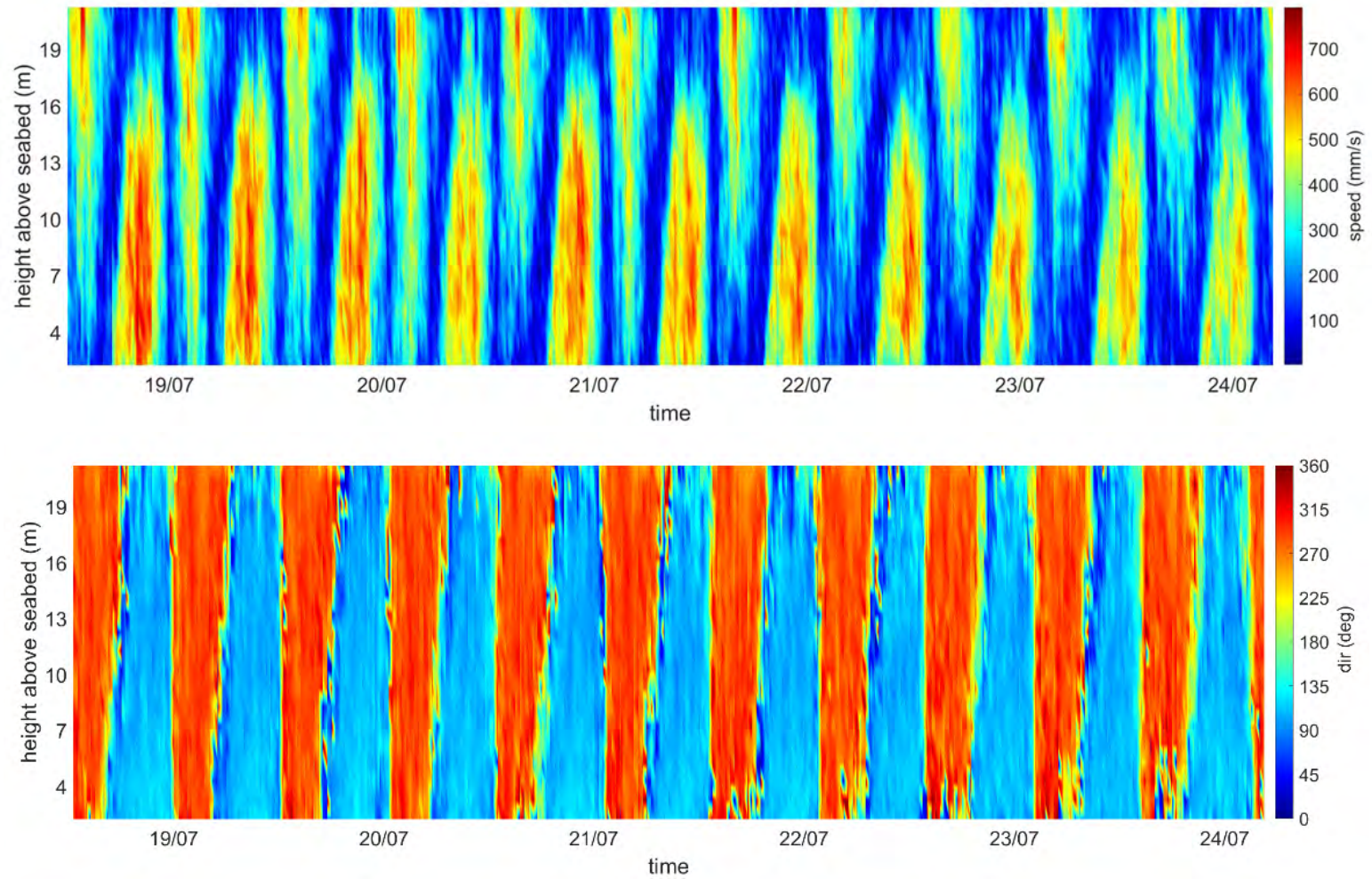


Figure 2.8 Current speed and direction at Matawhera, recorded by seabed mounted ADCP. Figure shows a subset of the period recorded for clearer visualization.

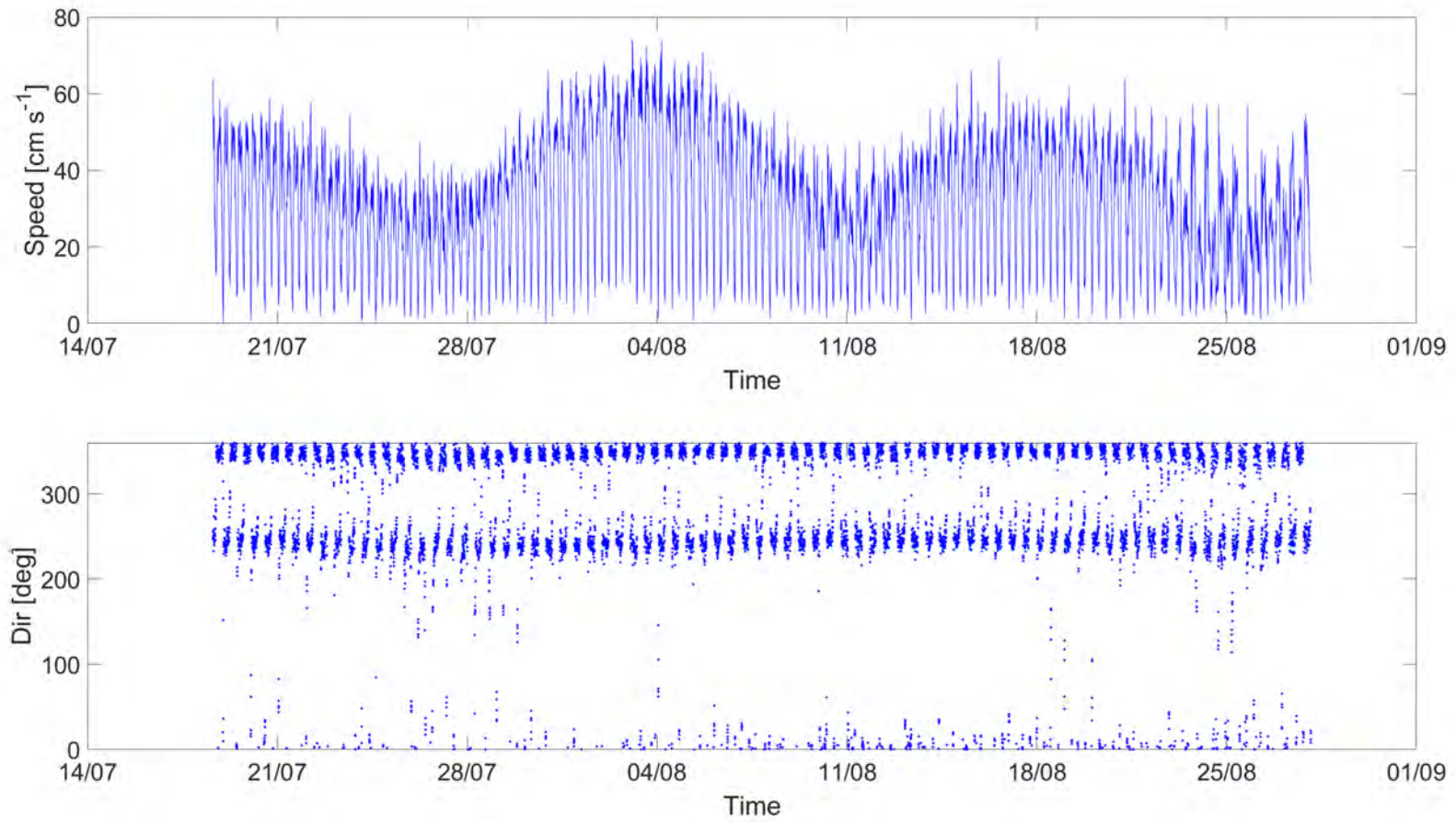


Figure 2.9 Current speed and direction at The Narrows, recorded by an FSI current meter.

3.Sub-Bottom Surveys – Scantec Ltd

The survey scope included measuring general stratigraphy and sediment thickness over bedrock in a triangular area of approx. 1.7 square kilometres. Equipment was mounted on a 5.5m vessel which was launched from the boat ramp at Rawene. A high powered 3.5kHz to 7kHz SBP system was used to penetrate the seabed and obtain reflections from bedrock. A Knudsen 320M 200kHz single beam echosounder was used to collect bathymetric data which needs to be collected as part of the SBP dataset to assist in data processing. The data was processed using seismic processing packages.

The Scantec report is included in Appendix A .

4. Numerical Modelling

4.1 Methodology

The release of pollutants in the oceanic environment through an outfall is a process that is generally continuous over time, but often subject to significant fluctuations in released quantities. The outcome of such releases is inherently non-deterministic and is governed, in part, by random variables such as currents, turbulence, wastewater network use and precipitation, it is therefore difficult to accurately predict.

However, the probability of future oceanic conditions can be assessed from the historical conditions, thereby allowing estimations of the general geographical dispersion expected. In the present study, the approach consisted of running year-long simulations within two contrasting historical contexts (La Niña /El Niño episodes, June 2010-June 2011, and June 2015-June 2016, respectively). This allows robust probabilistic estimates of the plume dispersion and dilution patterns to be determined and thus provide some guidance on expected concentration levels associated with the proposed outfall.

During El Niño conditions, New Zealand typically experiences stronger or more frequent westerly winds during summer. This leads to a greater risk of drier-than-normal conditions in east coast areas and more rain than normal in the west. In winter, colder southerly winds tend to prevail, while in spring and autumn, south-westerlies tend to be stronger or more frequent, bringing a mix of the summer and winter effects.

During La Niña conditions more north-easterly winds are characteristic, which tend to bring moist, rainy conditions to the north-east of the North Island, and reduced rainfall to the south and south-west of the South Island.

By considering both La Niña and El Niño episodes a robust probabilistic estimate of the plume dispersion and dilution patterns is able to be determined and thus provide guidance on expected concentration levels associated with the Hokianga Harbour WWTP discharges.

The discharge of waste-water into Hokianga Harbour has been modelled using a high-resolution local domain hydrodynamic model to characterise the salient hydrodynamics of the environment, while an Eulerian tracer technique has been applied in order to quantify the likely dilution of the discharged waste water.

The following sections detail the hydrodynamic models, including calibration and validation, and Eulerian tracer technique implemented for this specific study; assumptions around the discharge rates are also presented.

4.2 Hydrodynamic Model

4.2.1 Model description

The 2D and 3D baroclinic hydrodynamics of the Hokianga Harbour were modelled using the open-sourced hydrodynamic model SCHISM^{1,2}. The benefit of using open-source science models is the full transparency of the code and numerical schemes, and the ability for other researchers to replicate and enhance any previous modelling efforts for a given environment.

SCHISM is a prognostic finite-element unstructured-grid model designed to simulate 3D baroclinic, 3D barotropic or 2D barotropic circulation. The barotropic mode equations employ a semi-implicit finite-element Eulerian-Lagrangian algorithm to solve the shallow-water equations, forced by relevant physical processes (atmospheric, oceanic and fluvial forcing). A detailed description of the SCHISM model formulation, governing equations and numerics, can be found in Zhang and Baptista (2008).

The SCHISM model is physically realistic, in that well-understood laws of motion and mass conservation are implemented. Therefore, water mass is generally conserved within the model, although it can be added or removed at open boundaries (e.g. through tidal motion at the ocean boundaries) and water is redistributed by incorporating aspects of the real-world systems (e.g. bathymetric information, forcing by tides and wind). The model transports water and other constituents (e.g. salt, temperature, turbulence) through the use of triangular volumes (connected 3-D polyhedrons).

The finite-element triangular grid structure used by SCHISM has resolution and scale benefits over other regular or curvilinear based hydrodynamic models. SCHISM is computationally efficient in the way it resolves the shape and complex bathymetry associated with estuaries, and the governing equations are similar to other open-source models such as Delft3D and ROMS. SCHISM has been used extensively within the scientific community^{3,4}, where it forms the backbone of operational systems used to nowcast and forecast estuarine water levels, storm surges, velocities, water temperature and salinity⁵.

¹ <http://ccrm.vims.edu/schism/>

² http://www.ccrm.vims.edu/w/index.php/Main_Page#SCHISM_WIKI

³ http://www.stccmop.org/knowledge_transfer/software/selfe/publications

⁴ http://ccrm.vims.edu/schism/schism_pubs.html

⁵ https://tidesandcurrents.noaa.gov/ofs/creofs/creofs_info.html

4.2.2 Model domain and bathymetry

The model resolution was optimised to ensure replication of the salient hydrodynamic processes. The resolution ranged from 90 m at the boundary to 15 m within Hokianga Harbour and near the discharge locations.

Bathymetry is an essential requirement for coastal and estuaries numerical modelling. MetOcean Solutions has compiled an extensive national and regional bathymetric dataset derived from Electronic Navigation Charts (ENC). GEBCO data (Becker et al. 2009) was also used to characterise the deepest offshore areas. These datasets were updated with available hydrographic surveys for the region.

This included:

- LIDAR data available for parts of the harbour (Opononi-Omapere, Rawene and Kohukohu).
- Hydrographic surveys of the Hokianga Harbour completed by LINZ in 2015 (from the mouth to the upper reaches, see Figure 3).
- Hydrographic surveys of the Hokianga Harbour completed by NRC in 2006 (Motuti, Omapere and lower harbour).

Specialist data manipulation tools have been developed in-house to allow merging, interpolation and QA of raw bathymetric data to establish the numerical model domain (Figure 4.1 and Figure 4.2).

The triangular elements of the model domain mesh is shown in Figure 4.3 and associated bathymetry is presented in Figure 4.4.

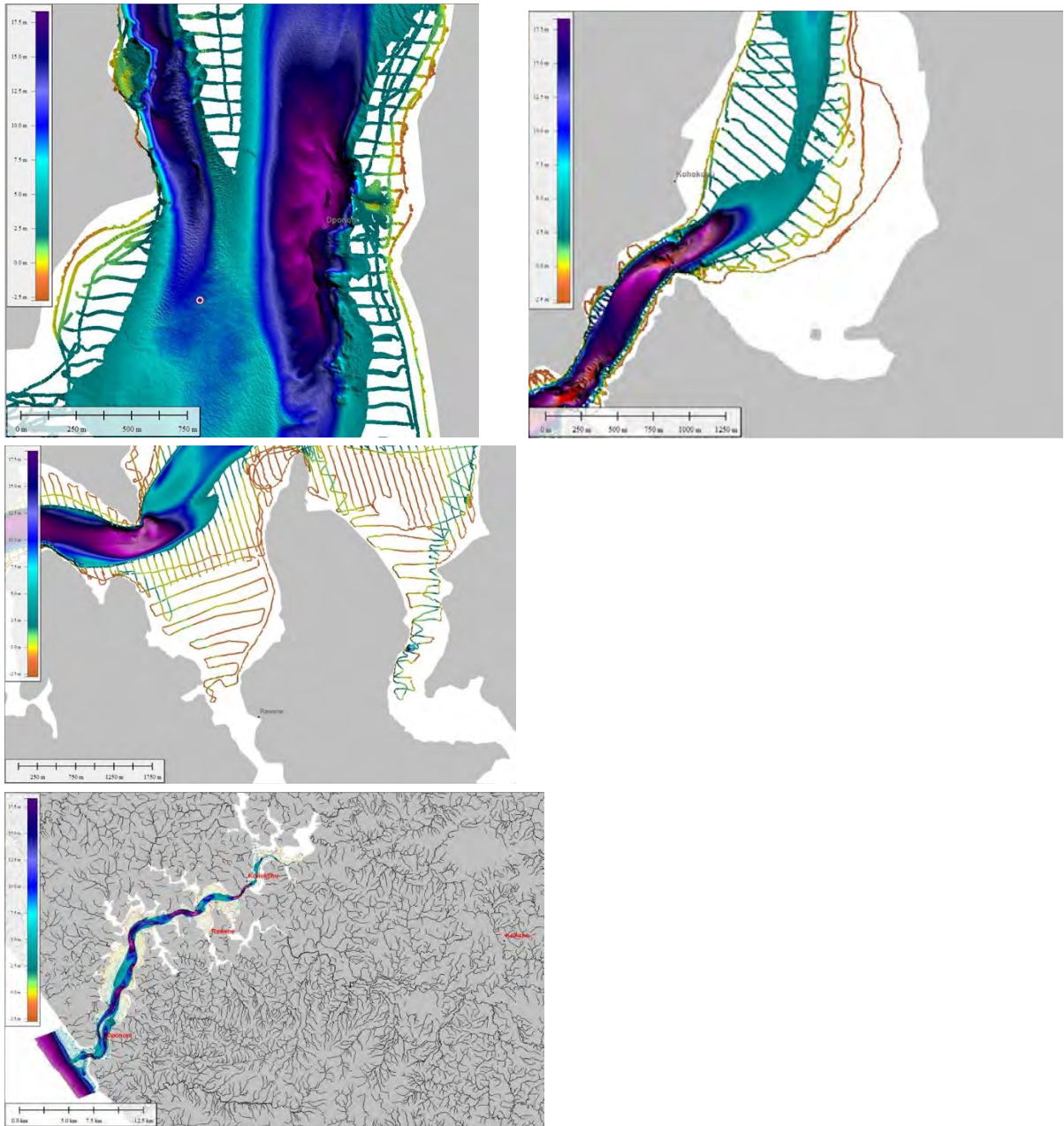


Figure 4.1: Hydrographic Survey for Hokianga Harbour completed by LINZ in 2015 near the WWTP (Top left: Opononi, Top right: Kohokohu, Bottom left: Rawene, Bottom right: Kaikohe)

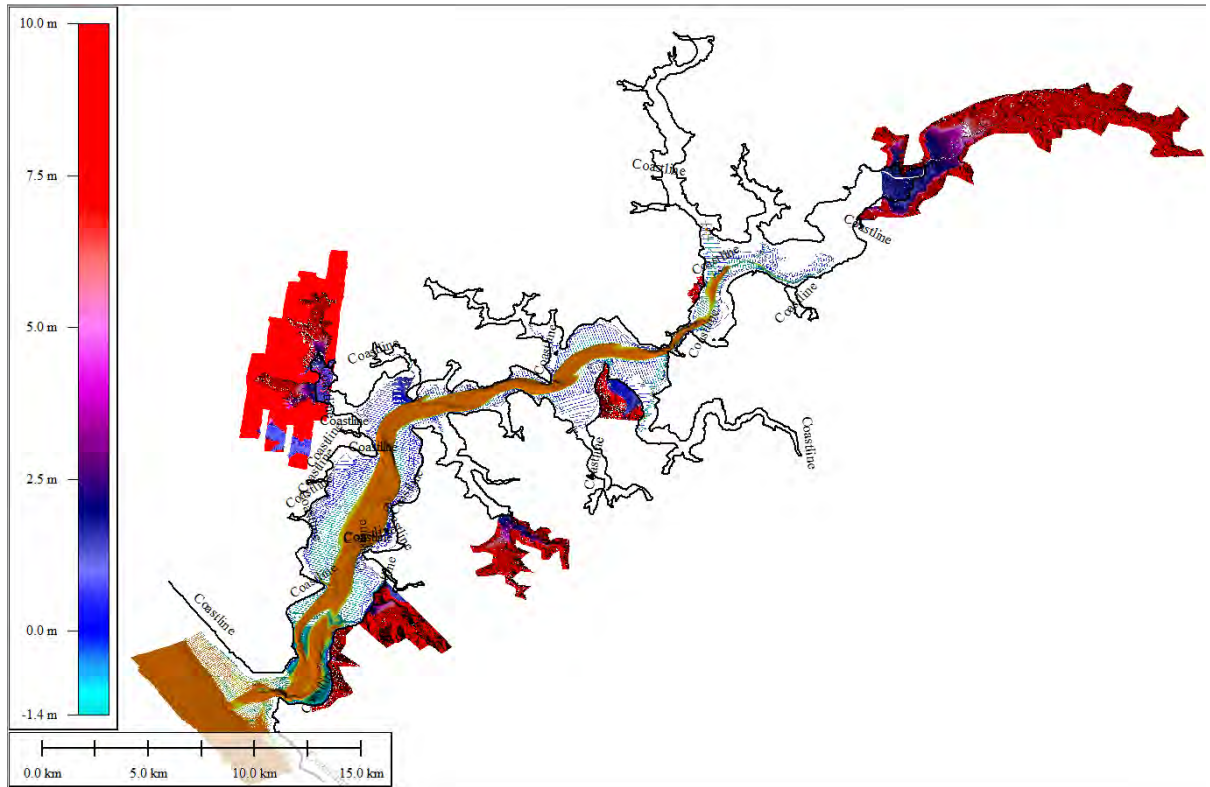


Figure 4.2: Compilation of all bathymetric data used to prepare the hydrodynamic model bathymetry of Hokianga Harbour.

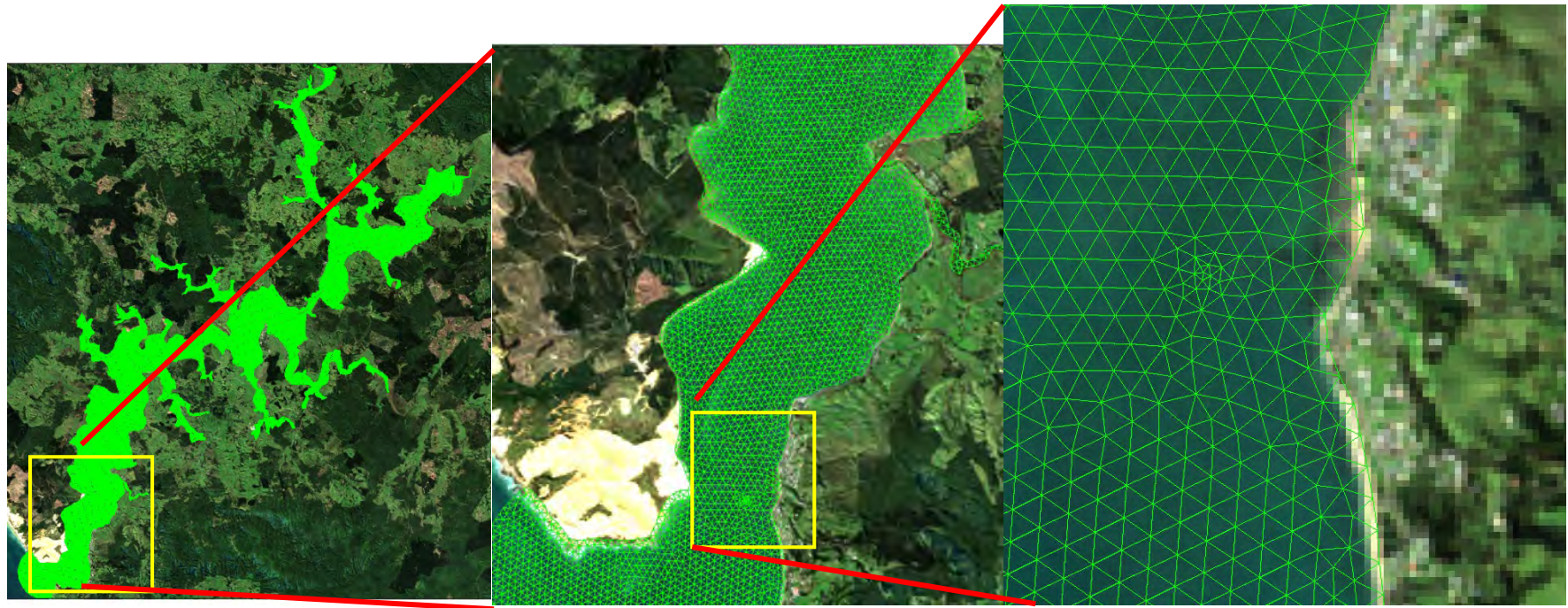


Figure 4.3 Triangular model mesh defined for the Hokianga Harbour. Left is the whole domain and right show the grid refinement around the Opononi discharge location.

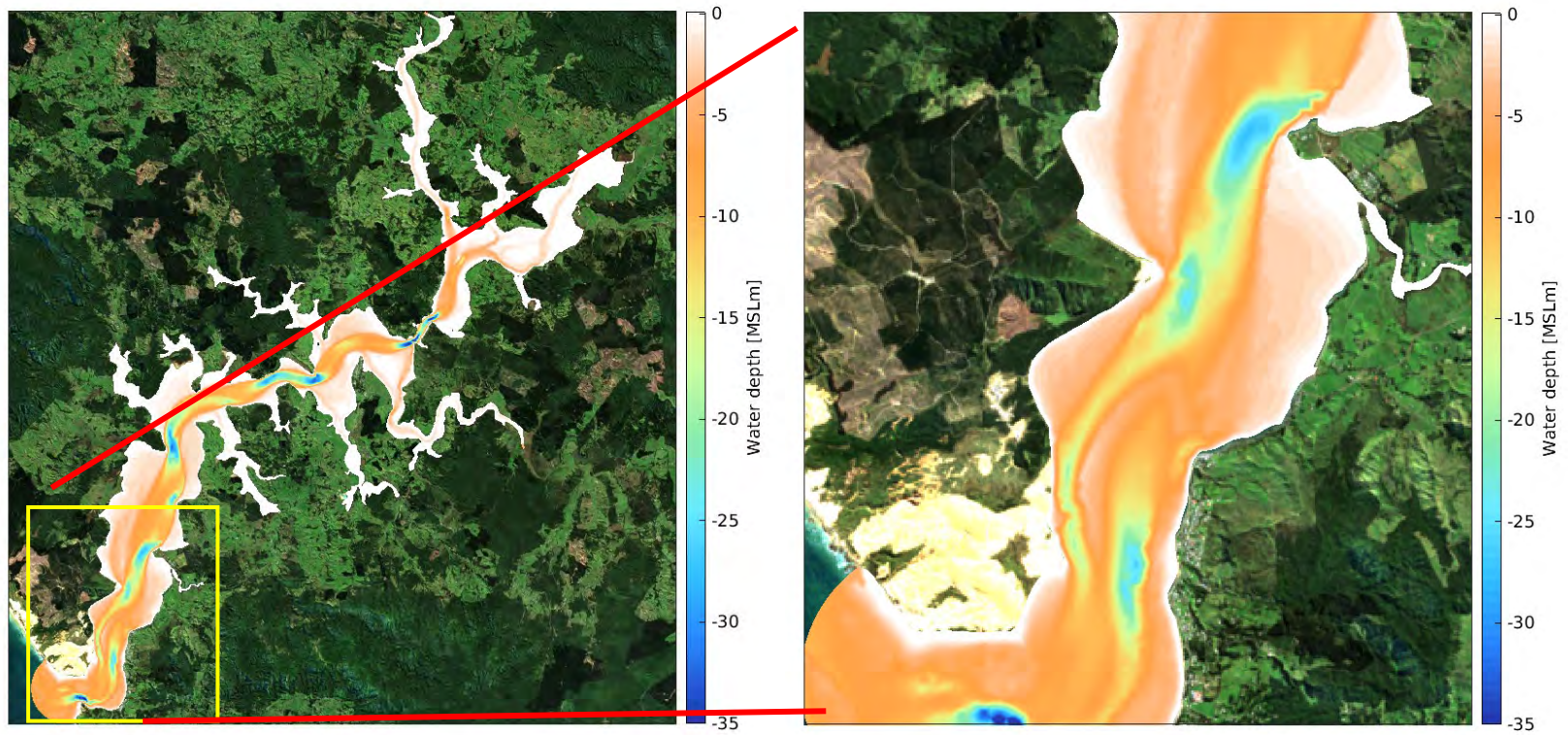


Figure 4.4 Bathymetry of model domain showing the water depth in m below mean sea level. Left is the whole domain and right is a zoom over the Opononi discharge location.

4.2.3 Vertical discretisation

For this model simulations, the vertical discretisation of the water column consisted of a Localized Sigma Coordinate system with Shaved Cell (LSC²), a type of terrain-following layers as described in Zhang et al. (2014).

The use of this type of vertical grid was dictated by the stratification of the water column as well as the shallows area in the Northern end of the Harbour. The vertical grid is constituted of quadratic terrain-following coordinate with 4 layers near in the shallow area (less than 2m) and 24 layers near the offshore boundary. A vertical section showing both the sigma layers and the water depths along a transect is presented in Figure 4.5.

For this study, the model was configured with increased vertical resolution at the surface. The vertical discretisation used in this study is appropriate for investigating the stratified flow regime that is expected within the harbour due to the mixing of the river fresh water and denser marine waters which leads to a concentration of fresh water in the upper levels of the water column.

In order to add more accuracy in the shallow region, the model was setup so that the minimum water depth calculated by the model is 0.001m. In other words, depth less than 1mm is considered dry.

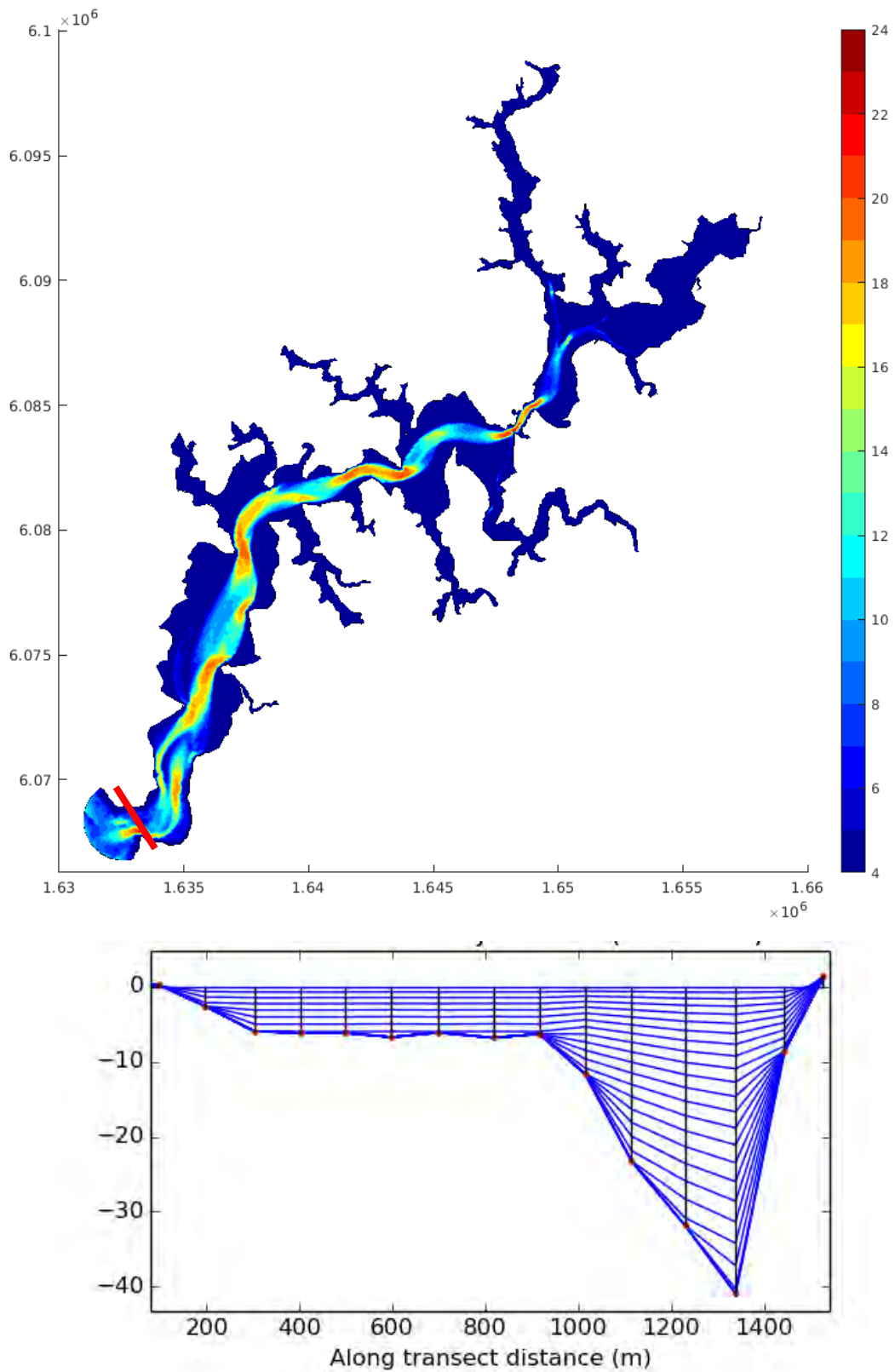


Figure 4.5 Map of Hokianga harbour showing the number of vertical level used in the model (left) and the cross section represented by the black line is shown on the right picture. Note the vertical resolution is increased near the surface to resolve the fresh water forcing.

4.2.4 Vertical mixing / turbulence closure

Vertical mixing was modelled using a *GLS* model with a (Kantha and Clayson 1994) stability function with minimum and maximum diffusivities set to 1×10^{-4} and 1×10^{-2} , respectively, following model validation and calibration. These values were adjusted as part of the model validation and calibration process.

The constant surface mixing length was held to the recommended default of 0.1 (i.e. 10% of the uppermost sigma layer); however, variations of the mixing length were examined during the validating and calibration process.

Frictional stress at the seabed was approximated with a quadratic drag law, with the drag coefficient (*CD*) determined using a manning coefficient of 0.01. Detailed explanations of the determination of the drag coefficient are given in (Zhang Y.L. and Baptista 2008).

4.2.5 Submerged Aquatic Vegetation

In order to include the mangroves ecosystem in the model, the Submerged Aquatic Vegetation (SAV) module was used. By using the SAV module the drag coefficient is increased (a coefficient of 1.13) and therefore affect the flow velocity.



Figure 4.6 Aerial photography of Hokianga Harbour showing in red the mangrove habitat used in the SCHISM model

4.3 Boundary Conditions and Forcing

4.3.1 Atmospherics Forcing

MetOcean Solutions maintains an up-to-date 12 km resolution New Zealand atmospheric hindcast reanalysis from 1979 to 2019 using the Weather and Research Forecasting (WRF) model and deriving boundary conditions from the global CFSR product. The improvement in resolution from the 35 km of CFSR adds accuracy and variability to the atmospheric fields that force the hydrodynamic models, especially over coastal margins where topography is known to substantially change the large-scale wind patterns and local responses. WRF reanalysis prognostic variables such as winds, atmospheric pressure, relative humidity, surface temperature, long and short wave radiation, and precipitation rate were used at hourly intervals to provide air-sea fluxes to force SCHISM in all domains, using a *bulk flux* parameterization (Fairall et al., 2003).

4.3.2 Open Boundary and Tidal Forcing

Tidal constituents were calculated from a greater New Zealand SCHISM domain (Figure 4.7). This New Zealand domain was run in hindcast baroclinic mode for a 10-year period spanning 2000-2009. Depth averaged velocity, elevations, tidal phases and amplitudes for the salient primary and secondary tidal constituents were derived near the Hokianga harbour entrance using harmonic analysis.

Residual surface elevation at the offshore boundary is a combined from multiple factors (Atmospheric pressure, tide and wave). In this study, the inverse barometric effect (IB) was calculated from the WRF mean sea level pressure. The impact of the wave on the offshore boundary was calculated using a basic wave set-up equation from Goda (1985), Where H_o is the wave height and L_o is the wavelength.

$$\text{Wave setup (Goda 1985): } \frac{0.01H_o}{\sqrt{\frac{H_o}{L_o} \left(1 + \frac{h}{H_o}\right)}} \quad (\text{Eq. 4.1})$$

The final residual surface elevation is the sum of the IB and the wave setup (Figure 4.8)



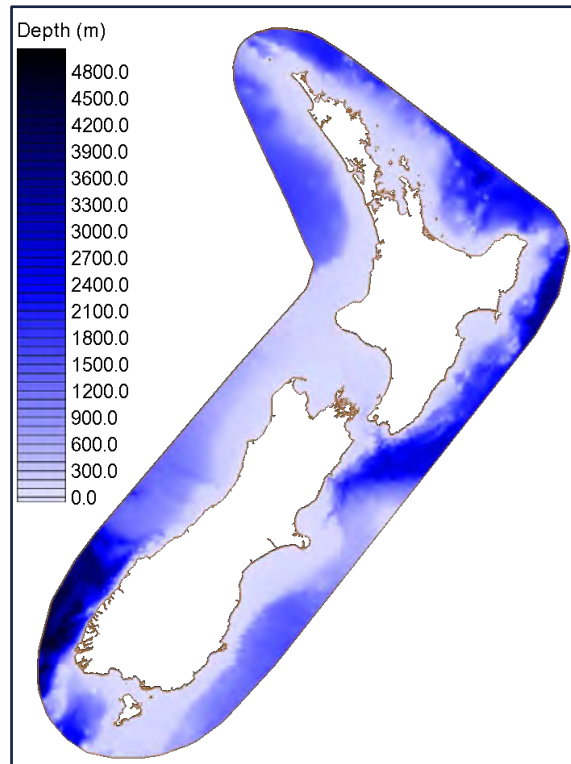


Figure 4.7 Extent of the NZ scale finite element domain used to derive tidal constituents at the Hokianga harbour entrance.

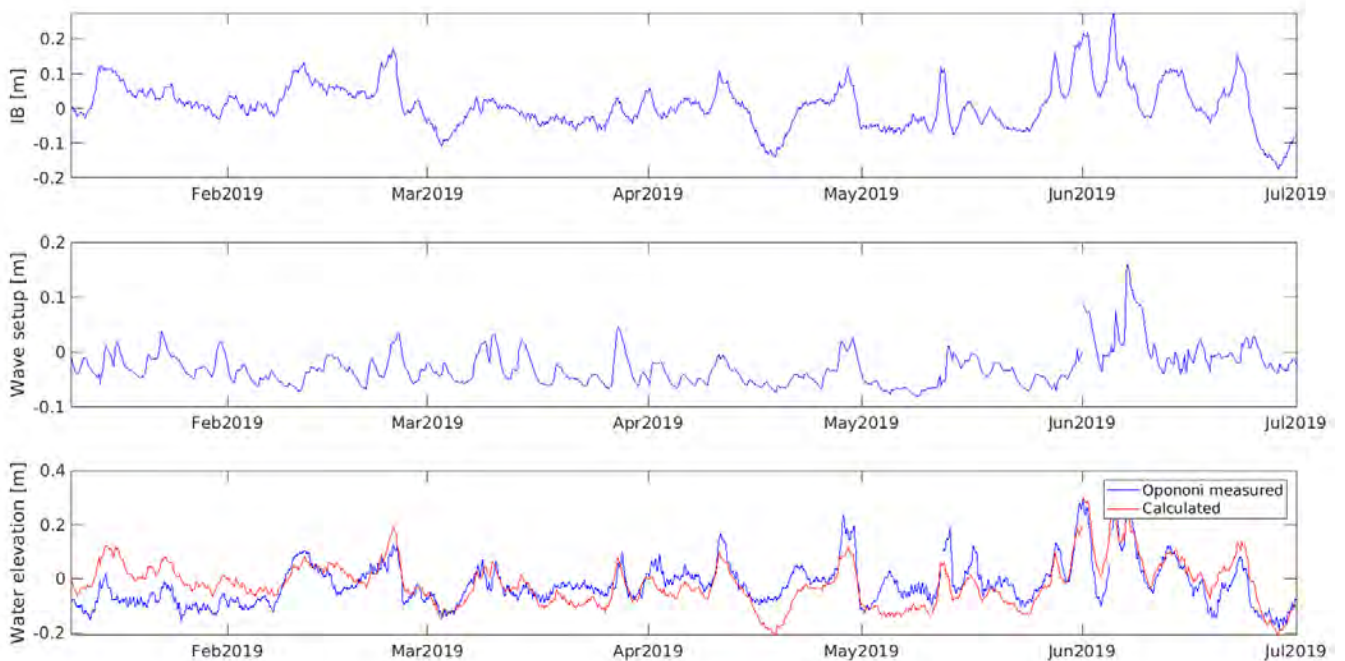


Figure 4.8 Time series of the IB calculated from the mean sea level pressure from WRF model (top). Timeseries of the wave setup calculated from the wave height at the offshore boundary using the equation from Goda 1985.(middle). Comparison of the residual elevation from IB and wave setup with the residual elevation measured at Opononi.



4.3.3 River Discharges

Only four major rivers were included in the model: Waima river, Waihou River, Orira River and the Mangamuka River (Figure 4.10).

Discharge records of Waihou and Waima rivers measured between 1989 and 2019 by NIWA and Northland Regional Council were processed to force the SCHISM domains. Due to the limited available data for Mangamuka River, a time series discharge rates for this river was estimated based on a ratio between the mean discharge rate from the Mangamuka and Waihou Rivers. The discharge from the Orira River was made constant and the mean discharge was used ($0.4 \text{ m}^3/\text{s}$)

In order to include the runoff from the surrounding streams, the rivers discharge were increased by a percentage calculated during the calibration of the model (Table 4.1).

Table 4.1 Factor used for each of the river in order to account for the run off in Hokianga harbour.

River	Factor
Waihou	1.16
Mangamuka	1.25
Waima	1.10

The time series of the Waima river and Waihou river discharges are presented in Figure 4.9

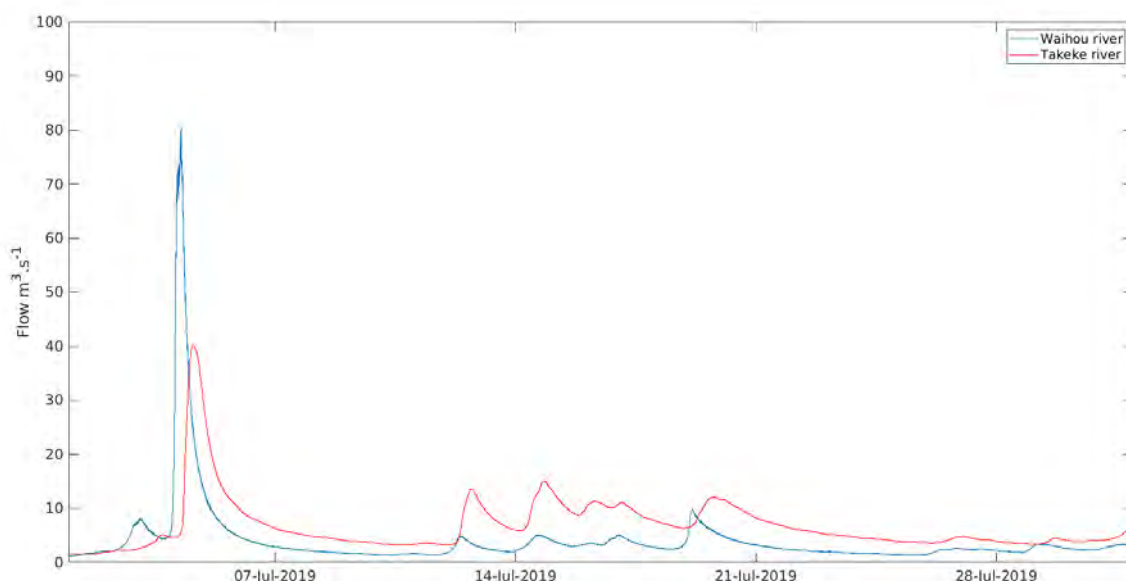


Figure 4.9 Timeseries of the Waihou and Waima river flow used during the validation period of the model.





Figure 4.10 Aerial photography showing in red the four rivers included in the model

4.3.4 Temperature and Salinity

A vertically and horizontally uniform salinity and temperature fields were applied to the open ocean model boundary from the HYCOM model.

River salinity was defined as fresh water (0 PSU), and river temperature was only measured at the Waiapa river (upstream from Waihou river).

The same temperature was used in all rivers. A time series of river temperature is presented in Figure 4.11.

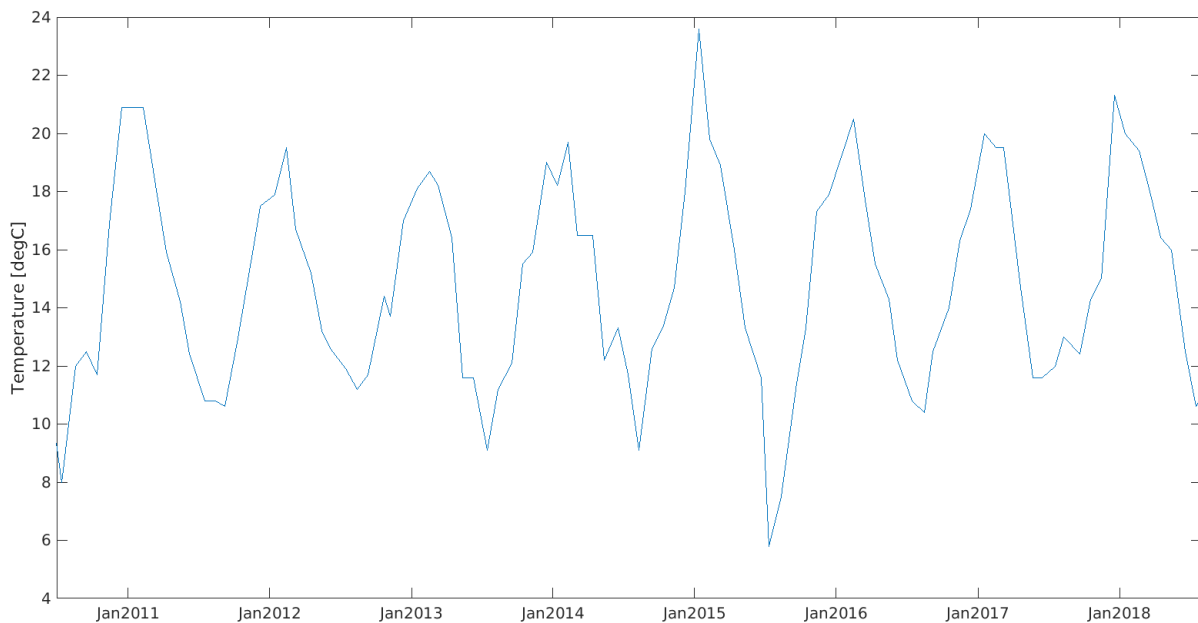


Figure 4.11 Timeseries of river temperature, measured at Waiapa river, used for all the rivers in the Hokianga Harbour model between 2010 and 2018

4.3.5 WWTP Discharges

As presented in the FNDC documents details of the WWTP discharges into Hokianga Harbour are as follows:

Opononi WWTP - 1634768E 6069462N (NZTM 2000)

- Discharged directly into the harbour via outfall pipe.
- Pumped from a holding pond and discharged into the harbour for maximum of 4 hours on an outgoing tide.
- Treated wastewater shall only be discharged to the Harbour for a max. of 3 hours each tidal cycle between one and four hours after high tide.
- Discharge Limit 450m³/day (revised from 685m³ previously)

Kohukohu WWTP – 1648973E 6085591N (NZTM 2000)

- Discharged into unnamed tributary of the Hokianga Harbour (tidal mud flat)
- Continuous gravity discharge. Known to have zero discharge in dry periods.
- Discharge limit 40m³/day (30 days average)

Rawene WWTP - 1645309E 6079915N (NZTM 2000)



- Discharged into Omanaia River (tidal mud flat)
- Continuous gravity discharge from the WWTP but once the discharge enters the drain it is controlled by a flood gate discharging to the Omanaia River. There are other contributors to the drain and therefore the discharge from the floodgate.
- Discharge limit 254m³/day (30 days average)

Kaikohe WWTP (1674845E 6079488N.)

- Discharged into unnamed tributary of the Wairoro Stream
- Continuous gravity discharge into freshwater that runs into the Hokianga Harbour.
- Discharge limit 1710m³/day (30 days average)

Nearfield:

Each of the four WWTP discharge are occurring either via an outfall pipe or via continuous gravity discharge which therefore did not have any structural design which would lead to complex dilution patterns (diffuser, multiple pipe arrangement..). The nearfield dilution is expected to simply occur as the discharge water mixes with the stream water or the Hokianga Harbour water. The SCHISM model represent the release of the contaminant as a discharge flow (with a tracer concentration [C]) in a model cell similarly to that a pipe on the seabed (or with gravity discharge on dry land). The near field dilution is then occurring within that model cell .The representation in the numerical model as a discharge source is therefore suitable for assessing the fate and dispersion of the WWTP waters in the harbour.

Discharge Timeseries:

In order to model the four discharges a review of the discharge rate timeseries data was undertaken (see Figure 4.12) and an annual representation of the variability in the discharge rate, as well as a maximum, close to the proposed resource consent was chosen for each of the four discharge locations (Figure 4.13 and Figure 4.14). If needed, the discharge was increased to reach the resource consent limit.

Opononi was set up to only discharge up to four hours following high tide.

The probability of future estuarine conditions can be assessed from the historical conditions, thereby allowing estimations of the general geographical dispersion expected. In the present study, the approach consists in running year-long simulations



within two contrasting historical contexts (La Niña /El Niño episodes, June 2010 - June 2011, and June 2015 - June 2016, respectively).

The yearlong run simulation was extended by two days with a discharge rate increased to the highest discharge recorded in order to assess the impact of an extreme isolated event (Figure 4.14).

Different passive Eulerian tracers (i.e. neutrally buoyant , no decay) were used for each WWTP discharge. A nominated concentration value of 1 mg/L was used so that dilution can be calculated at various distance from the source. Specific contaminant concentration levels can then be determined using concentration ratios and the expected, or measured, discharged value.

For the Kaikohe WWTP the discharge occurs more than 30 km upstream of the Waima River connection to Hokianga Harbour. The WWTP contaminant concentration gets diluted as it flows from Kaikohe to the harbour due to the little tributaries joining along the stream. Timeseries of river discharge data are only available further downstream of the discharge and closer to the harbour (i.e. 'Punakitere at Taheke' data from NRC).

A modelled discharge point closer to the harbour was therefore implemented. A dilution factor of 1/18.4 between the Kaikohe discharge location and the point where the modelled Waima river discharges into the harbour was adopted. Comparing the volume of water from the NIWA river maps service (<https://shiny.niwa.co.nz/nzrivermaps/>) data, at these two locations allow us to consider all the fresh water input from all the small tributaries between the WWTP discharge point and the modelled discharge point in the harbour. The mean flow value extracted from the NIWA site where 0.768m³/s near the Kaikohe discharge location and 14.1m³/s near the modelled Waima river point, this leads to a ratio of 18.4. It is noted that based on the available data (mean flow, mean annual low flow, 1 in 5-year low flow) this dilution ratio can vary between approximately 1/16 to 1/23.



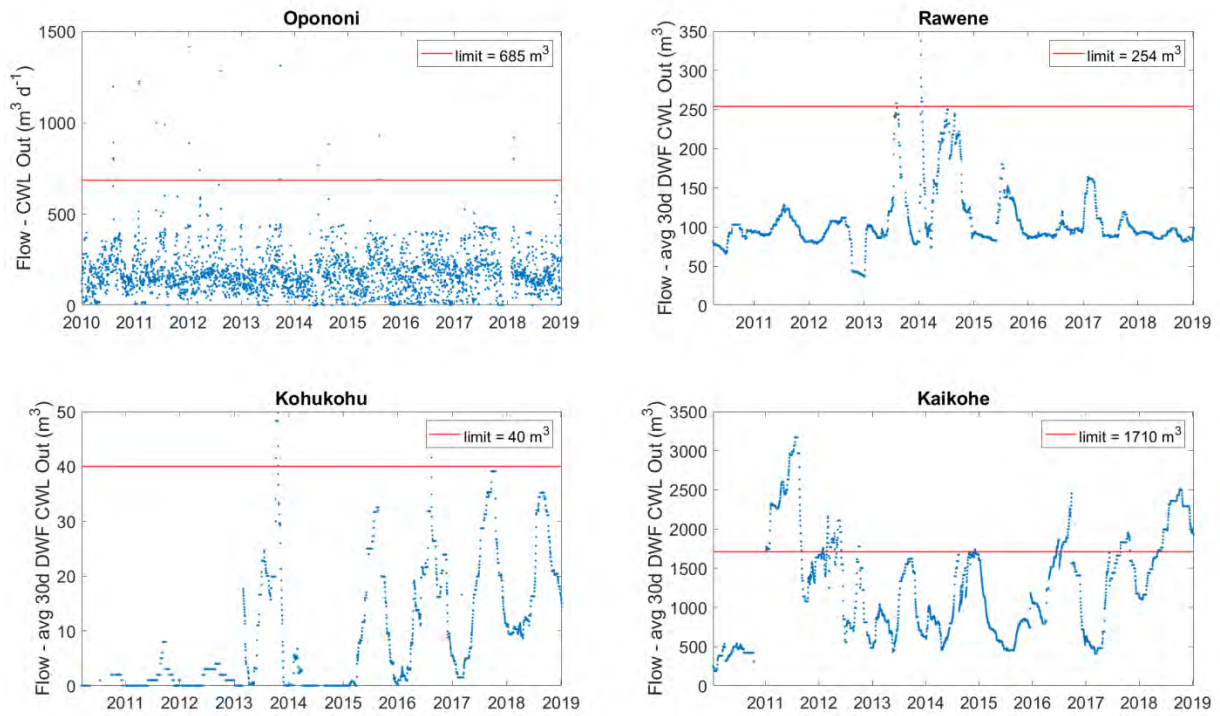


Figure 4.12 Discharge timeseries (blue) and council limits (red) from the four locations

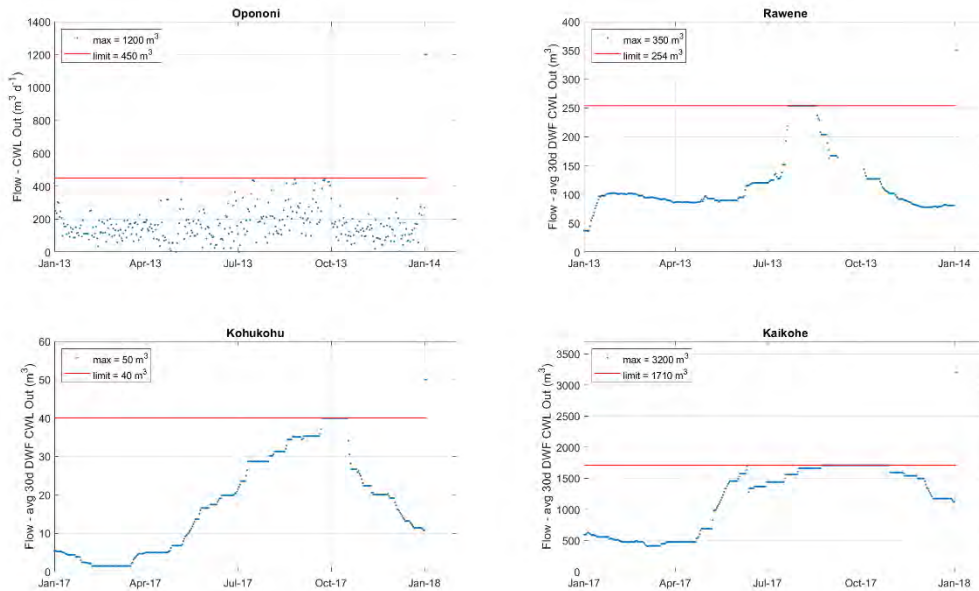


Figure 4.13 Discharge timeseries (blue) and council limits (red) from the four locations selected for use in the modelling



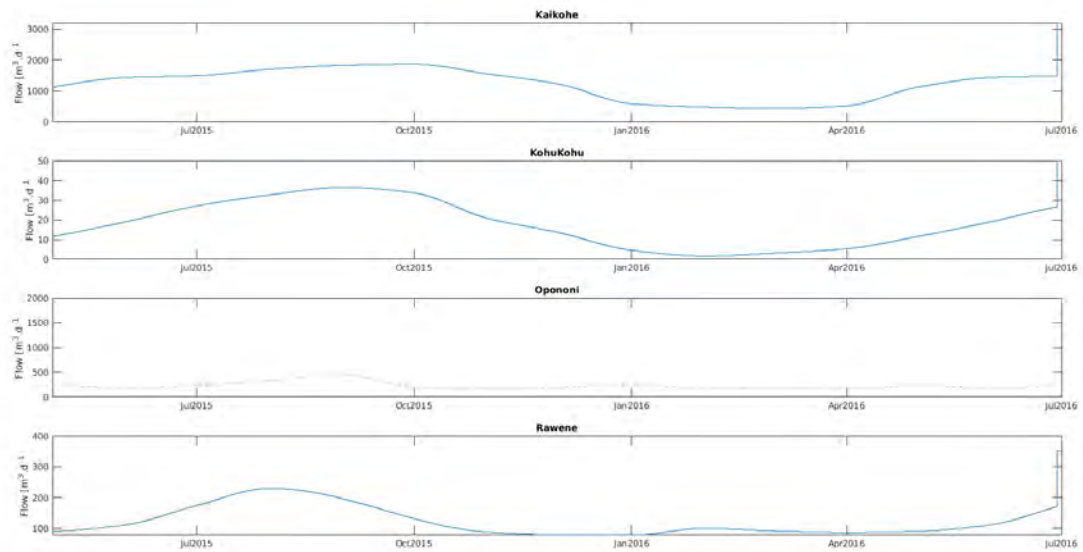


Figure 4.14 Modelled timeseries of discharge rate (in m³/day) from the four discharge locations. Note Opononi was only released during the first four hour of the ebb tide.

Contaminants:

Can you please proceed with doing concentration maps for the 50th and 95th percentile , then colorbar legend should be concentration in mg/L (based on a 1mg/L discharge concentration).

And then change Axis labels for time series



5.Results

5.1 Model validation

5.1.1 Elevation

Time series of measured water elevations have been processed and the residual elevations are separated from the tidal elevations.

The amplitudes and phases from M2, S2, N2, K2, K1 and L2 tidal constituents extracted from all data collection sites are shown from Table 5.1 to Table 5.6. Time series of total elevations are shown in Figure 5.1. Residual time series are presented in Figure 5.2.

Comparisons show that the model successfully reproduces the propagation of the tidal wave inside the harbour, with good agreement between both amplitudes and phases of the principal tidal constituents. The misalignment in the time series of the measured and modelled water level at Onoke and The Narrows are due to the movement of the instrument which occurred during the deployment as discussed in Section 2.1.3, nevertheless the water level variations are in good agreement.

Table 5.1 Comparison of measured and modelled amplitude and phase for the M2 constituent at all sites.

M2 constituent	Amplitude [m]		Phase [deg]	
	Measured	Modelled	Measured	Modelled
Omapere	0.98	1.01	291.28	289.23
Onoke	1.11	1.08	293.48	296.86
Matawhera	1.14	1.10	302.13	301.65
The Narrows	1.24	1.10	307.76	311.17



Table 5.2 Comparison of measured and modelled amplitude and phase for the S2 constituent at all sites

S2 constituent	Amplitude [m]		Phase [deg]	
Site name	Measured	Modelled	Measured	Modelled
Omapere	0.25	0.25	322.28	316.62
Onoke	0.30	0.29	326.00	322.83
Matawhera	0.28	0.31	336.87	326.98
The Narrows	0.30	0.32	339.20	335.93

Table 5.3 Comparison of measured and modelled amplitude and phase for the N2 constituent at all sites

N2 constituent	Amplitude [m]		Phase [deg]	
Site name	Measured	Modelled	Measured	Modelled
Omapere	0.21	0.19	286.87	276.65
Onoke	0.24	0.20	292.74	286.25
Matawhera	0.24	0.20	299.92	291.98
The Narrows	0.26	0.20	306.89	301.51

Table 5.4 Comparison of measured and modelled amplitude and phase for the K2 constituent at all sites

K2 constituent	Amplitude [m]		Phase [deg]	
Site name	Measured	Modelled	Measured	Modelled
Omapere	0.08	0.08	320.89	322.66
Onoke	0.12	0.12	321.54	338.78
Matawhera	0.09	0.14	327.36	344.99
The Narrows	0.12	0.16	308.89	356.66



Table 5.5 Comparison of measured and modelled amplitude and phase for the K1 constituent at all sites

K1 constituent	Amplitude [m]		Phase [deg]	
	Measured	Modelled	Measured	Modelled
Omapere	0.06	0.07	34.14	33.88
Onoke	0.08	0.07	41.38	38.59
Matawhera	0.07	0.07	41.31	41.17
The Narrows	0.09	0.07	32.81	46.16

Table 5.6 Comparison of measured and modelled amplitude and phase for the L2 constituent at all sites

L2 constituent	Amplitude [m]		Phase [deg]	
	Measured	Modelled	Measured	Modelled
Omapere	0.05	0.01	283.54	232.30
Onoke	0.06	0.03	250.81	253.33
Matawhera	0.08	0.04	284.07	259.66
The Narrows	0.04	0.04	271.83	270.39



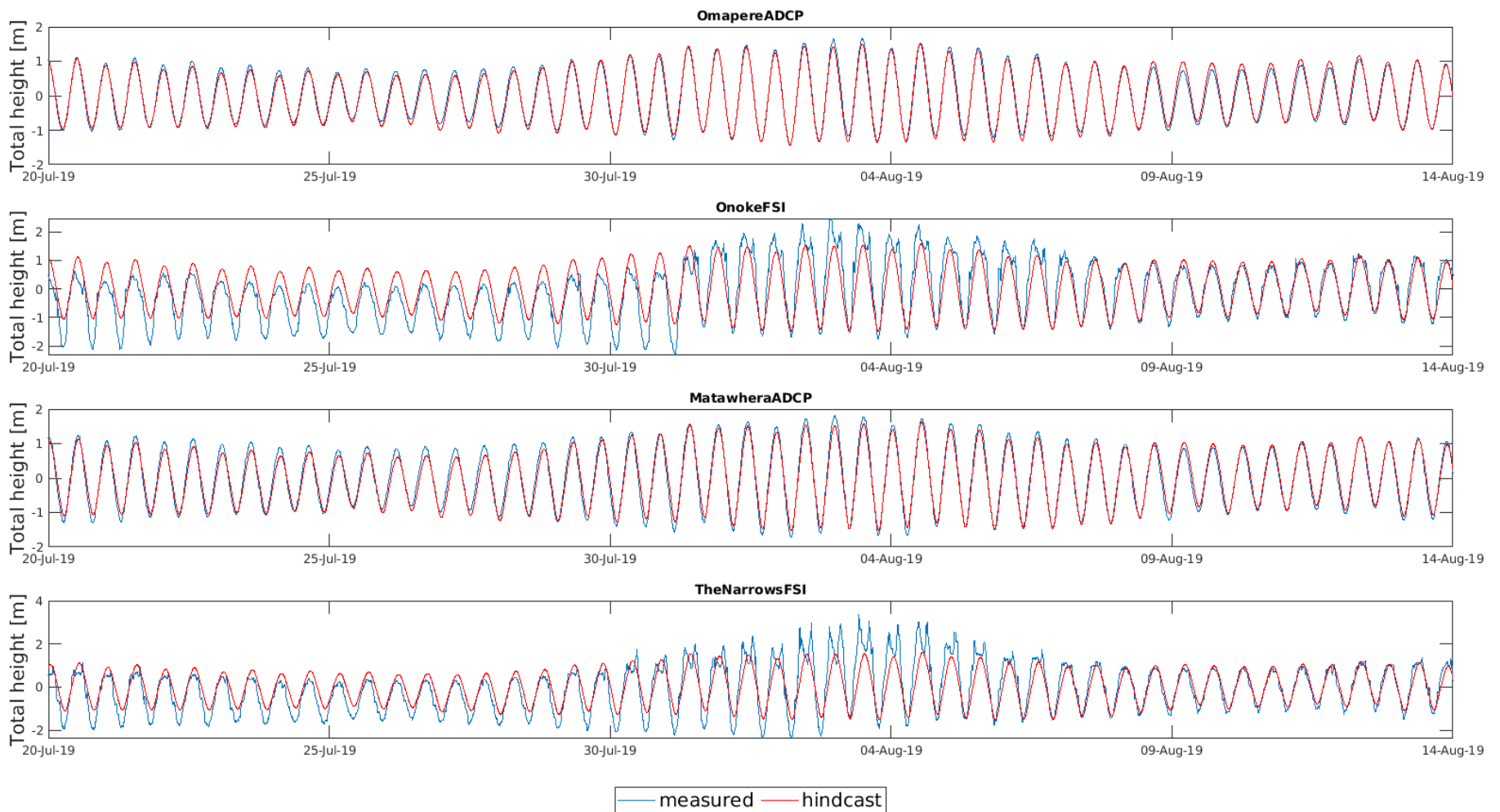


Figure 5.1 Timeseries of water elevation measured at the four sites (blue) and modelled (red) between July 2019 and August 2019. Note: the two FSI sites have moved positioned during the measurement period.



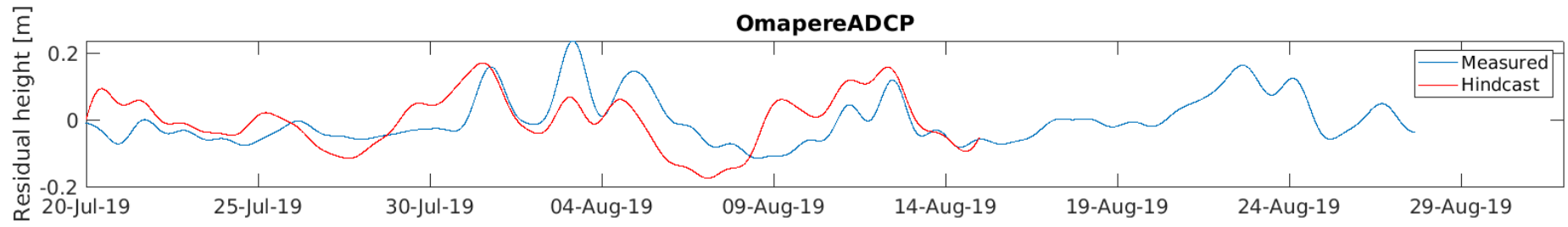


Figure 5.2 Timeseries of residual water elevation measured at Opononi sites (blue) and modelled (red) between July 2019 and August 2019



5.1.2 Velocities

The comparison of the total current speeds and directions at three levels in the water column at the Omapere ADCP site are presented in Figure 5.3 and Figure 5.4 respectively. Tidal signal was removed from the velocities, and currents were rotated in the channel axes. The resultant velocities are presented in Figure 5.5.

Comparison of current speeds and direction at Onoke and The Narrows are presented in Figure 5.6 and Figure 5.10 respectively. For both FSI sites, the extraction of the tidal signal was not possible due to the shift of the instrument during the deployment.

The comparison of the total current speeds and directions at three levels in the water column at the Matawhera ADCP site are presented in Figure 5.7 and Figure 5.8 respectively. Tidal signal was removed from the velocities, and currents were rotated in the channel axes. The resultant velocities are presented in Figure 5.9.

At all sites, the model reproduces well the tidal signal in the entire water column. More precisely, the amplitude difference between the ebb and flood current is modelled correctly especially at the Matawhera site (Figure 5.7).

The model tends to reproduce the current more accurately toward the end of the deployment (in August). This could be due to the freshwater influence on the environment. Higher precipitation rate and higher discharge from the river were observed between the 14th and 20th of July 2019 (Figure 4.9).



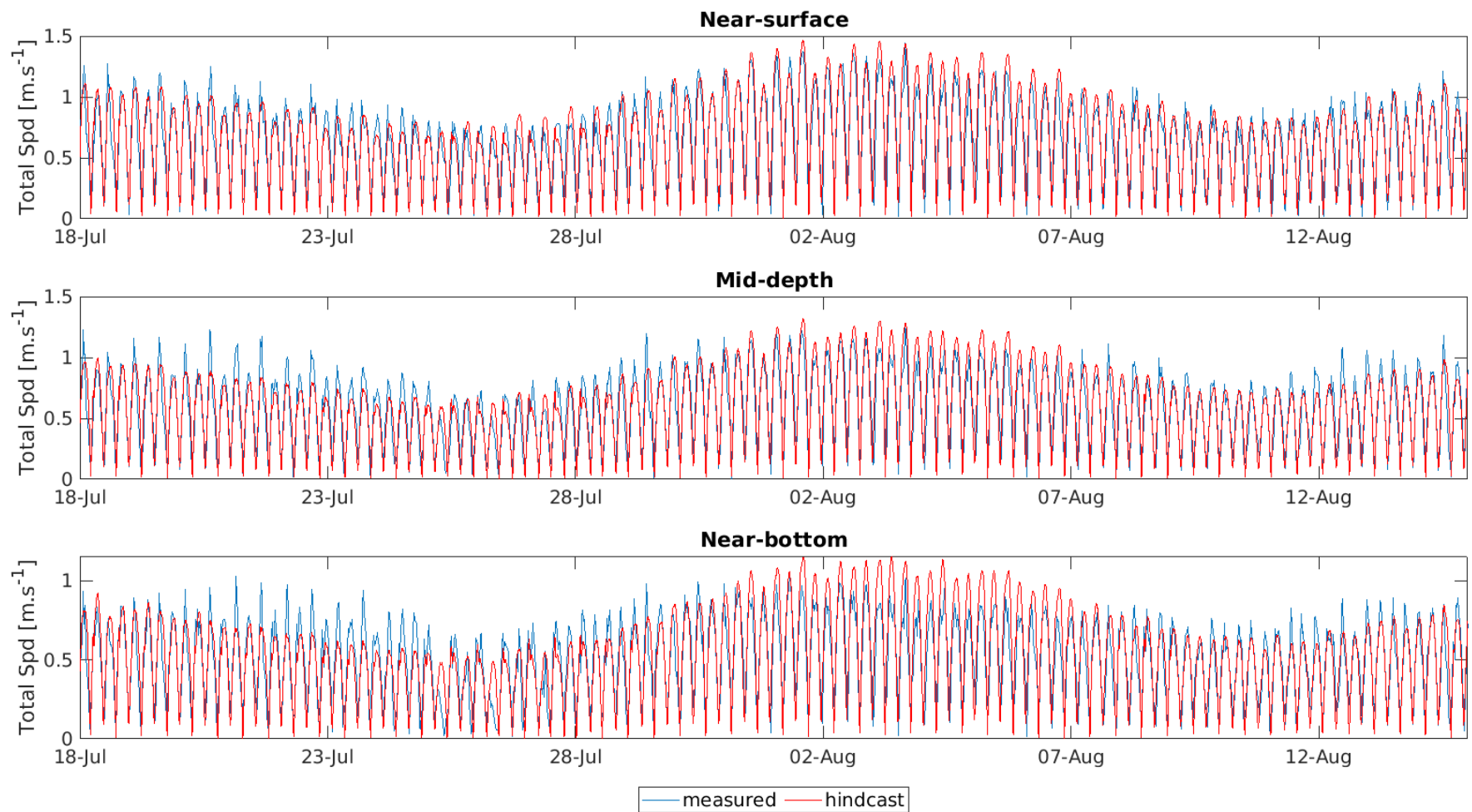


Figure 5.3 Measured (blue) and modelled (red) total near-surface (top), mid-depth (middle), and near-bottom (bottom), current speeds at Omapere ADCP site from July 2019 to August 2019.



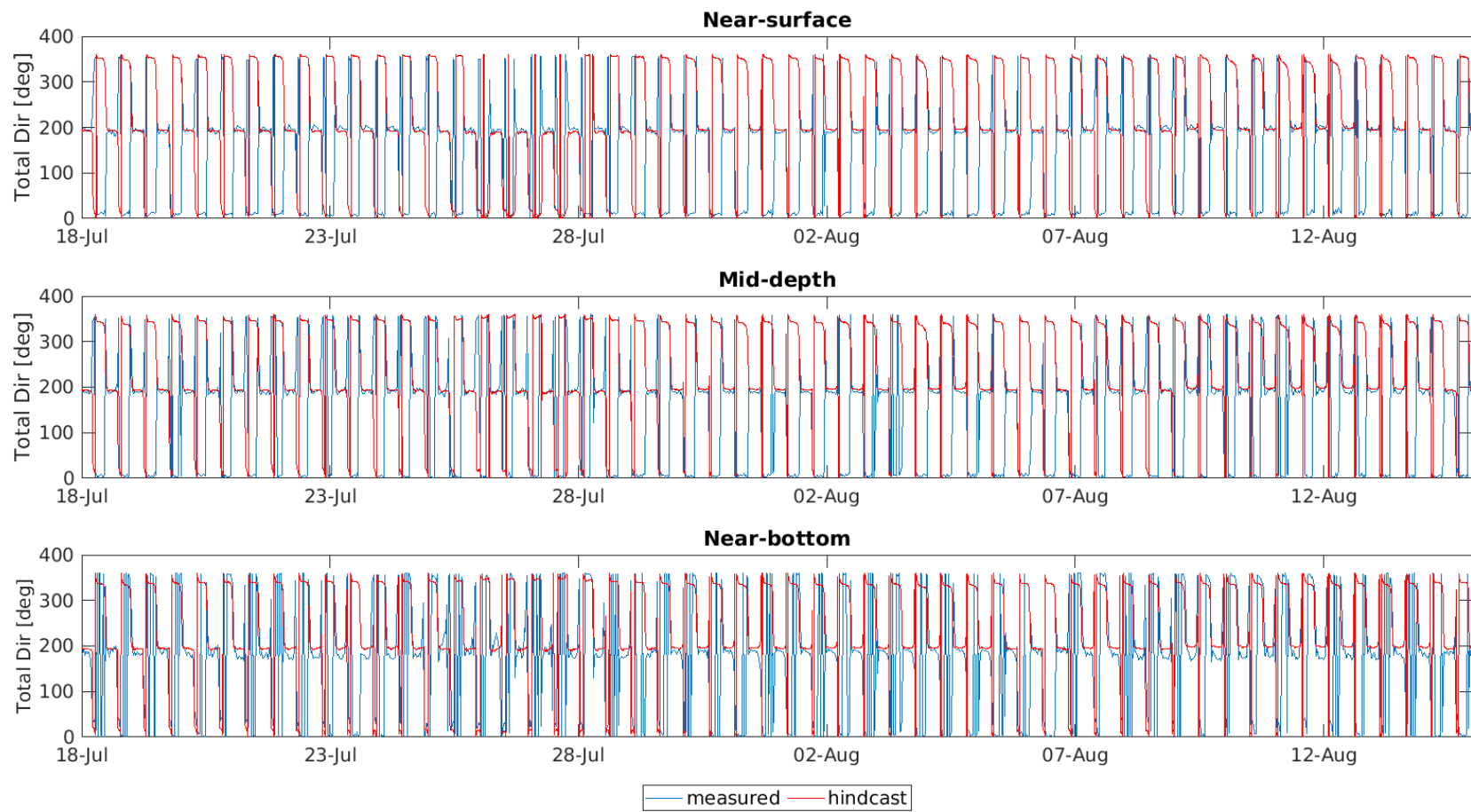


Figure 5.4 Measured (blue) and modelled (red) total near-surface (top), mid-depth (middle), and near-bottom (bottom), current direction at Omapere ADCP site from July 2019 to August 2019

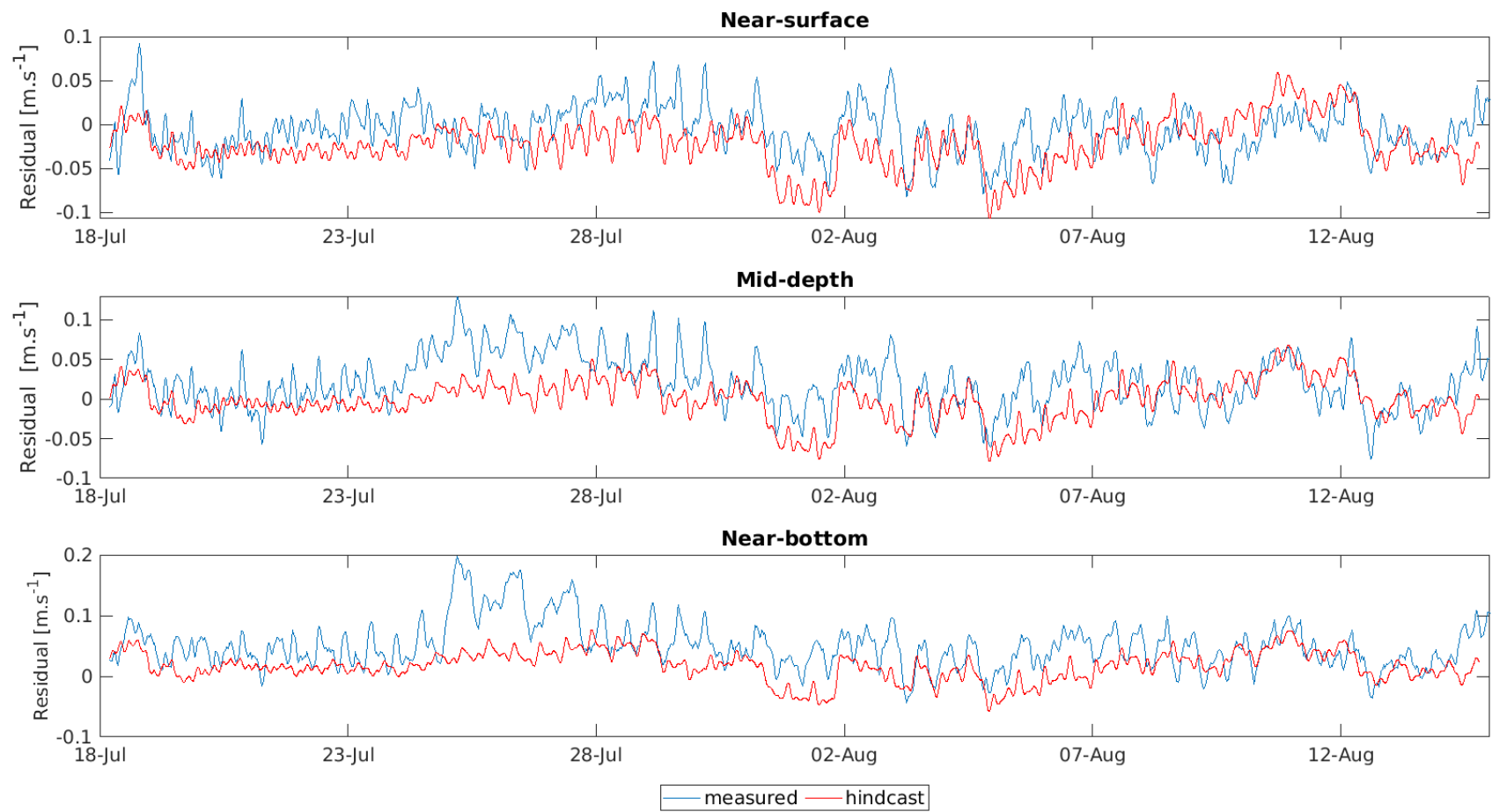


Figure 5.5 Measured (blue) and modelled (red) total near-surface (top), mid-depth (middle), and near-bottom (bottom), Residual velocities at Omapere ADCP site from July 2019 to August 2019. Note the current were rotated to be aligned with the main channel.



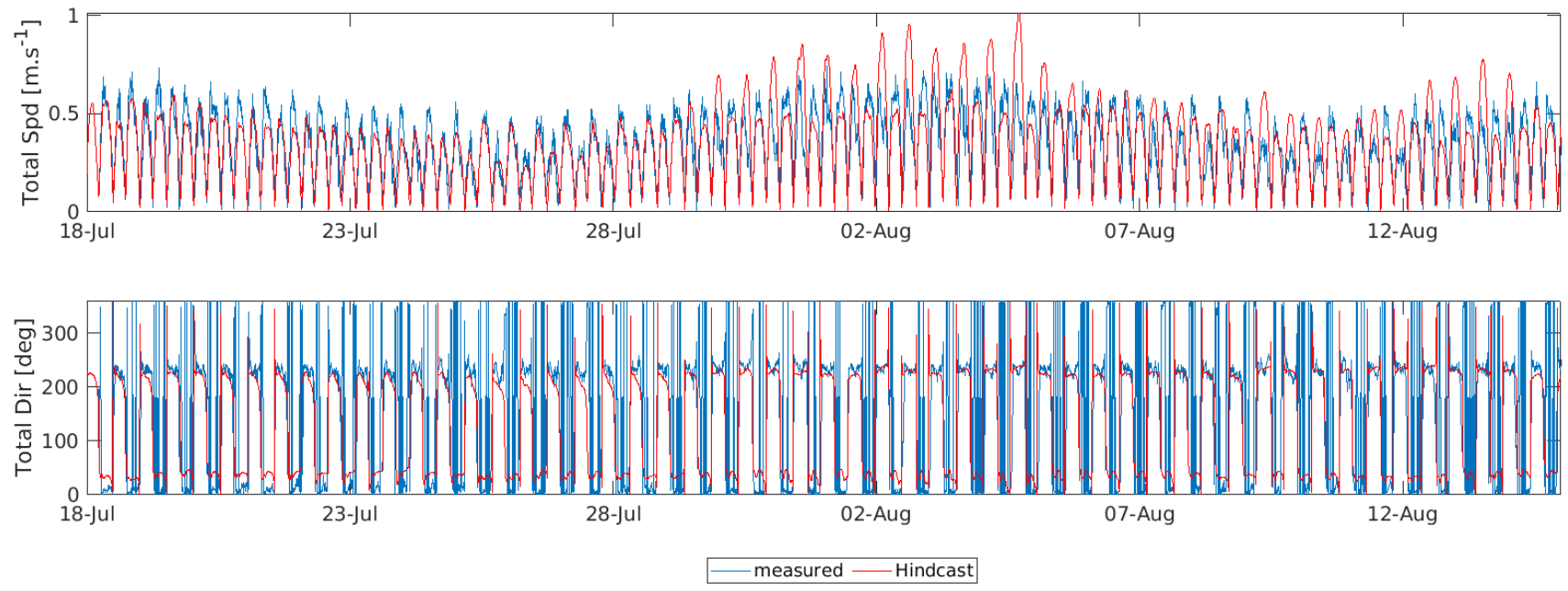


Figure 5.6 Measured (blue) and modelled (red) total mid-depth current speeds (top) and direction (bottom) at Onoke FSI site from July 2019 to August 2019

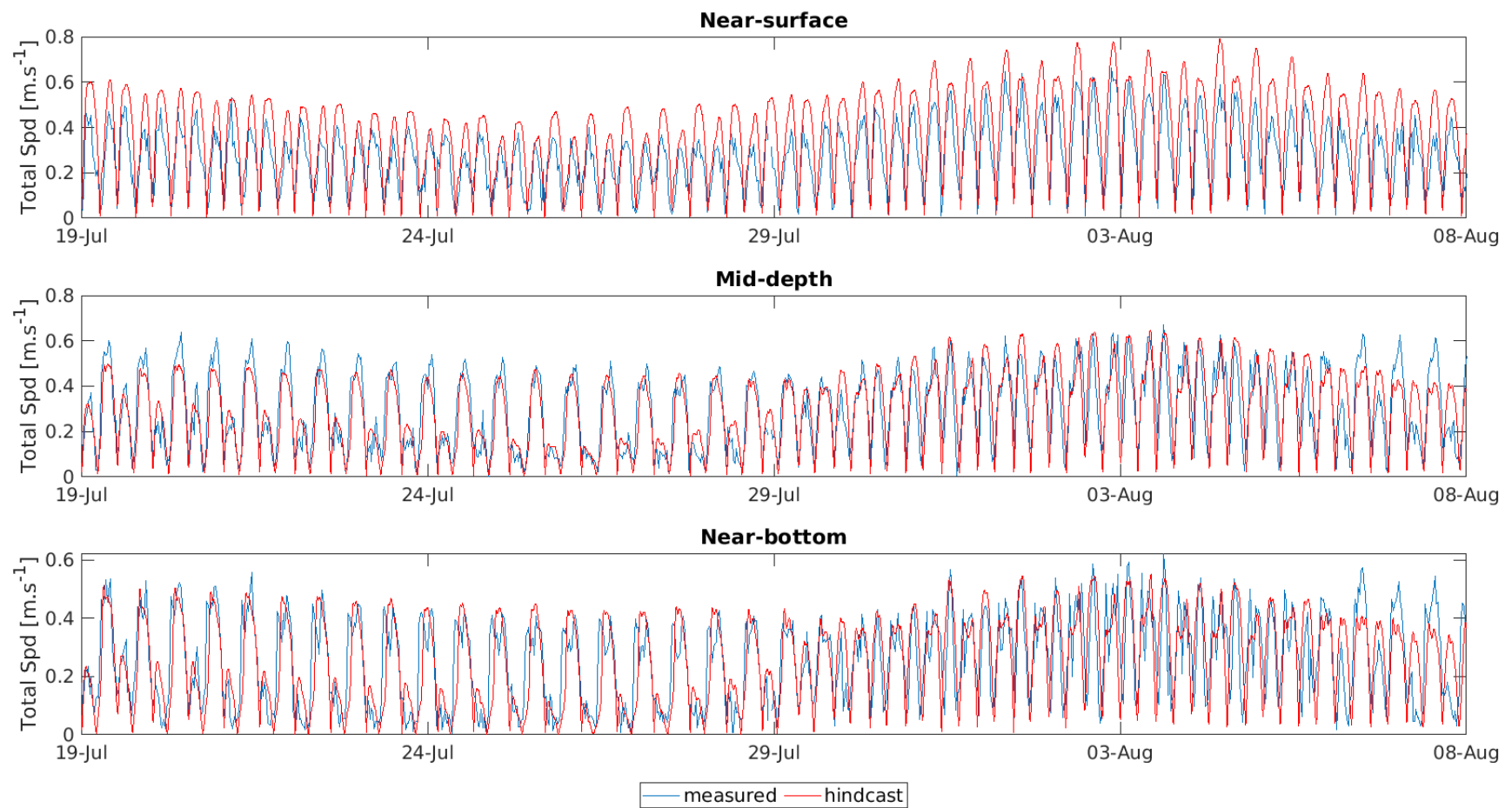


Figure 5.7 Measured (blue) and modelled (red) total near-surface (top), mid-depth (middle), and near-bottom (bottom), current speed at Matawhera ADCP site from July 2019 to August 2019



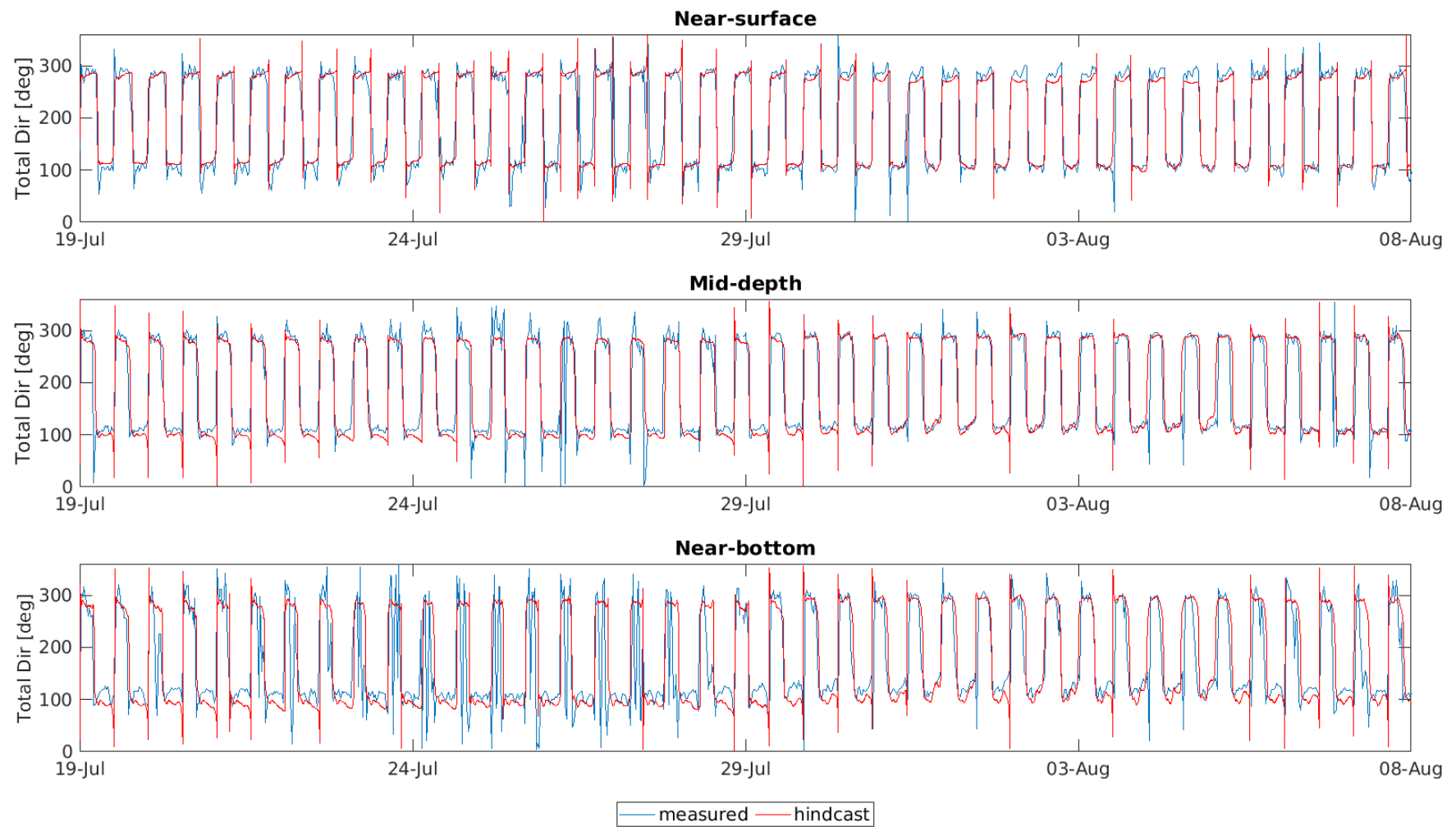


Figure 5.8 Measured (blue) and modelled (red) total near-surface (top), mid-depth (middle), and near-bottom (bottom), current direction at Matawhera ADCP site from July 2019 to August 2019



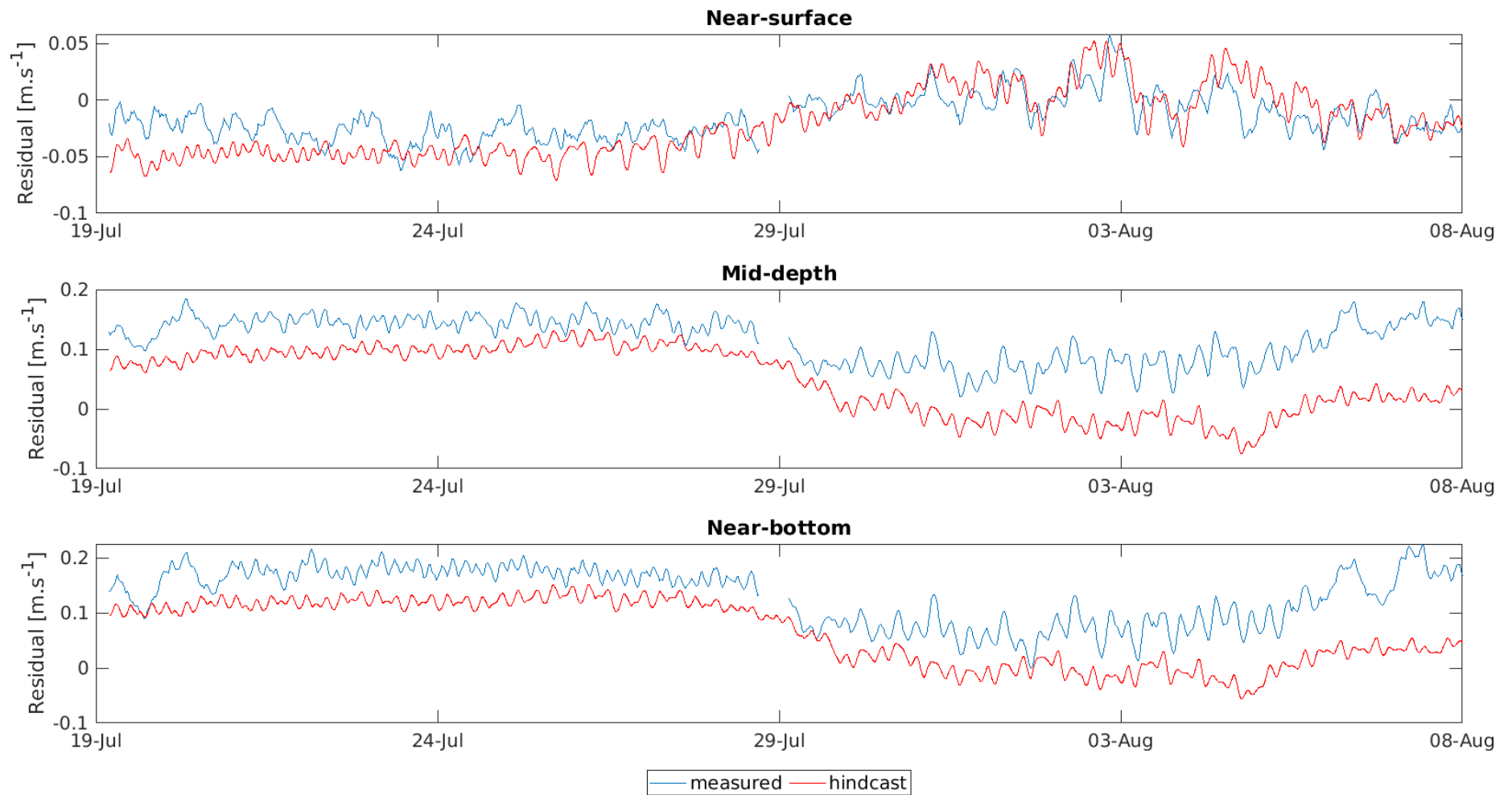


Figure 5.9 Measured (blue) and modelled (red) total near-surface (top), mid-depth (middle), and near-bottom (bottom), Residual velocities at Matawhera ADCP site from July 2019 to August 2019. Note the current were rotated to be aligned with the main channel



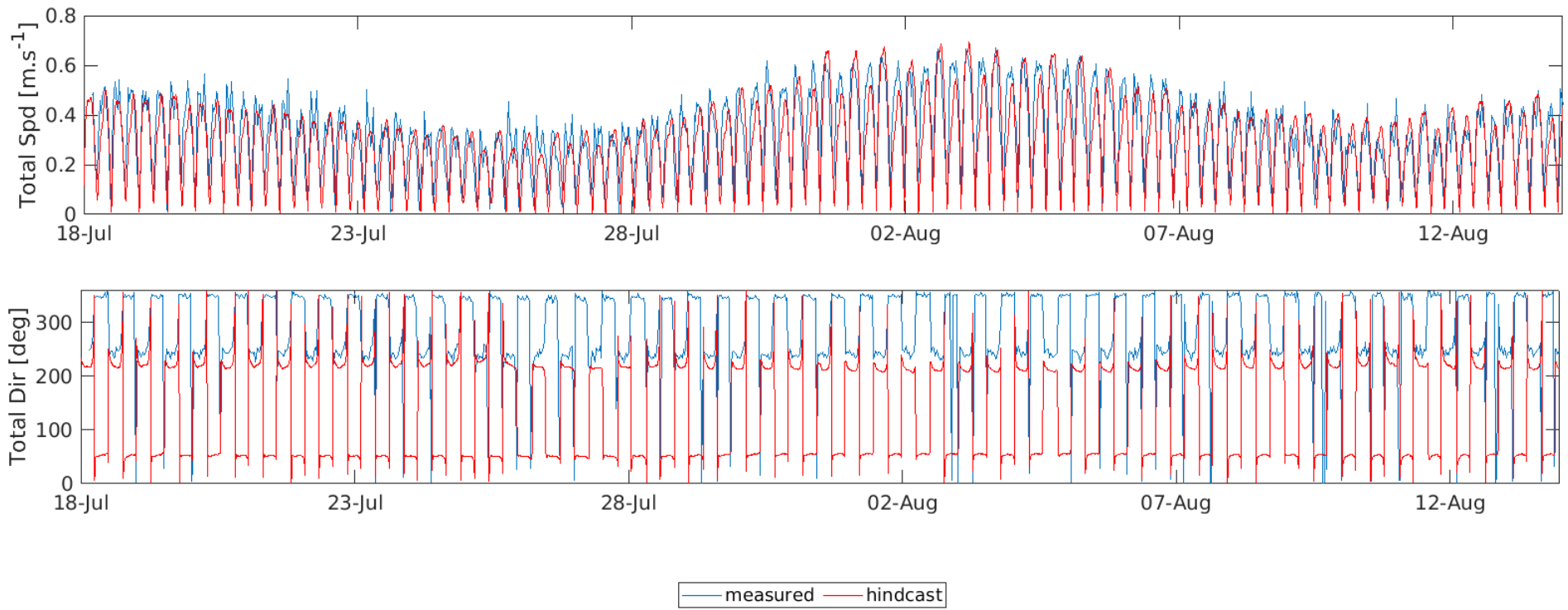


Figure 5.10 Measured (blue) and modelled (red) total mid-depth current speeds (top) and direction (bottom) at The Narrows FSI site from July 2019 to August 2019



5.1.3 Temperature and salinity

Timeseries of near-bottom temperature at all sites are presented in Figure 5.11. The temperature at the entrance of the harbour is modelled more accurately than the northern part of Hokianga Harbour.

Comparisons of mid-depth salinities are presented in Figure 5.12.

The variation and trend in temperature and salinity over the measurement period is well described by the model. Difference in the absolute temperature and salinity values are observed, however these are mostly related to the minimal information available to setup the initial conditions in the model .



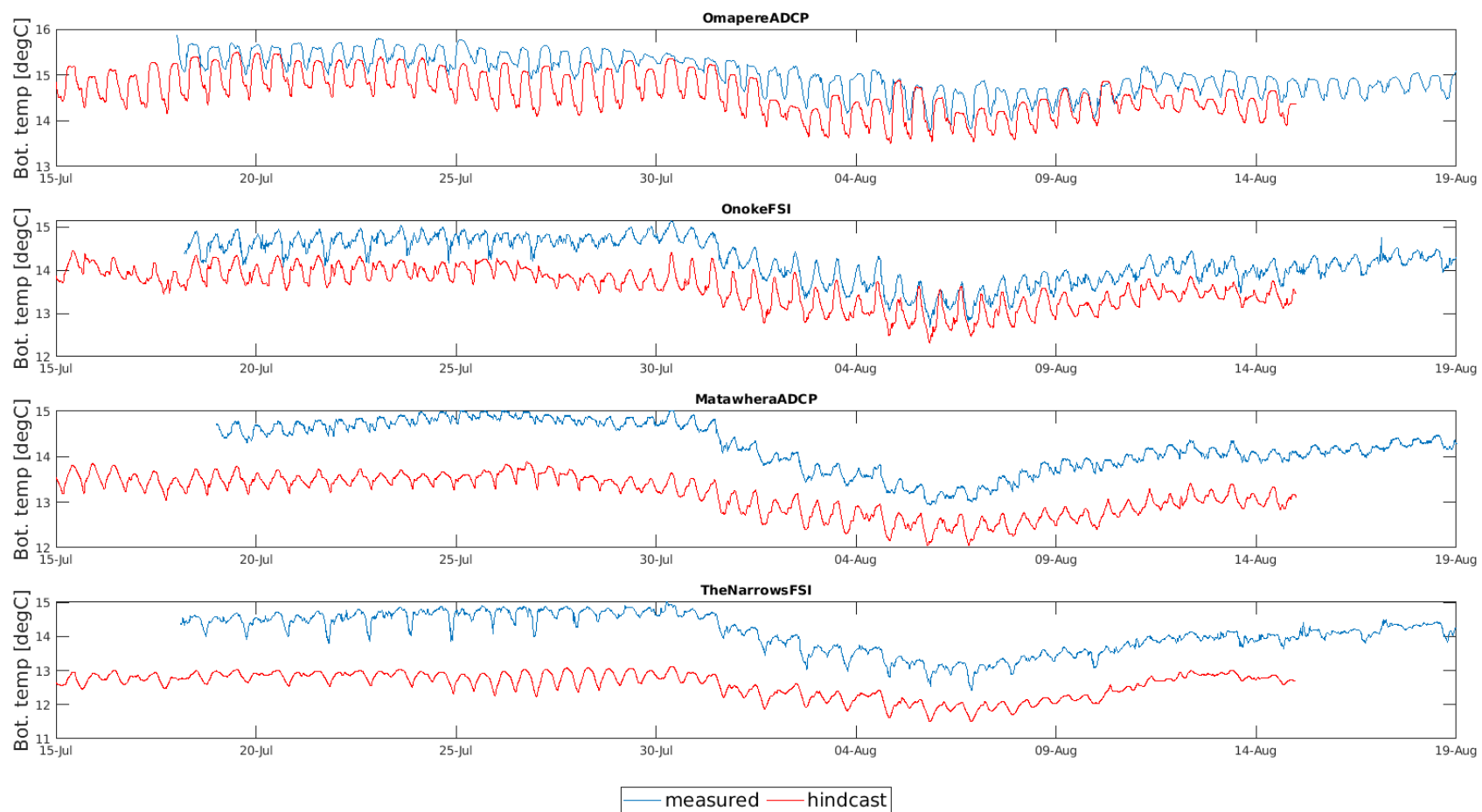


Figure 5.11 Comparison of bottom temperature measured (blue) and modelled (red) at all sites by the FSI and ADCP sensors during July 2019 to August 2019.



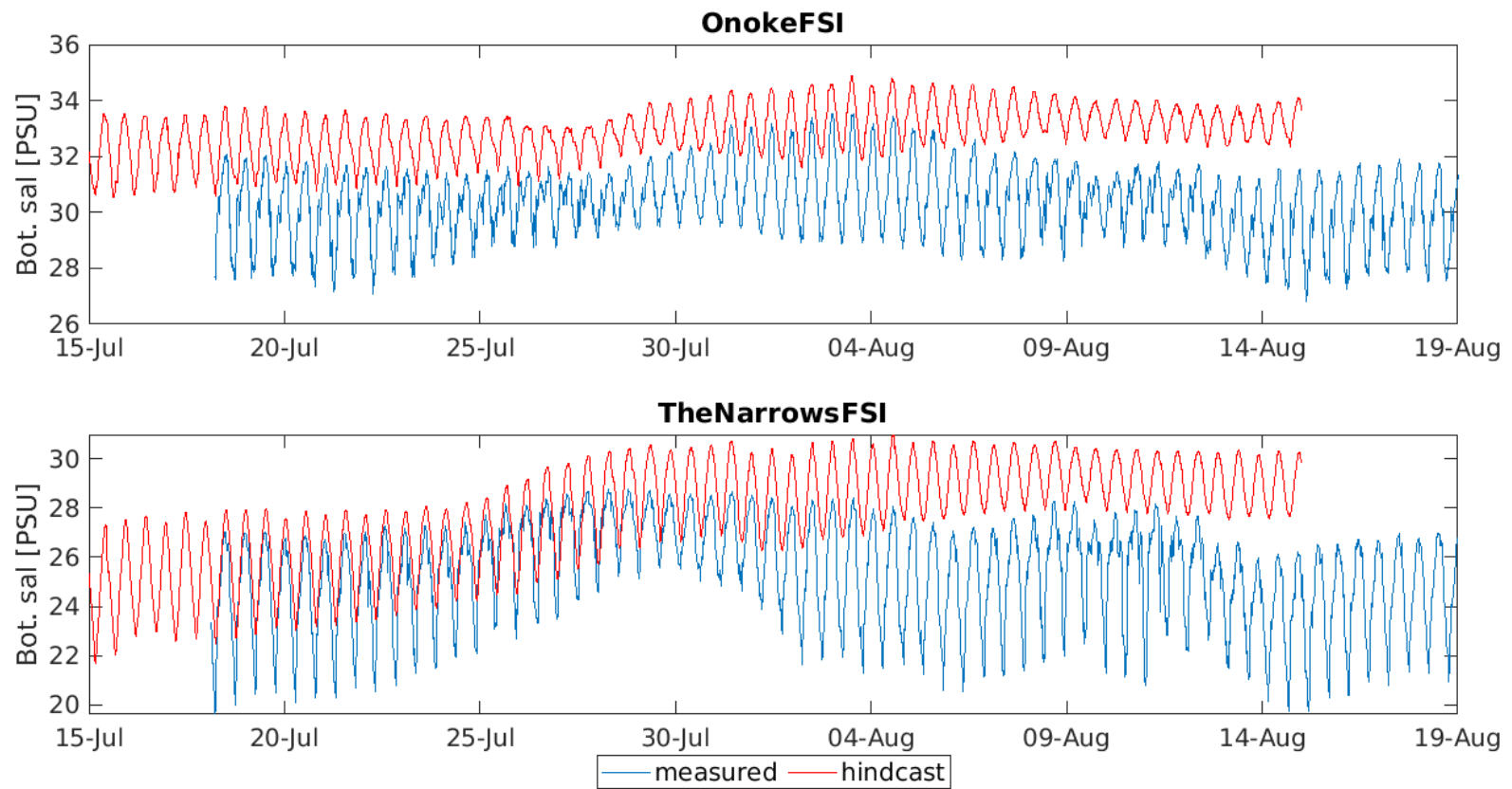


Figure 5.12 Comparison of bottom temperature measured (blue) and modelled (red) at Onoke and The Narrows sites by the FSI sensors during July 2019 to August 2019



5.2 Model results

Surface and bottom velocities in Hokianga harbour are represented in Figure 5.13 and Figure 5.14 during ebb and flood tide. The strong difference of flow between the two tides can be seen at the surface and the bottom of the Harbour.

The horizontal temperature and salinity are shown in Figure 5.15.



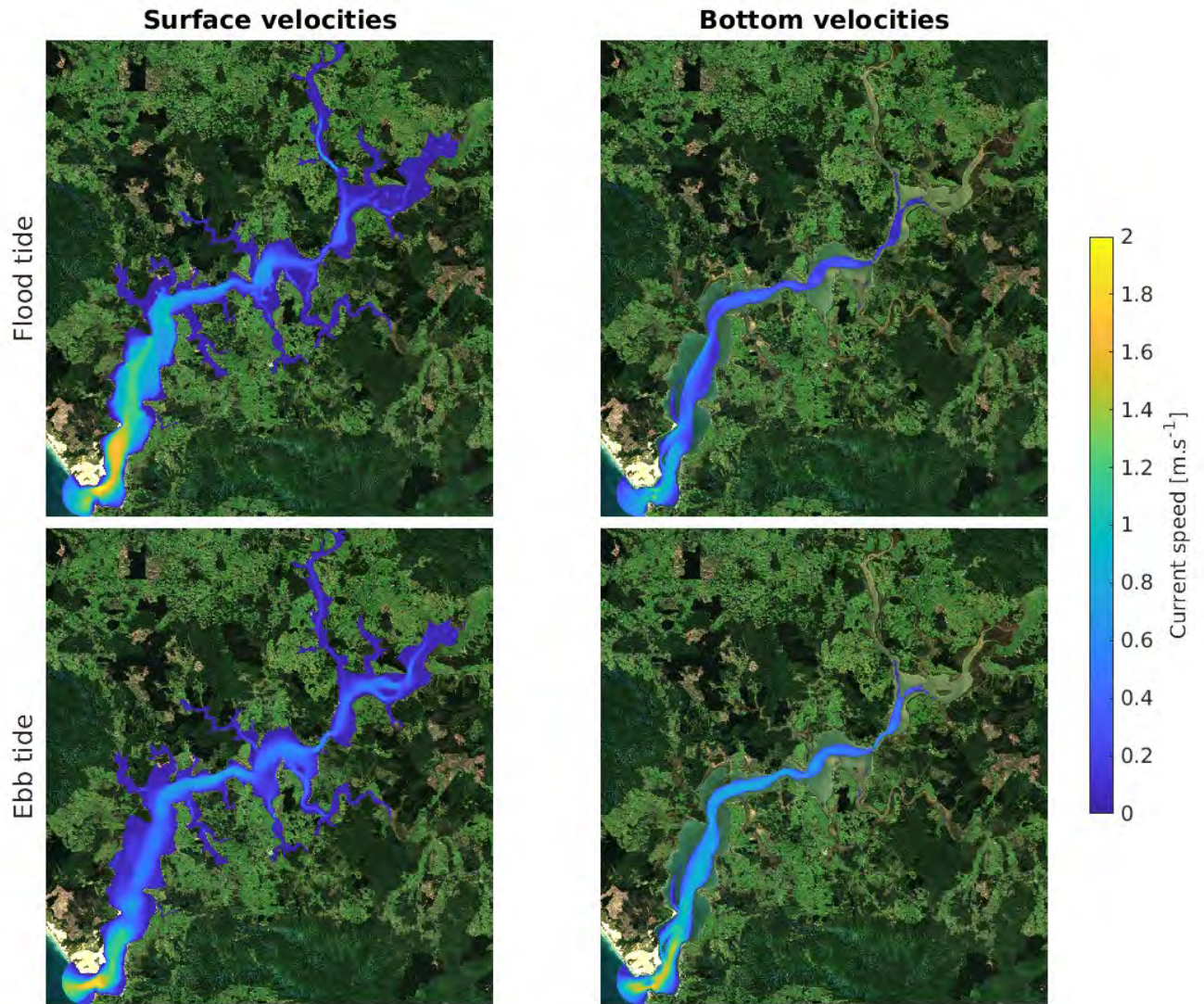


Figure 5.13 Aerial image from Hokianga harbour showing the peak surface (left) and bottom (right) velocities during the flood tide (top) and ebb tide (bottom).

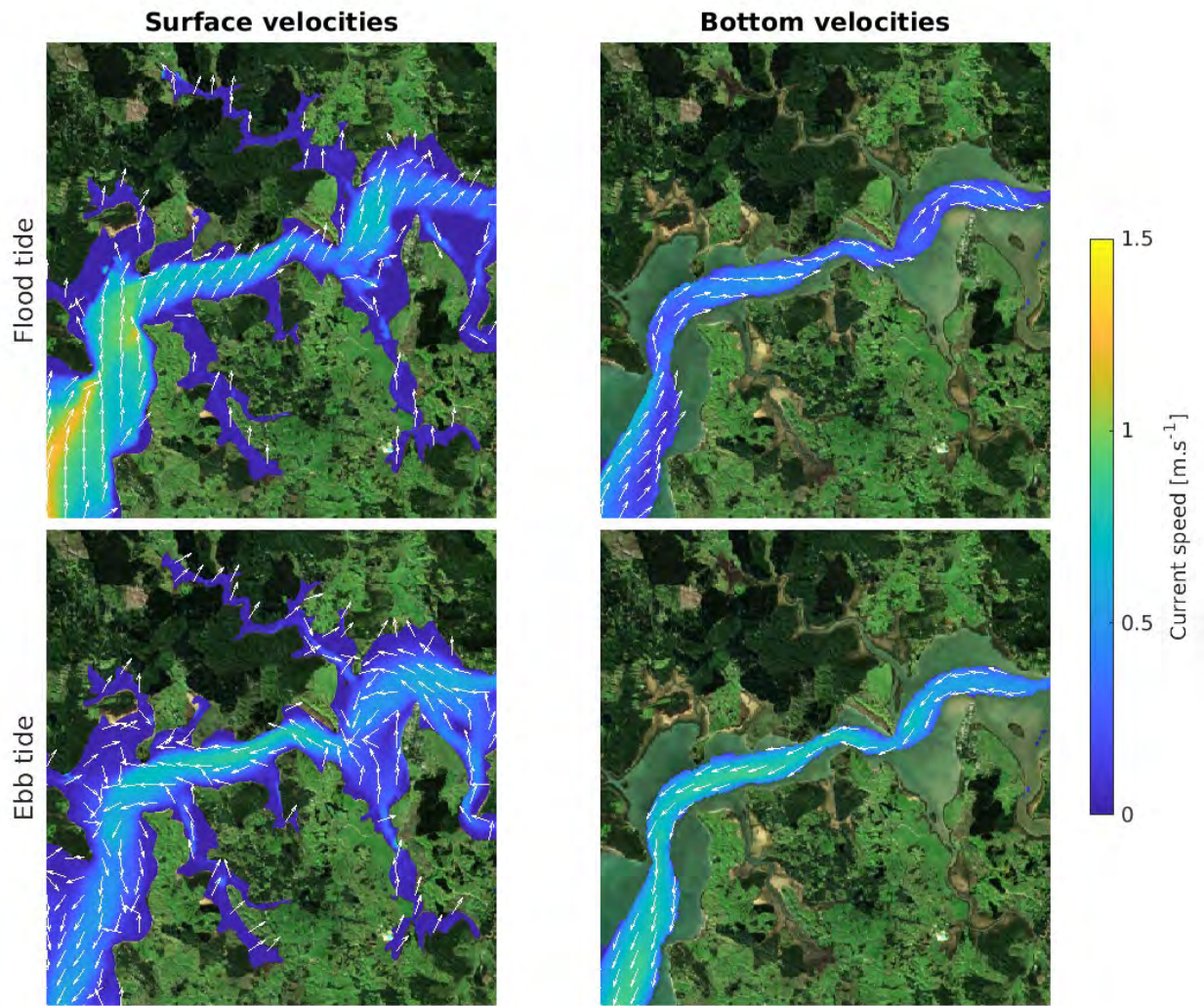


Figure 5.14 Aerial image zoom over Matawhera showing the peak surface (left) and bottom (right) velocities during the flood tide (top) and ebb tide (bottom).

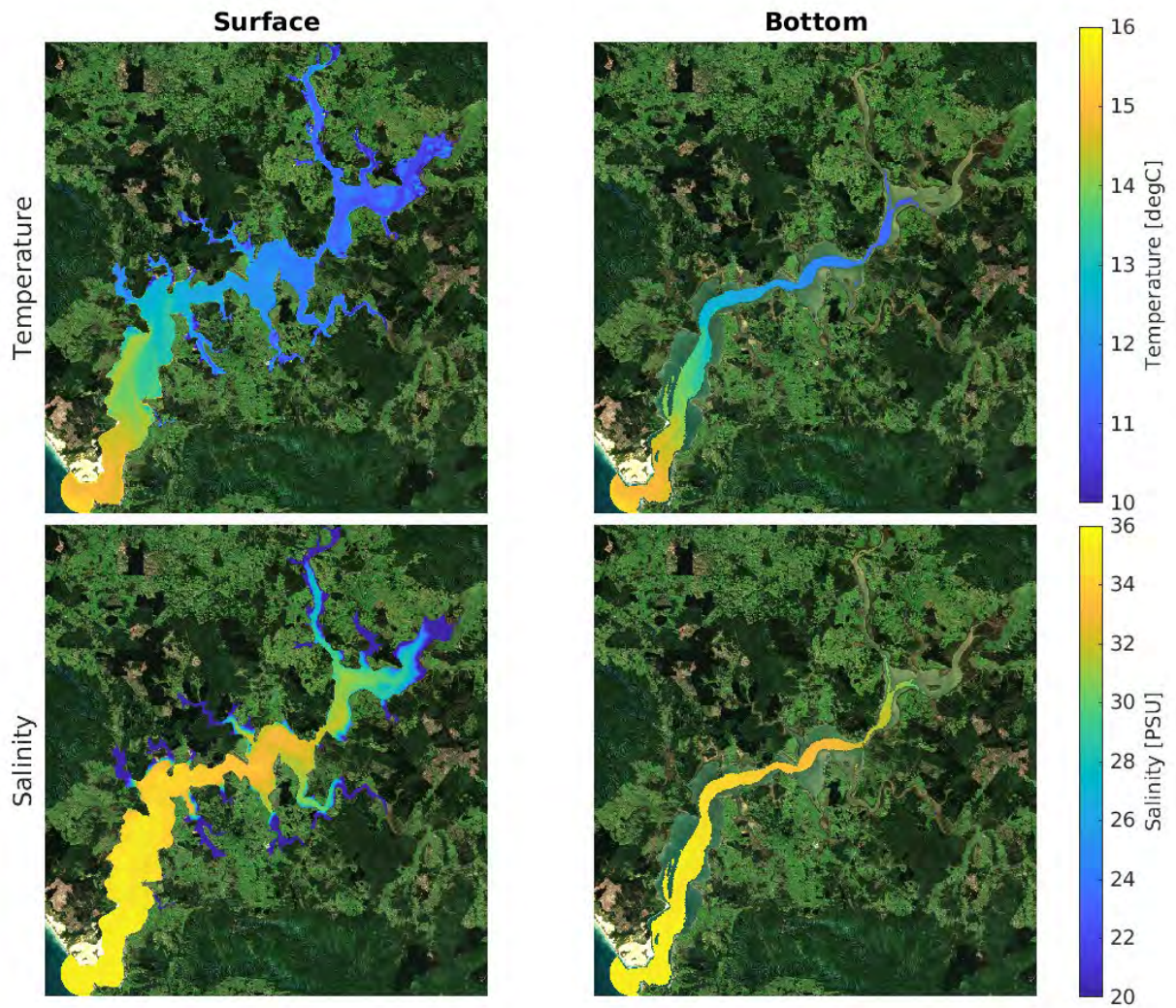


Figure 5.15 Aerial image from Hokianga harbour showing the surface (left) and bottom (right) temperature (top) and salinity (bottom) in July 2015.

5.3 WWTP Discharge Simulations

Simulations were undertaken for a full El Nino (July 2015-June 2016) and La Nina (July 2010 to June 2011) years. The WWTP discharges timeseries presented in Figure 4.14 were used together with a nominated tracer concentration of 1mg/L for each WWTP discharge. The model simulation results were processed in terms of dilution factors which were determined by dividing the tracer concentration at any grid point to the discharged concentration. A dilution factor of 1:1000 therefore indicates the contaminant concentration (e.g. Ammoniacal Nitrogen, Total Suspended Solids, Biological Oxygen Demand.) at that location is 1000 times smaller than discharged at the WWTP. Specific contaminant concentration levels at environmental receptors will be determined by consultants doing the QMRA, using concentration ratios and the expected or measured discharged value.

5.3.1 50th Percentile and 95th Percentile Maps

Results are presented in Figure 5.16 to Figure 5.23, in terms of 50th and 95th percentile maps of dilution factor and tracer concentration in mg/L (based on a 1mg/L concentration at the discharge point). The percentiles were calculated using the hourly output from the model over the full year.

The 50th percentile maps present the dilution factors and concentration (in mg/L) expected to be exceeded 50% of the time.

The 95th percentile maps present the dilution factors and concentration (in mg/L) expected to be exceeded 5% of the time (or not exceeded for 95% of the time).

The 50th and 90th percentile dispersion for each contaminant (e.g. E.coli / Faecal coliforms, Total Suspended Solids, Biological Oxygen Demand, Total Ammoniacal Nitrogen) can be visually estimated by multiplying the concentration seen on the maps by the expected concentration to be discharged or the Consent limit. However, it should be noted that the contaminants estimate may be conservative as no decay was considered for the passive tracer used in the simulations.

The results show dilution factors for the combination of all the four discharges together, which illustrate the potential cumulative effects of all discharges (Note: They assume that the same tracer concentration is being released simultaneously at each WWTP). The 50th and 95th percentile maps of dilution factor and tracer concentration in mg/L (based on a 1mg/L concentration at the discharge point) for the four WWTP combined are presented in Figure 5.24 and Figure 5.25.



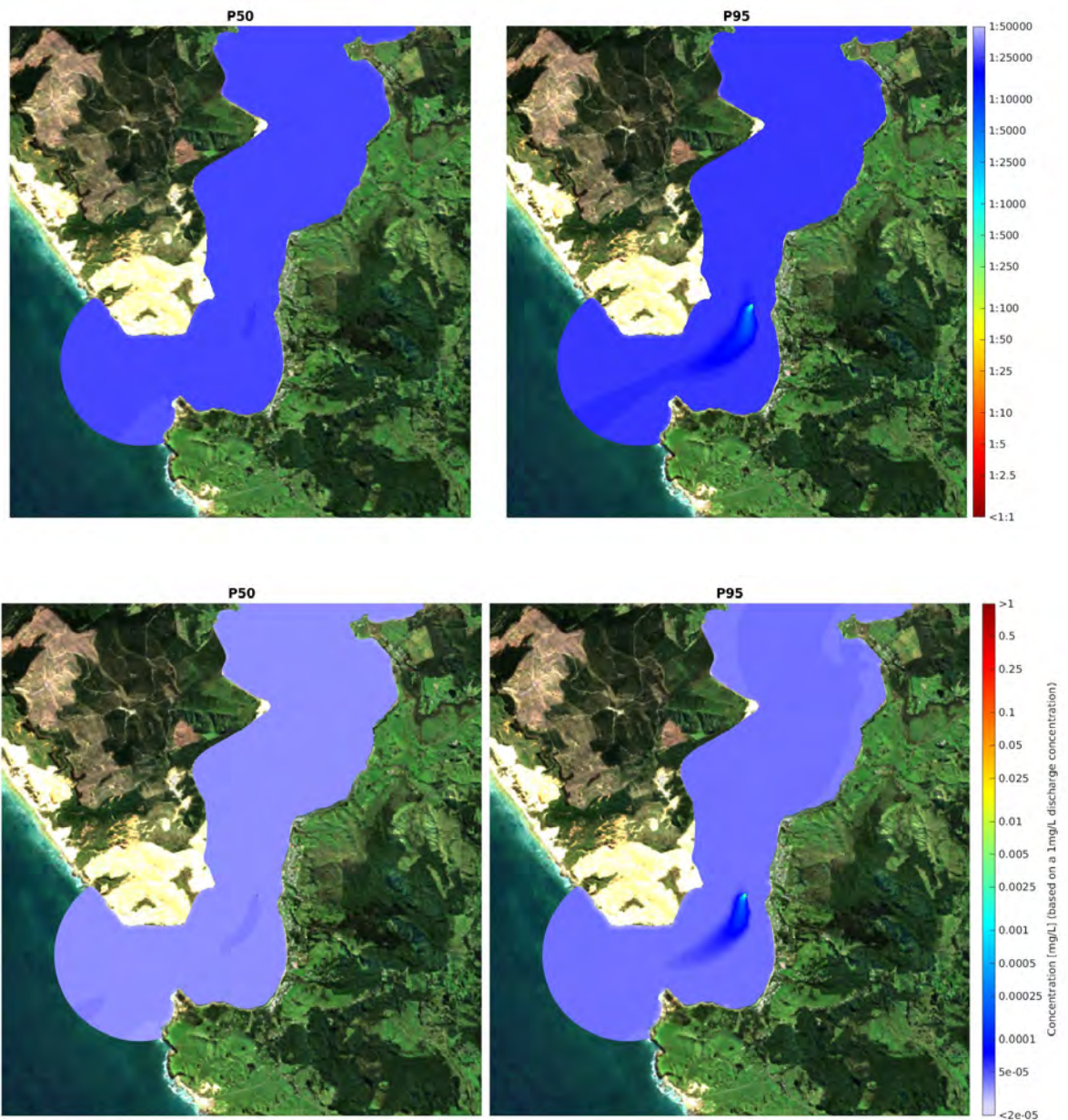


Figure 5.16 50th Percentile and 95th Percentile Dilution factor (top) and tracer concentration in mg/L (bottom) for Opononi WWTP during El Niño year



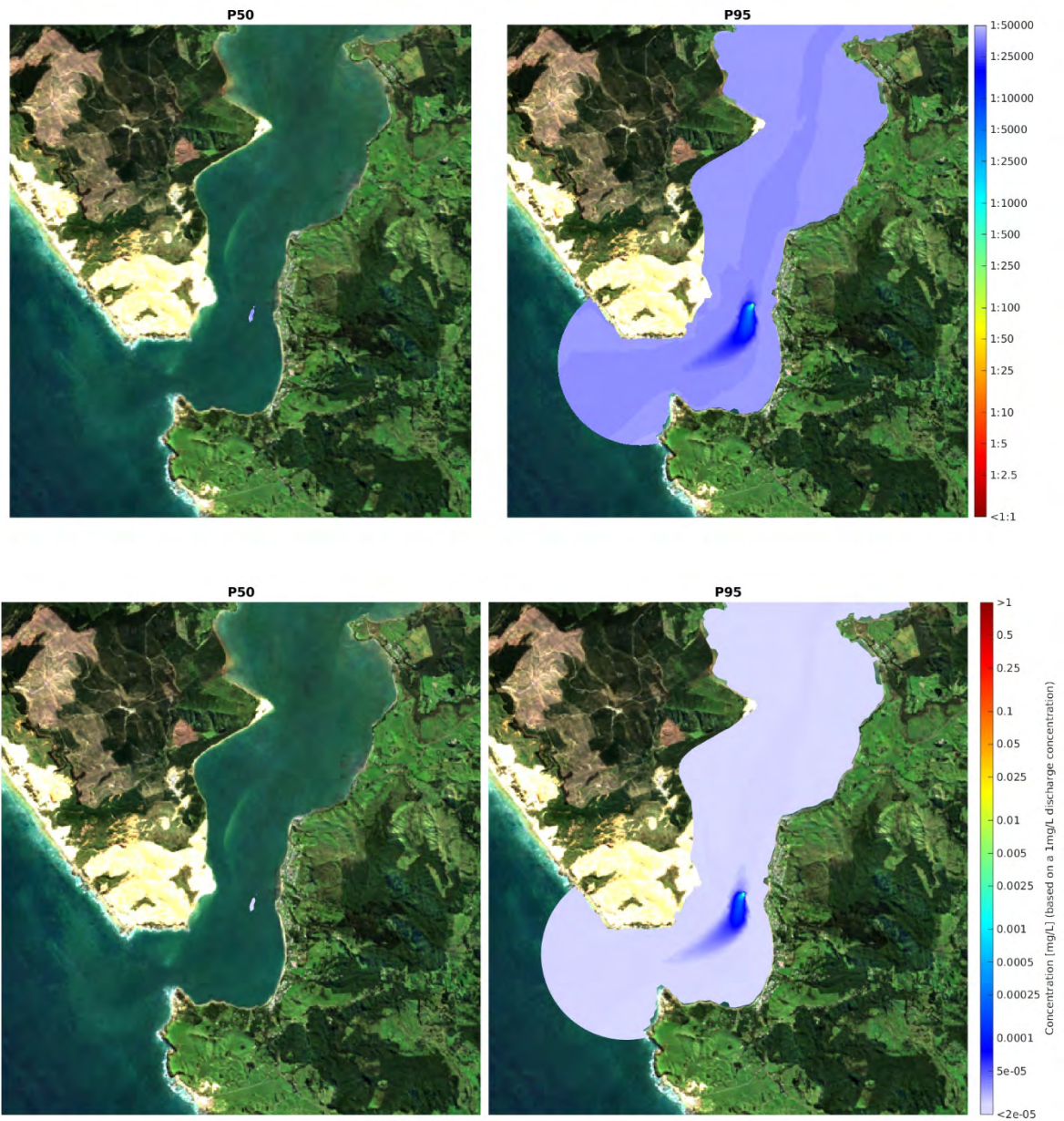


Figure 5.17 50th Percentile and 95th Percentile Dilution factor (top) and tracer concentration in mg/L (bottom) for Opononi WWTP during La Nina year.



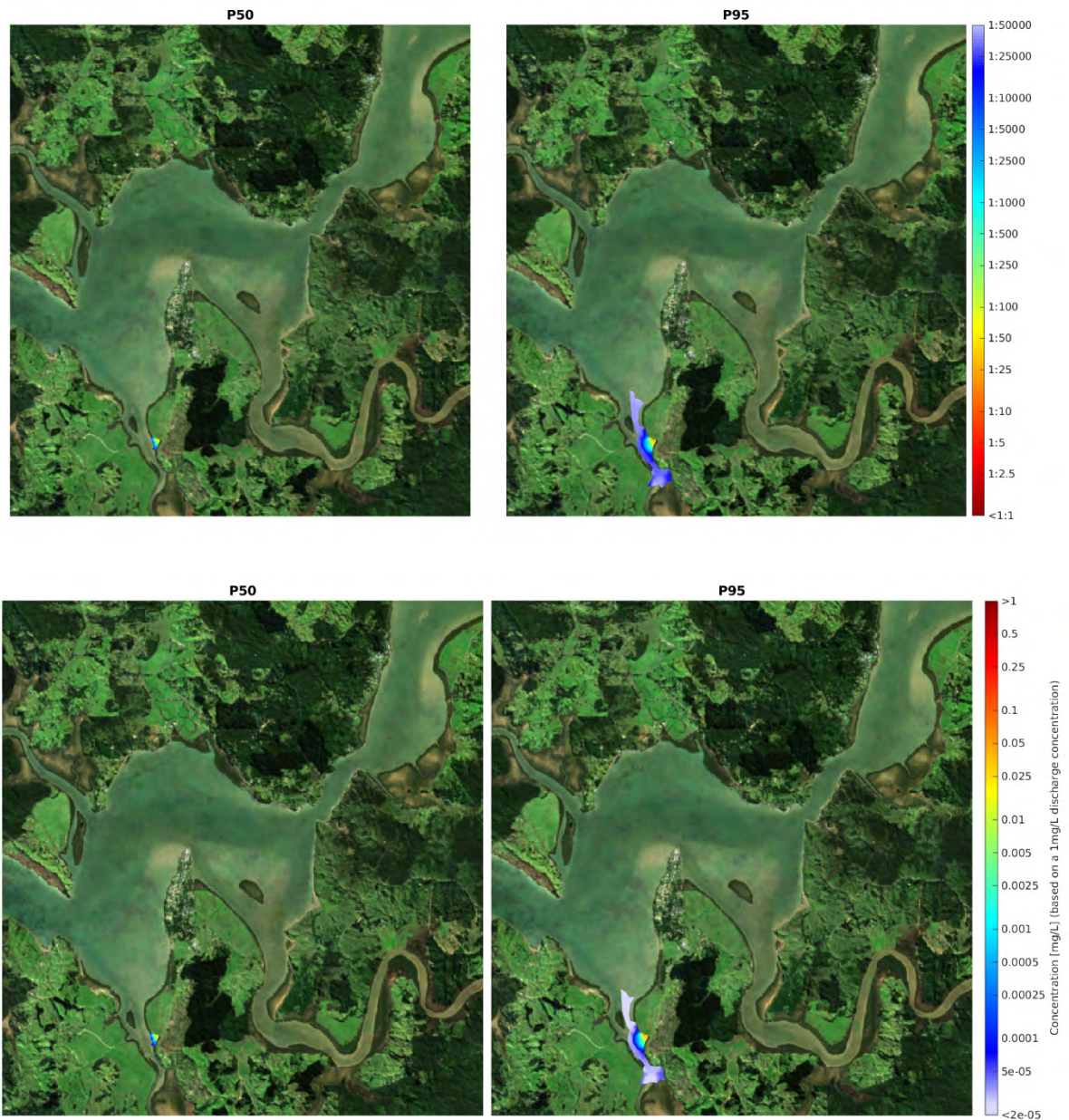


Figure 5.18 50th Percentile and 95th Percentile Dilution factor (top) and tracer concentration in mg/L (bottom) for Rawene WWTP during El Niño year.

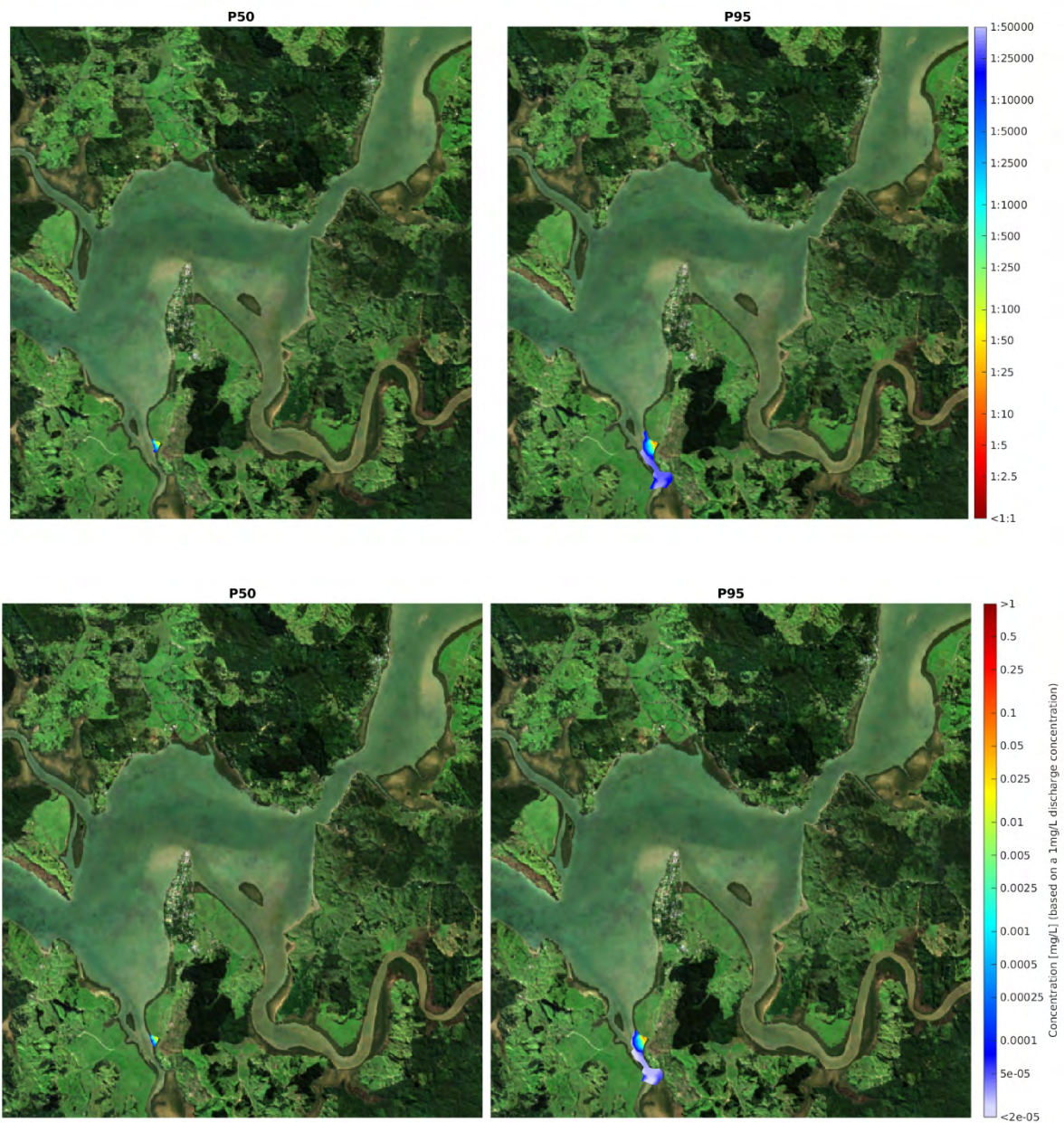


Figure 5.19 50th Percentile and 95th Percentile Dilution factor (top) and tracer concentration in mg/L (bottom) for Rawene WWTP during La Nina year.



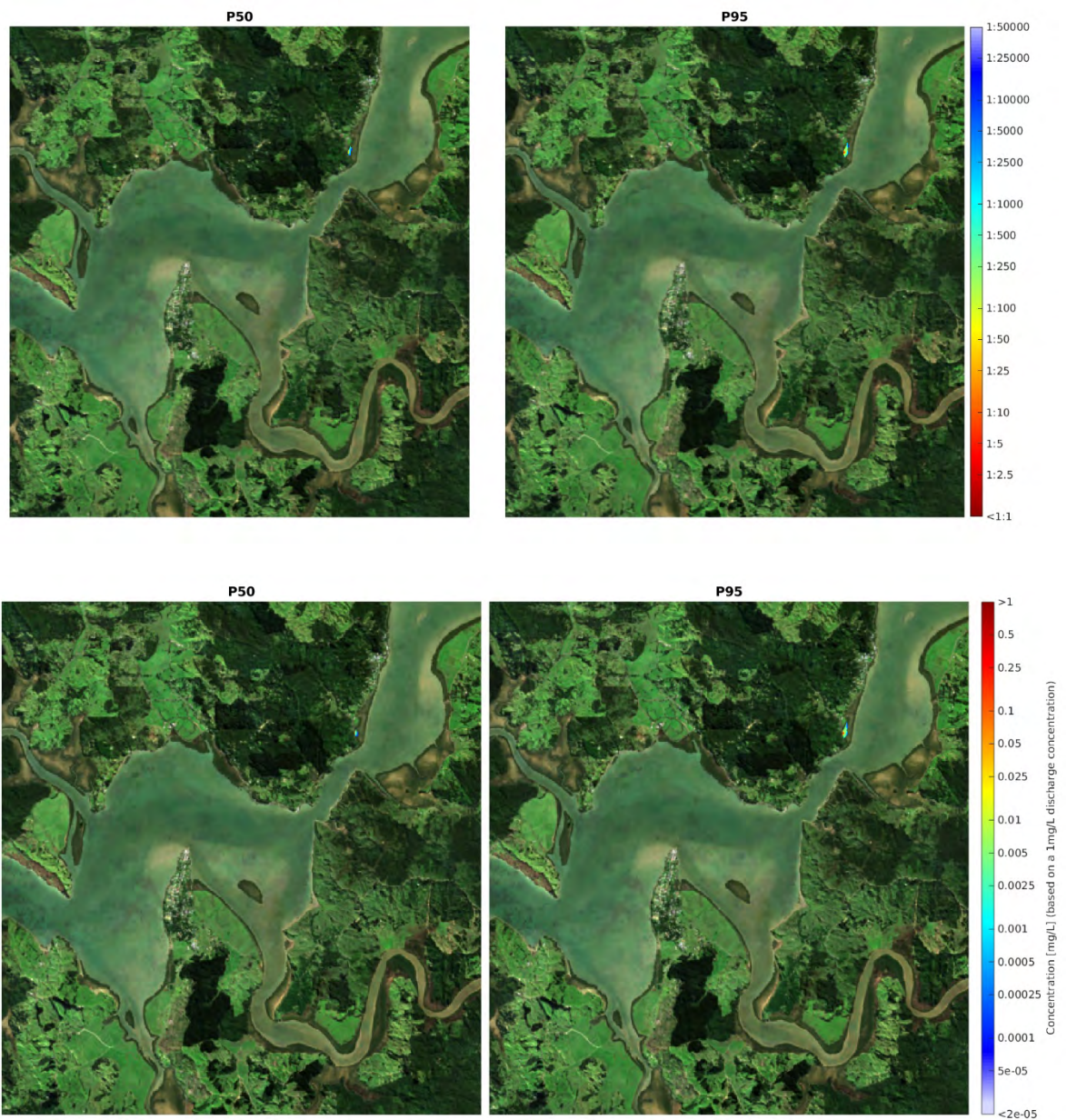


Figure 5.20 50th Percentile and 95th Percentile Dilution factor (top) and tracer concentration in mg/L (bottom) for Kohukohu WWTP during El Niño year.

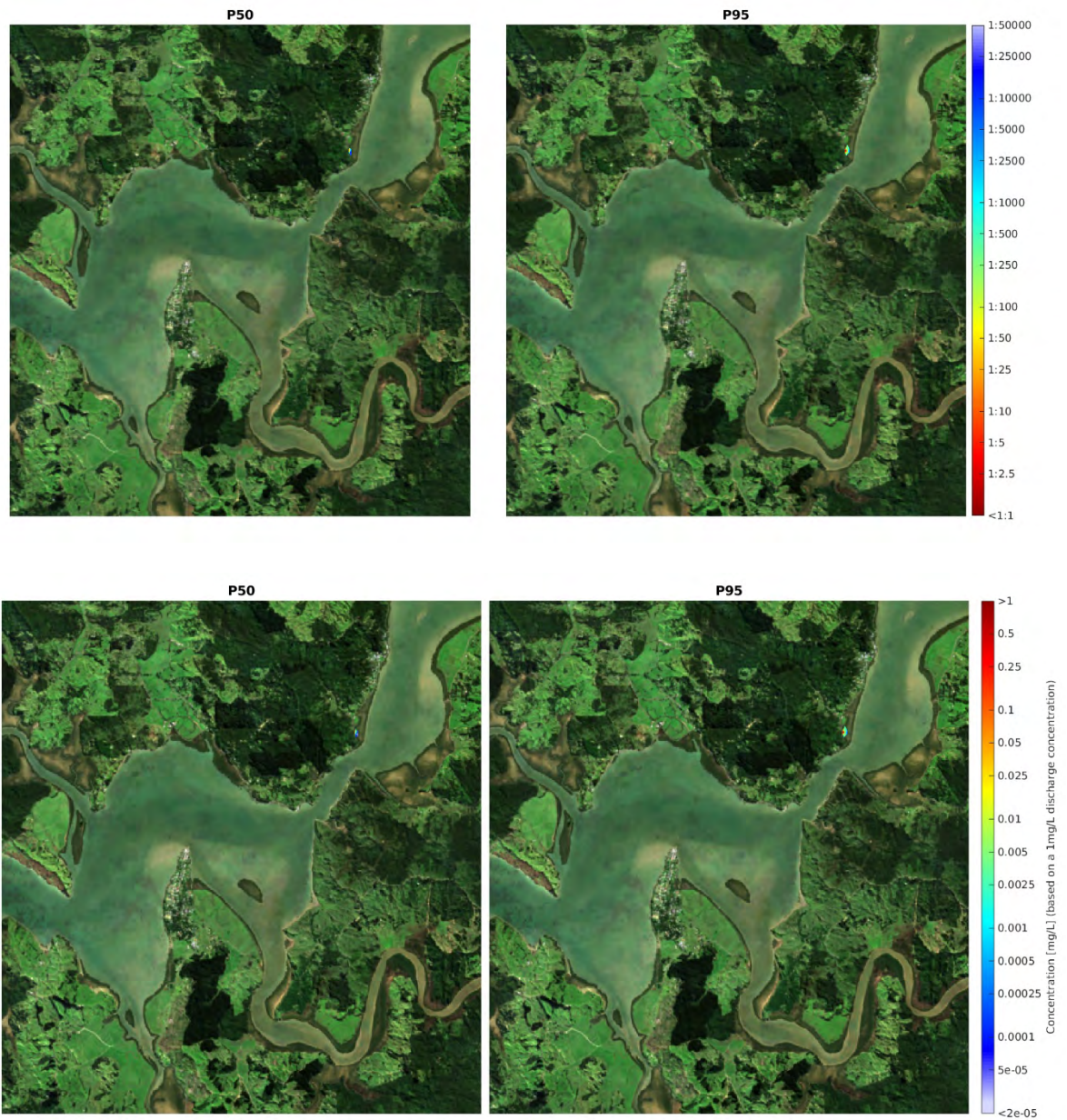


Figure 5.21 50th Percentile and 95th Percentile Dilution factor (top) and tracer concentration in mg/L (bottom) for Kohukohu WWTP during La Nina year.

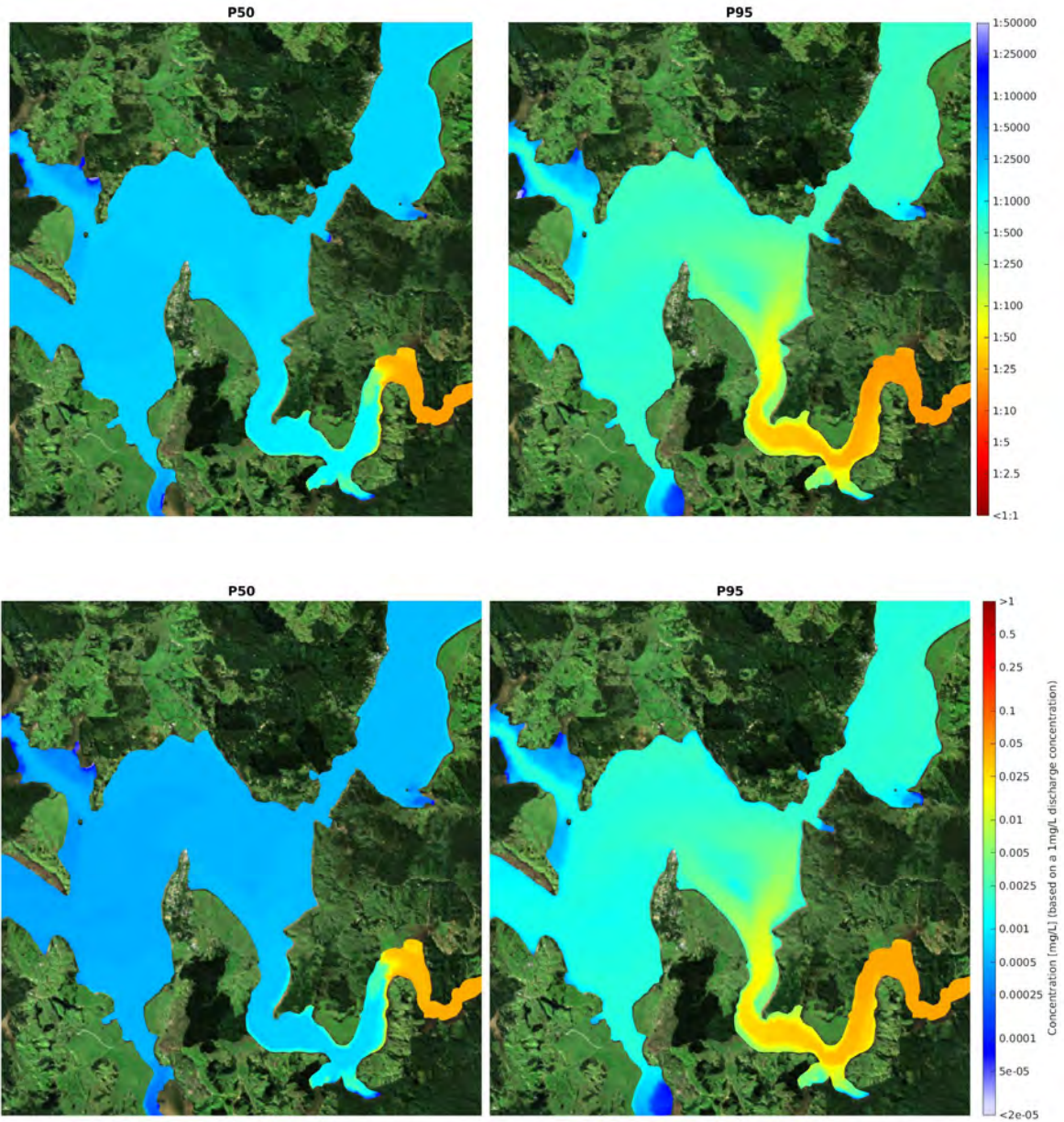


Figure 5.22 50th Percentile and 95th Percentile Dilution factor (top) and tracer concentration in mg/L (bottom) for Kaikohe WWTP during El Niño year.

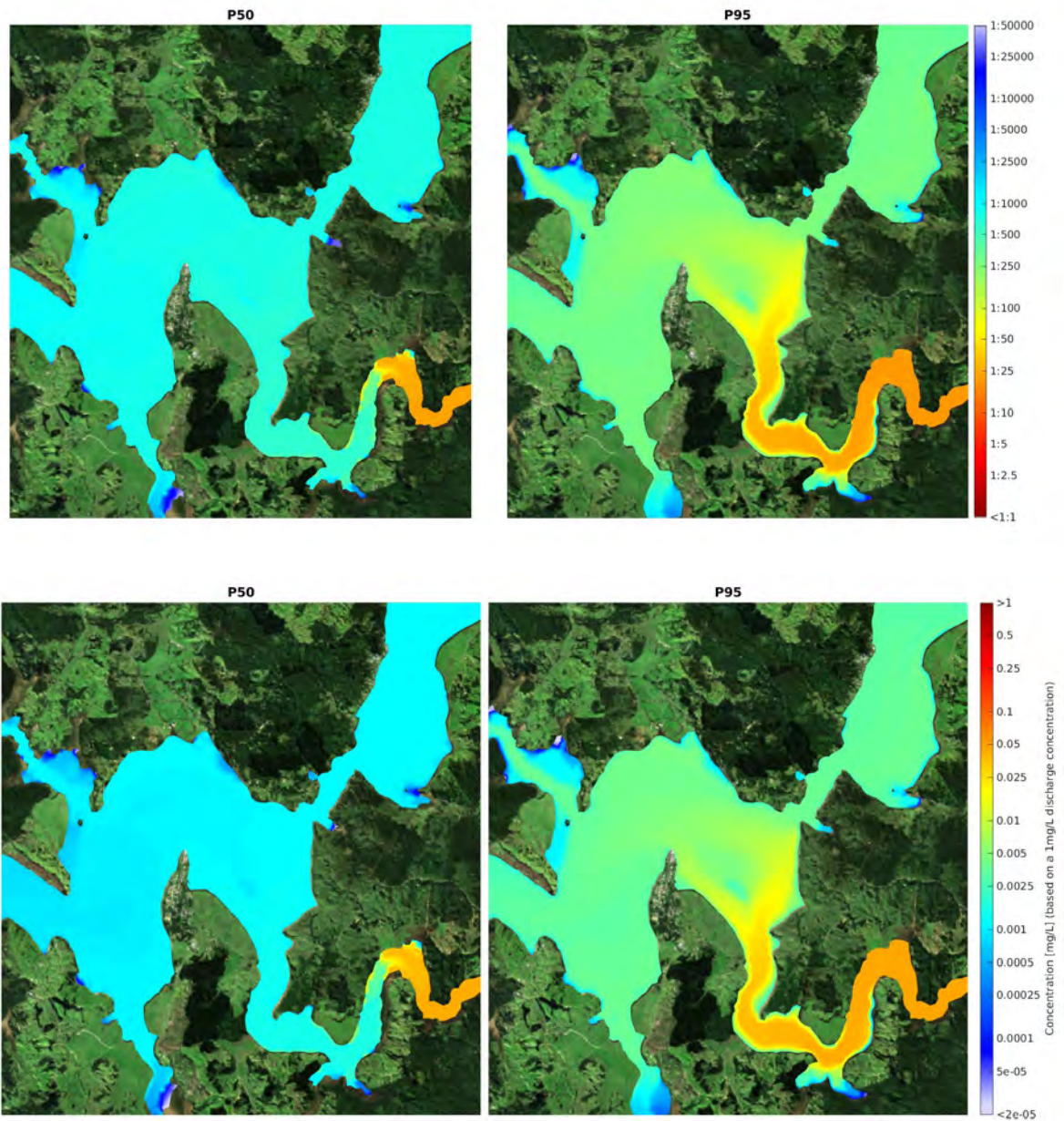


Figure 5.23 50th Percentile and 95th Percentile Dilution factor (top) and tracer concentration in mg/L (bottom) for Kaikohe WWTP during La Nina year.

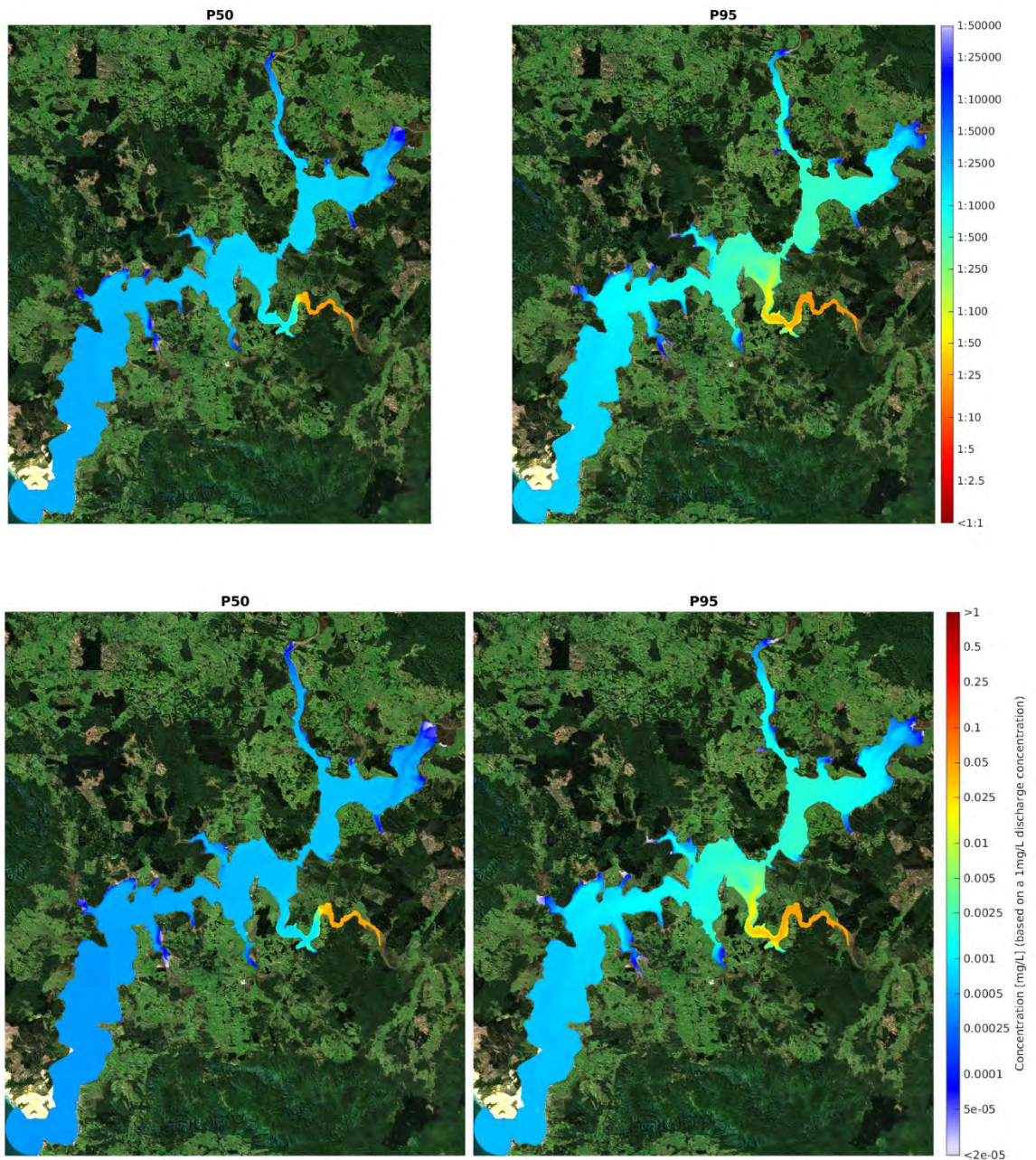


Figure 5.24 50th Percentile and 95th Percentile Dilution factor (top) and tracer concentration in mg/L (bottom) for the four WWTPs combined during El Nino year.



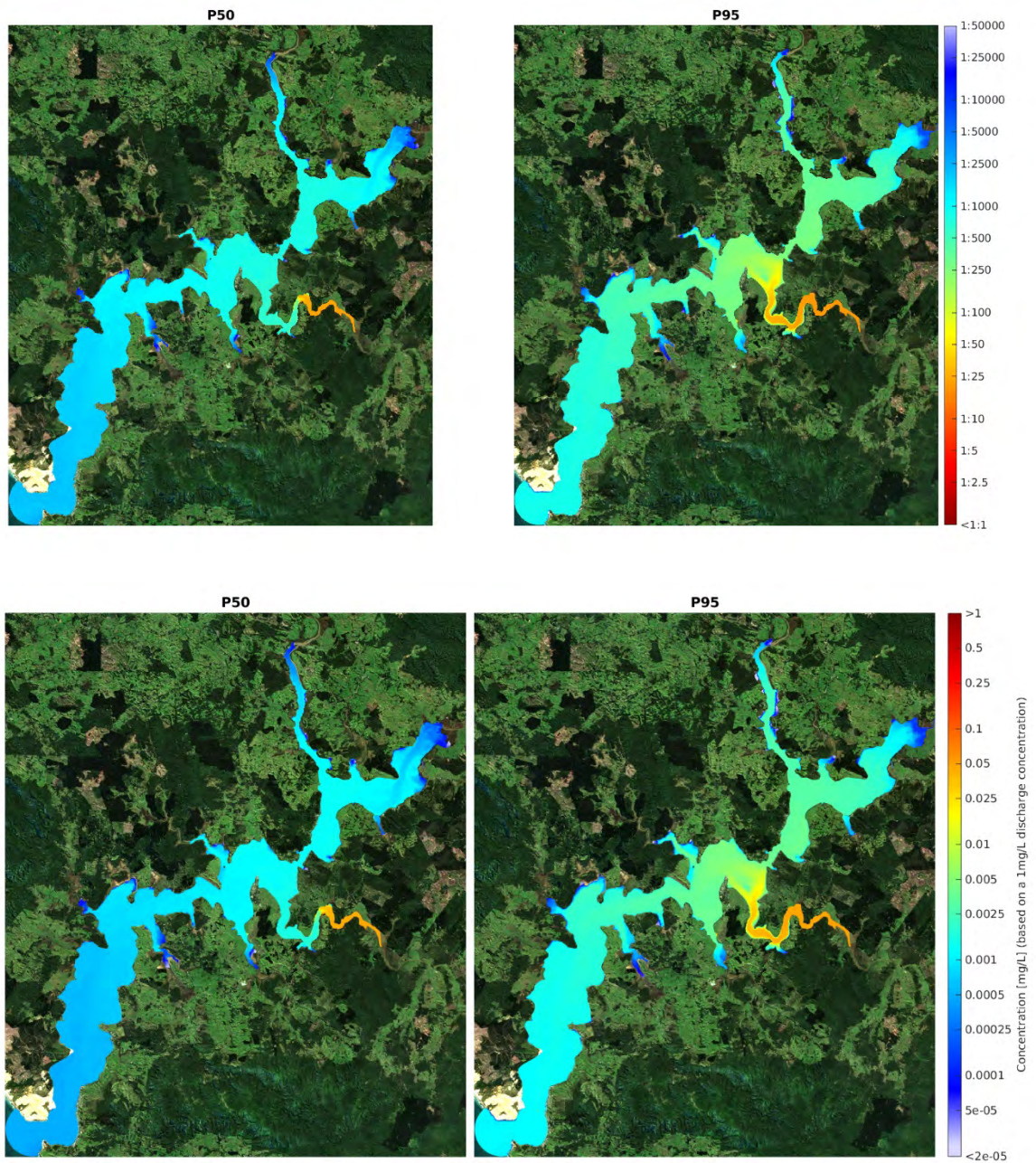


Figure 5.25 50th Percentile and 95th Percentile Dilution factor (top) and tracer concentration in mg/L (bottom) for the four WWTPs combined during La Nina year.



5.3.2 Time Series of dilution

Time-series of tracer concentrations were extracted at selected locations (see Figure 5.26) within Hokianga Harbour. Figure 5.27 to Figure 5.31 presents the time-series tracer concentration in mg/L (based on a 1mg/L concentration at the discharge point) at location P1, P2, P3, CR1 and CR4. Locations near Opononi have been selected following communications with Streamlined Ltd (who is currently undertaking the QMRA for Opononi WWTP) and the timeseries data was provided to them for the assessment.

The concentration for each contaminant (e.g. E.coli / Faecal coliforms, Total Suspended Solids, Biological Oxygen Demand, Total Ammoniacal Nitrogen) can be estimated by multiplying the timeseries concentration by the expected concentration to be discharged or the Consent limit. However, it should be noted that the contaminants estimate may be conservative as no decay was considered for the passive tracer used in the simulations.

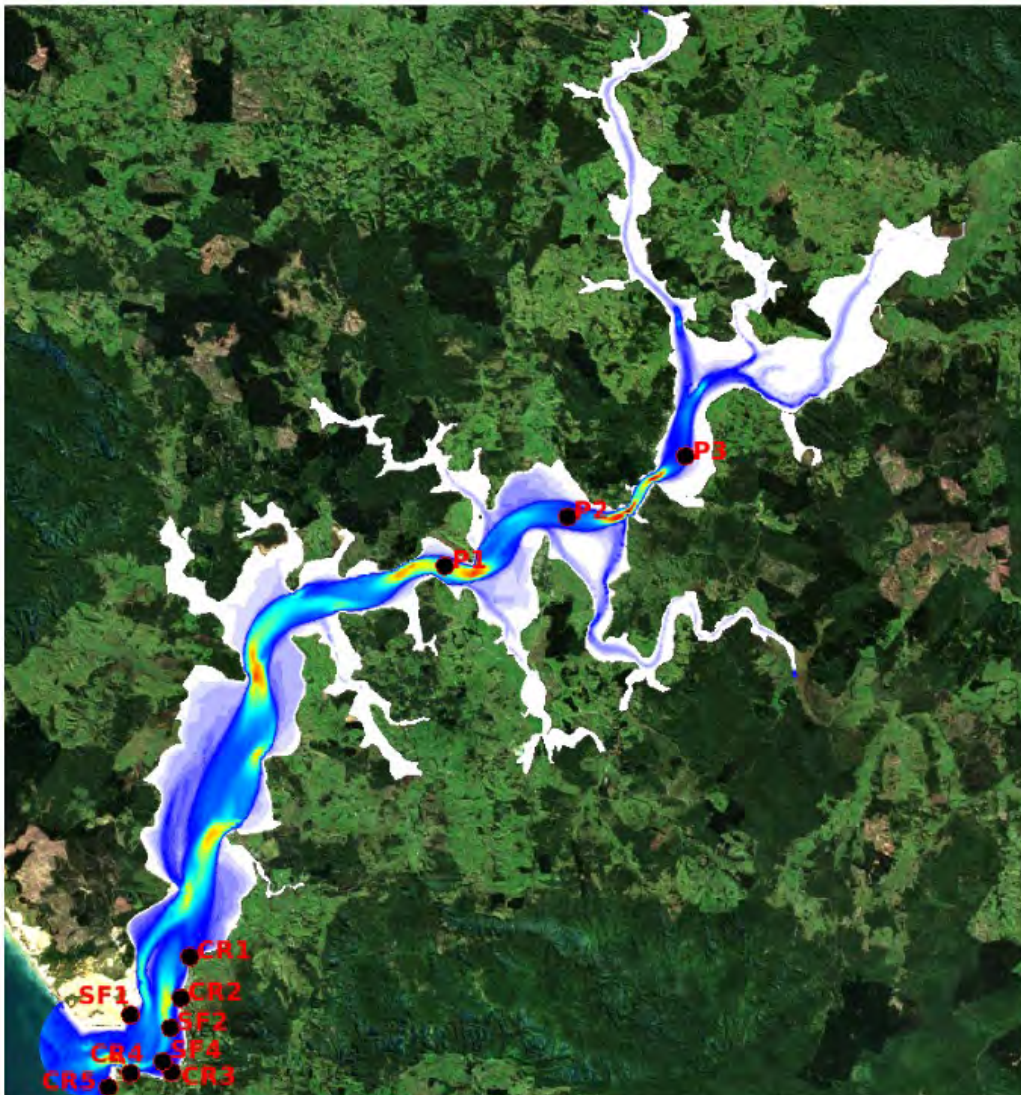


Figure 5.26 Location for tracer concentration timeseries extraction and analysis

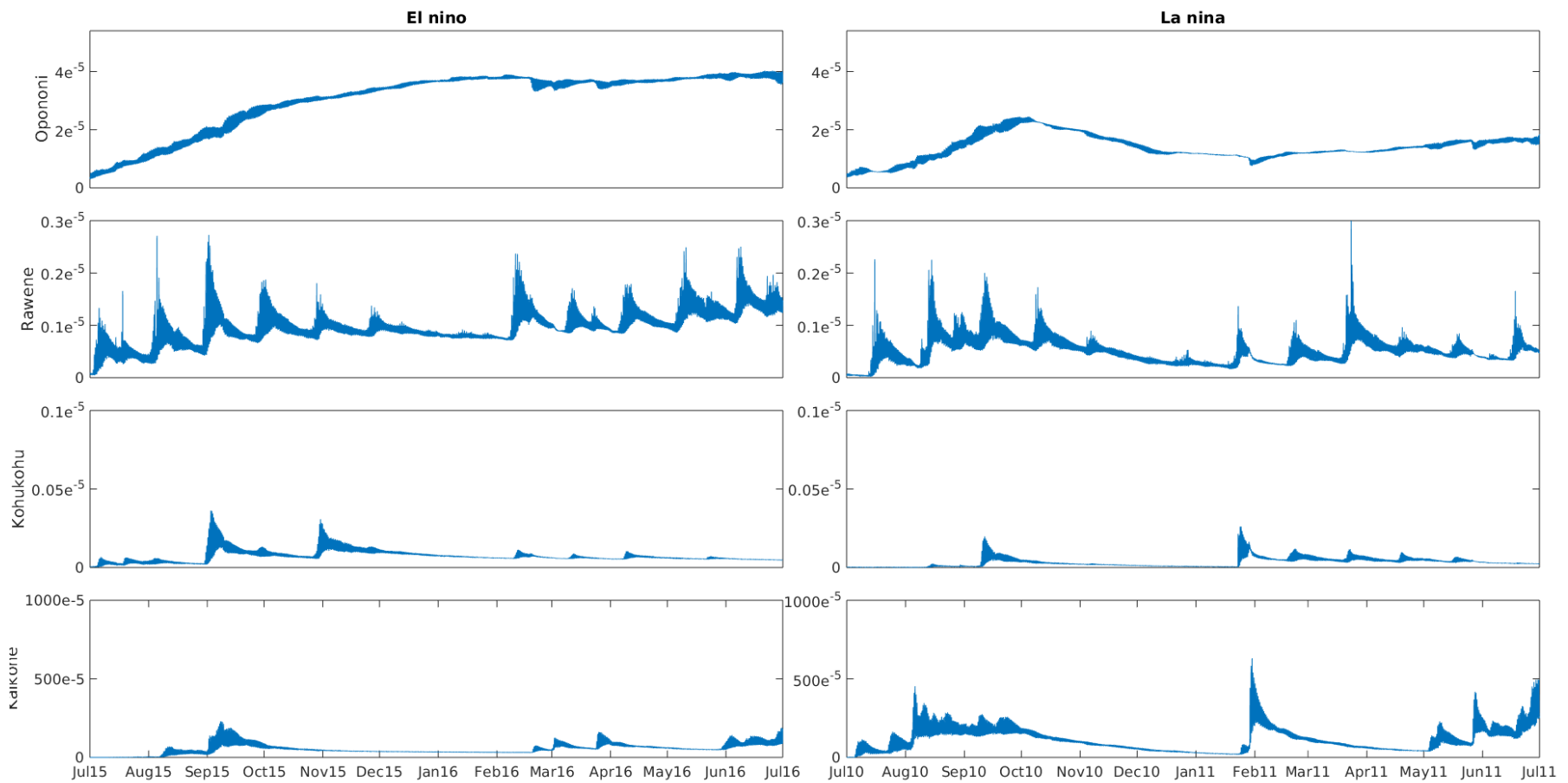


Figure 5.27 Timeseries of tracer concentration in mg/L (based on a 1mg/L concentration at the discharge point) at location P1 for each WWTP discharge for the El Nino and La Nina year simulations.



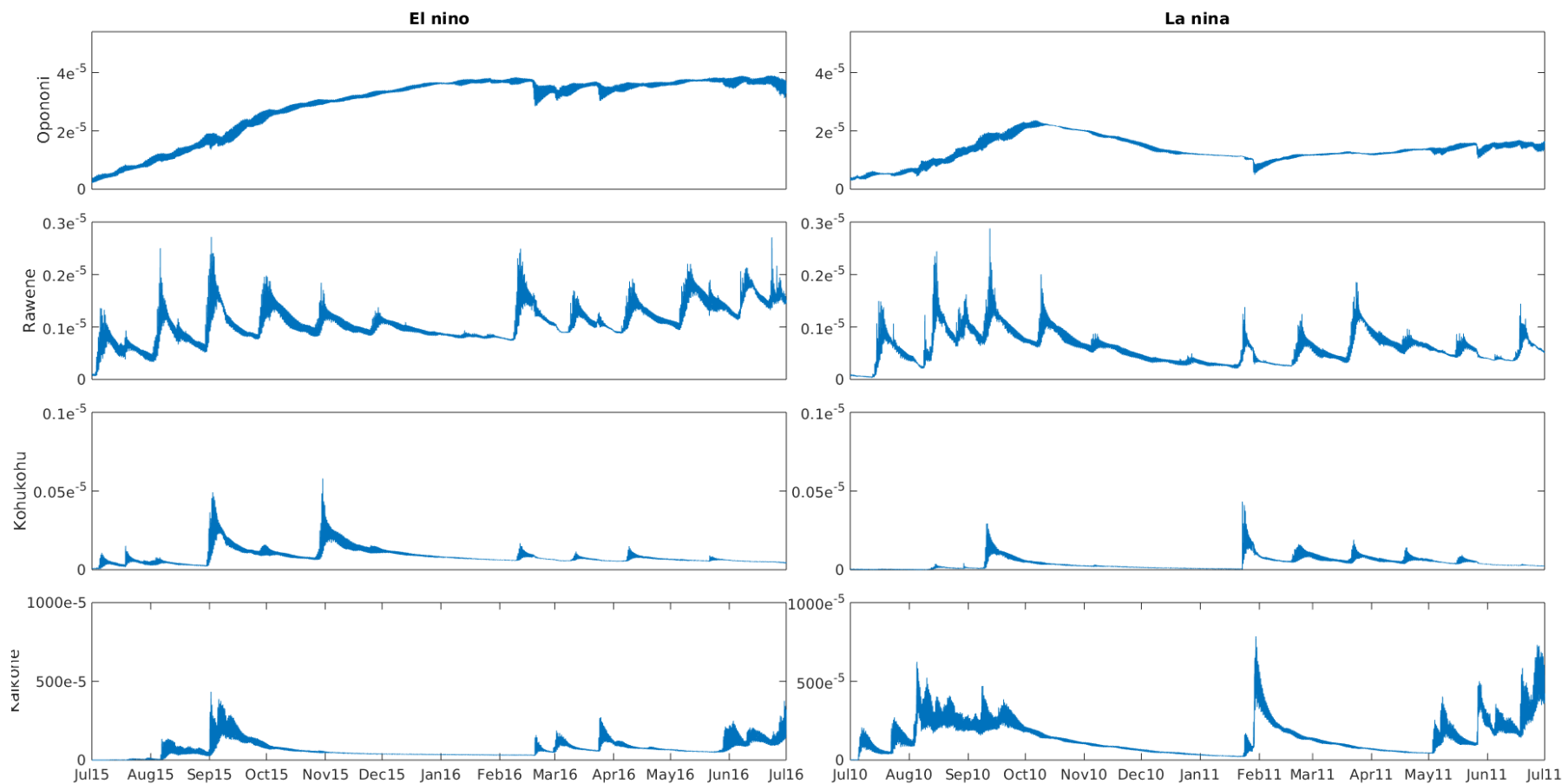


Figure 5.28 Timeseries of tracer concentration in mg/L (based on a 1mg/L concentration at the discharge point) at location P2 for each WWTP discharge for the El Nino and La Nina year simulations.



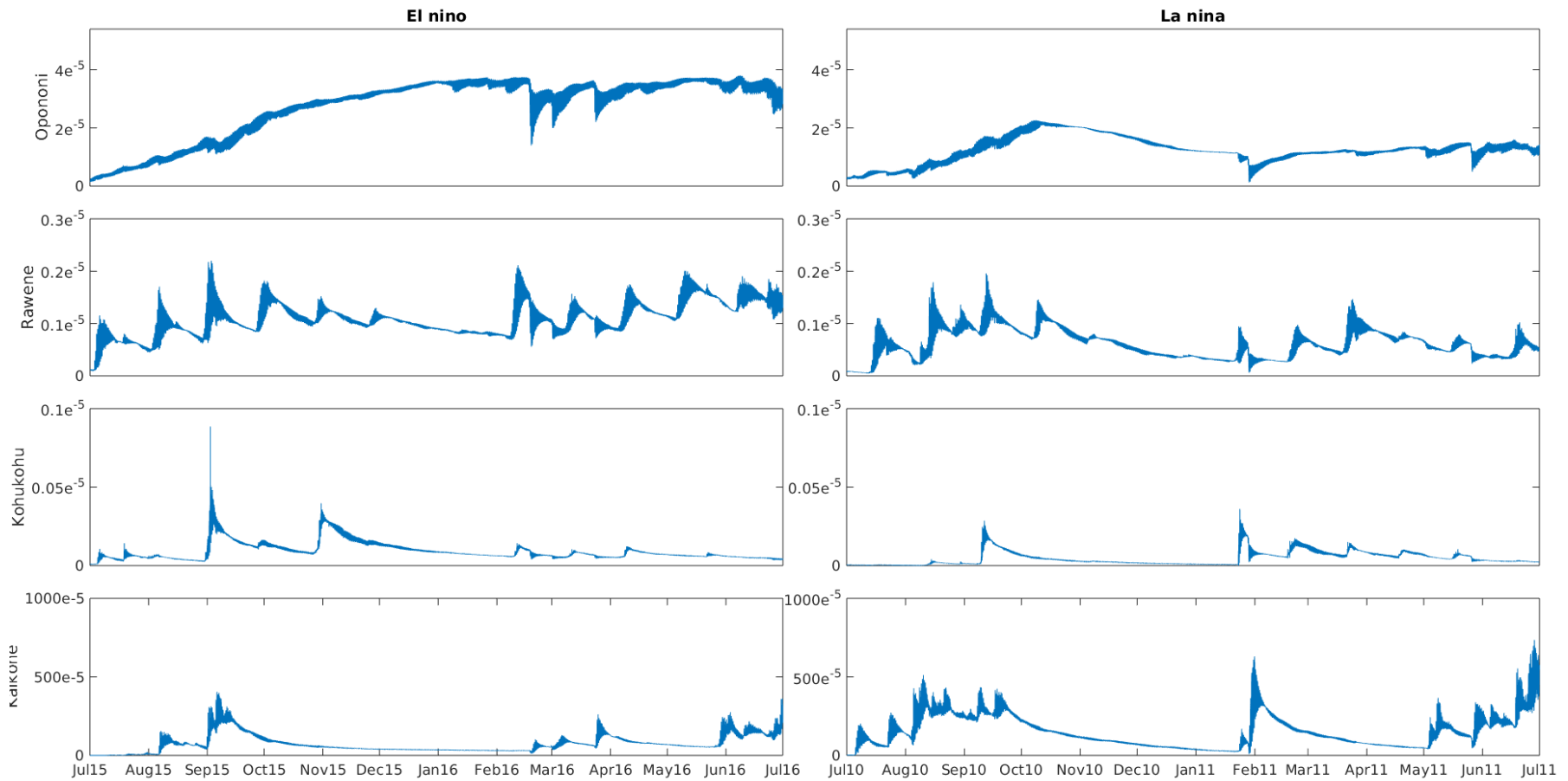


Figure 5.29 Timeseries of tracer concentration in mg/L (based on a 1mg/L concentration at the discharge point) at location P3 for each WWTP discharge for the El Nino and La Nina year simulations.



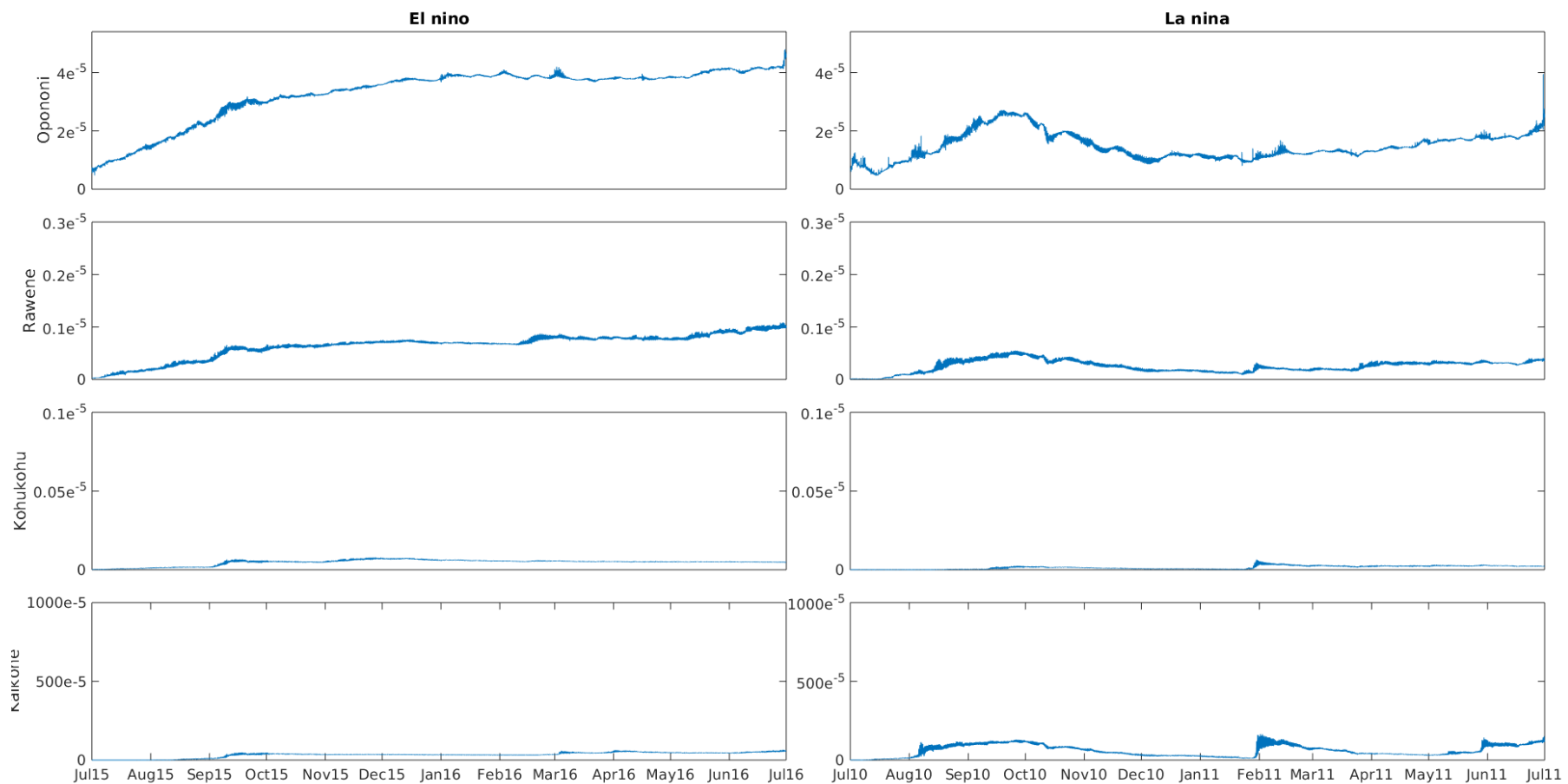


Figure 5.30 Timeseries of tracer concentration in mg/L (based on a 1mg/L concentration at the discharge point) at location CR1 for each WWTP discharge for the El Nino and La Nina year simulations.



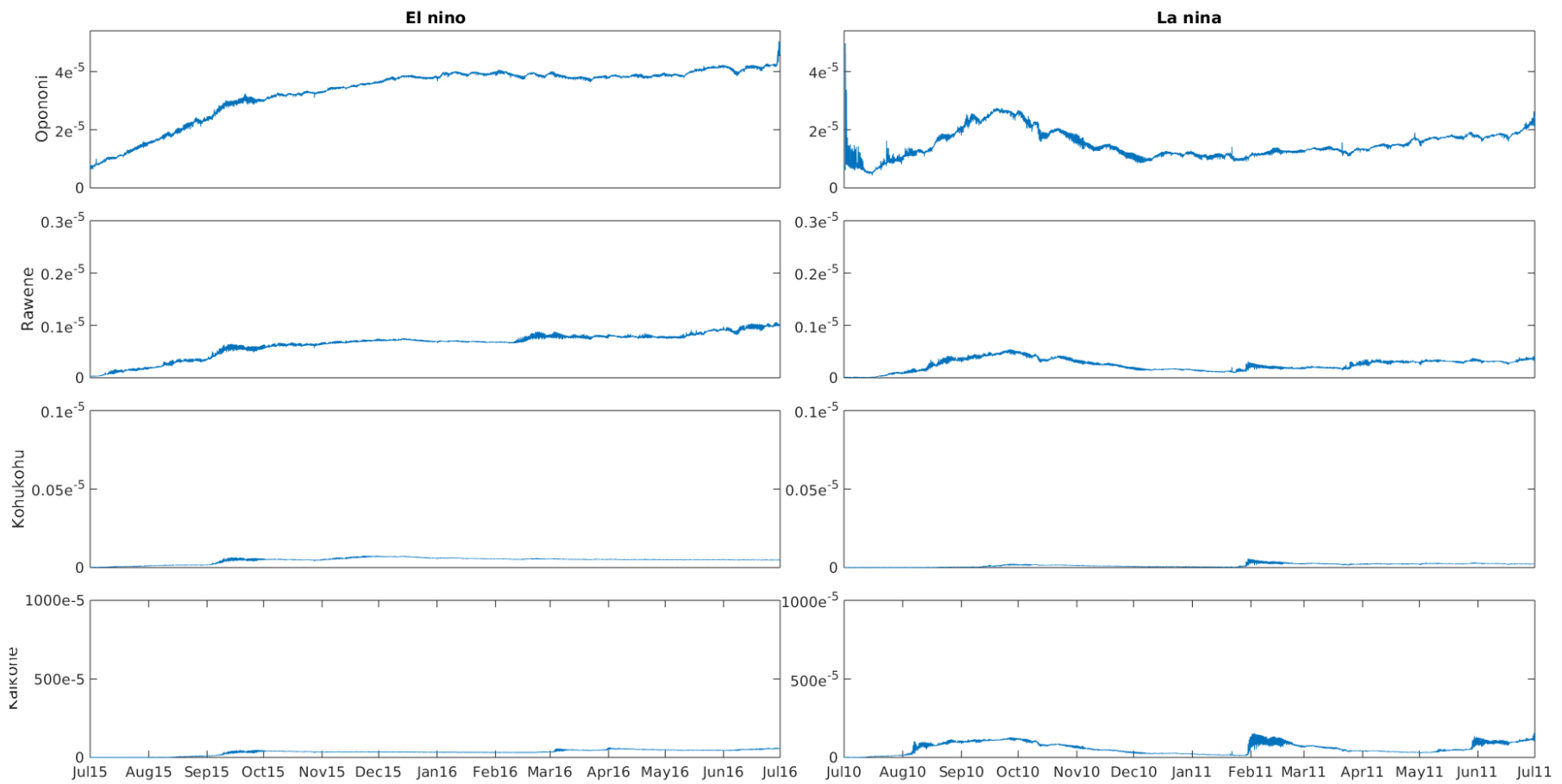


Figure 5.31 Timeseries of tracer concentration in mg/L (based on a 1 mg/L concentration at the discharge point) at location CR4 for each WWTP discharge for the El Nino and La Nina year simulations.



5.3.3 Discussion

Opononi WWTP :

The modelled discharge at the Opononi WWTP typically varied from approximately 100 m³/day to the proposed limit of 450 m³/day . Results show that the dilution factor is about 1 in 25,000 near the discharge for the 50th percentile and about 1 in 1000 for the 95th percentile for both El Nino and La Nina. The plume followed the tidal currents and mostly extended toward the entrance of the harbour with a dilution of 1 in 5,000 at about 750m for El Nino and 500m for La Nina. Near the shoreline the dilution is about 1 in 25,000 or more.

Rawene WWTP :

The modelled discharge at the Opononi WWTP typically varied from approximately 50 m³/day to the proposed limit of 254 m³/day. Results show that the plume is mostly contained within the Omanaia River and dilution factor at about 100 m from the discharge is about 1 in 5,000 near for the 50th percentile (El Nino and La Nina) and about 1 in 500 for the 95th percentile and 1 in 1000 for the 95th percentile. The plume mostly extended north and south, with a 95th percentile dilution of 1 in 50,000 at about 1000 m (El Nino) and 300 m (La Nina) towards the north and about 700 m towards the south for both El Nino and La Nina.

Kohukohu WWTP :

The modelled discharge at the Kohukohu WWTP typically varied from approximately 2 m³/day to the proposed limit of 40 m³/day . Results show that the plume is mostly confined to the vicinity of the discharge location with a dilution factor of 1 in 50,000 at approx. 50 m and 100 m for the 50th percentile and 95th percentile respectively.

Kaikohe WWTP :

The modelled discharge at the Kaikohe WWTP typically varied from approximately 500 m³/day to the proposed limit of 1710 m³/day. As discussed previously more than 30 km upstream of the Waima River connection to Hokianga Harbour. The WWTP contaminant concentration gets diluted as it flows from Kaikohe to the harbour due to the little tributaries joining along the stream.

Results show that the 50th percentile dilution factor is about 1 in 25 up to 1000 m upstream of the Motukiore Road within the Waima River. Dilution then increase to about 1 in 2500 as it reaches the harbour near Rawene.



Dilution factor for the 95th percentile is about 1 in 25 as far as the 'Y' junction where the Waima River connect to the harbour. Near Rawene the dilution is about 1 in 100.

Results are similar for both El Nino and La Nina with a slight increase in dilution during El Nino.



6. Conclusions

A hydrodynamic modelling study was undertaken to investigate dispersion of four WWTP discharge waters into Hokianga Harbour.

A field measurement campaign was first undertaken by Cawthron Institute and provided the necessary field data for calibration and validation of the hydrodynamic model. Water level and current were measured at four locations within Hokianga Harbour, Omapere, Matawhera, Onoke and The Narrows.

The open-source SCHISM system was setup and used to run high-resolution hydrodynamics and tracer dispersion simulations of the Opononi, Rawene, Kohukohu and Kaikohe WWTP discharge.

Comparisons between the model and measured water elevations show that the model captures the propagation of the tidal wave within the model domain well, including the phasing and amplitudes at various points. Principal model and measured tidal constituents show good agreement.

The shift of the FSI during the deployment period restricted the suitable methods that could be used to separate the total measured velocity into tidal and residual components.

Comparison of the total velocity indicates that the model generally reproduces well the phase and amplitude of tidal flows within the harbour. The stronger ebb tide compared to the flood tide can be seen in the model results.

Comparing the residual component of the velocity shows deviations between the model and in-situ measurements; most of the episodes are correctly reproduced. Interestingly, the model tends to reproduce the direction of change (i.e. velocity increase or decrease) but not always the velocity magnitude.

Overall, the comparisons indicate that the model reproduces the measured velocities, water elevations and salinity to a reasonable degree. In particular, the model appears to robustly reproduce the tidal dynamics in the study region, which makes it fit for the present purpose of producing waste-water studies inside the harbour.

Tracer dispersion simulations were undertaken for a full El Nino and La Nina year. The model simulation results were processed in terms of dilution factors which were determined by dividing the tracer concentration at any grid point to the discharged concentration. Results were presented in terms of the 50th and 95th percentile concentration and dilution factors which consists of a statistical representation of the plume extent.



Timeseries of concentration levels were extracted at selected location within the harbour and provided to consultants undertaking the QMRA.

Results shows that each WWTP discharges present very different plume extents due to their location within the harbour and the actual discharge volumes. Some of the key features for each discharge are:

- The Opononi WWTP discharge presents an elongated plume stretching toward the entrance of Hokianga harbour. Dilution factors for the 50th percentile are as high as 1 in 5000 within 100 m of the discharge.
- The Rawene WWTP discharge plume is mostly contained within the Omanaia River and dilution factors for the 50th percentile are about 1 in 5000 at 100 m from the discharge location
- The Kohukohu WWTP discharge plume is mostly confined to the vicinity of the discharge location with a dilution factor of 1 in 50,000 at approx. 50 m for the 50th percentile.
- The Kaikohe WWTP discharge plume present dilution factors of 1 in 25 within the Waima River as far as downstream as the last bend before Motukiore Road. Dilution is about 1 in 1000 to 1 in 2500 within the harbour.



7. References

- Becker, J. J., D. T. Sandwell, W. H. F. Smith, J. Braud, B. Binder, J. Depner, D. Fabre, et al. 2009. "Global Bathymetry and Elevation Data at 30 Arc Seconds Resolution: SRTM30_PLUS." *Marine Geodesy* 32 (4): 355–371.
- Fairall, C. W., Bradley, E. F., Hare, J. E., Grachev, A. A., and Edson, J. B. 2003. "Bulk Parameterization of Air-Sea Fluxes: Updates and Verification for the COARE Algorithm." *Journal of Climate* 16 (4): 571–91.
- Goda, Y. 2000. *Random Seas and Design of Maritime Structures (Advanced Series on Ocean Engineering)*. Second. Vol. 15. World Scientific.
- Kantha, L. H., and C. A. Clayson. 1994. "An Improved Mixed Layer Model for Geophysical Applications." *Journal of Geophysical Research* 99 (C12): 25235–66.
- Zhang, Y. L., and A. M. Baptista. 2008. "A Semi-Implicit Eulerian-Lagrangian Finite Element Model for Cross-Scale Ocean Circulation." *Ocean Modelling* 21: 71–96.
- Zhang, Yinglong, Eli Ateljevich, Hao-Cheng Yu, Chin Wu, and Jason Yu. 2014. "A New Vertical Coordinate System for a 3D Unstructured-Grid Model." *Ocean Modelling* 85 (November). <https://doi.org/10.1016/j.ocemod.2014.10.003>.



Appendix A: Sub-bottom Profile Survey, Rawene,
Hokianga Harbour (Scantec Ltd)



Technical Report

Sub-bottom Profile Survey, Rawene, Hokianga Harbour

Project: MS971

Client: MetOcean Solutions /
Far North District Council

Location: Rawene, Hokianga Harbour

Date: Aug-Dec 2019

Technical Staff: Matt Watson
Don Molloy
Kirsty Hamlin

Release Date: 20-12-19

CONTENTS

1.0 Introduction

- 1.1 Scope of Survey

2.0 Survey Methodology

- 2.1 Bathymetry Survey
- 2.2 Sub Bottom Profiling

3.0 Results

- 3.1 Bathymetry Survey
- 3.2 Sub Bottom Profiling

4.0 Summary

LIST OF FIGURES

- Figure 1 Hokianga Harbour – SBP (Sub-bottom Profile) Survey Area
- Figure 2 Bathymetry 200kHz
- Figure 3 Bathymetry with aerial photo
- Figure 4 Bathymetry – 3D projection
- Figure 5 Interpretation of depth to bedrock
- Figure 6 Interpretation of depth to bedrock, 3D projection
- Figure 7 Estimate of estuarine mud thickness (SBP)
- Figure 8 Estimate of estuarine mud thickness (SBP) with aerial photo
- Figure 9 SBP Section H3, H5
- Figure 10 SBP Section H6, H10
- Figure 11 SBP Section H11, H13, H19
- Figure 12 SBP Section H12

1.0 Introduction

ScanTec Ltd was requested by MetOcean Solutions to carry out a sub-bottom profile (SBP) survey covering a predefined area of the Hokianga Harbour near Rawene.

The work was carried out on the vessel Sidescan1, and included 3.5kHz, 7kHz SBP measurements and also 200kHz bathymetric sonar.

The coverage area for the survey is shown as Figure 1 (see attached A3 figure sheets).

Site work was carried out during 3 shifts in August and November 2019. Weather conditions were fine, with low wind strength.

2.0 Survey methodology

2.1 Bathymetric Survey

A Knudsen 320M 200kHz single beam echosounder was used to collect bathymetric data, which needs to be collected as part of the SBP dataset to assist in data processing. Sonar equipment was linked to a RTK GPS positional system and TSS DMS-05 dynamic motion sensor.

Data was processed in custom software and bathymetric data generated in SURFER. Digital data is presented as XYZ dat, GRD, and CAD compatible DXF files.

2.2 Sub-Bottom Profiling (SBP)

A Raytheon PTR-106 Sub bottom profiler system and 24bit ADC controller were used for SBP data acquisition. The 3.5kHz and 7kHz transducer was mounted off the side of the vessel. Measurements were synchronized with the Trimble/ Omnistar DGPS data and were recorded at a boat speed of between 1.5knot (confined areas) and 2.5knots. Multiple runs were recorded over some lines using different acquisition settings to obtain optimum results.

The PTR-106 is a high resolution seismic (acoustic) system that transmits a high power (2kW+) 3.5kHz to 7kHz frequency pulse stream into the water which has sufficient energy to penetrate deep into sand and sediment. The sonar equipment is connected to a USB ADC converter to digitise the data in high resolution and store as seismic SEG-Y format.

Data processing

All measurements were processed using processing software, REFLEX-W seismic processing software, RADAN 6.5 and SURFER v13. Data processing involved;

- converting from SEG-Y to SEG2 and DZT format
- high and low pass frequency filtering
- linear gain ramp
- horizontal background removal
- predictive deconvolution

Positional and height datum

Positional and bathymetric data (seabed elevation) are presented in NZTM and NZVD 2016

3.0 Results

3.1 Bathymetric Survey

Results of the Bathymetric survey are shown as figures 1 to 4.

Figure 2 Bathymetry 200kHz
Figure 3 Bathymetry with aerial photo
Figure 4 Bathymetry – 3D projection

3.2 Sub Bottom Profile (SBP) data

The SBP data is presented as the following figures;

Figure 5	Interpretation of depth to bedrock
Figure 6	Interpretation of depth to bedrock, 3D projection
Figure 7	Estimate of estuarine mud thickness (SBP)
Figure 8	Estimate of estuarine mud thickness (SBP) with aerial photo
Figure 9	SBP Section H3, H5
Figure 10	SBP Section H6, H10
Figure 11	SBP Section H11, H13, H19
Figure 12	SBP Section H12

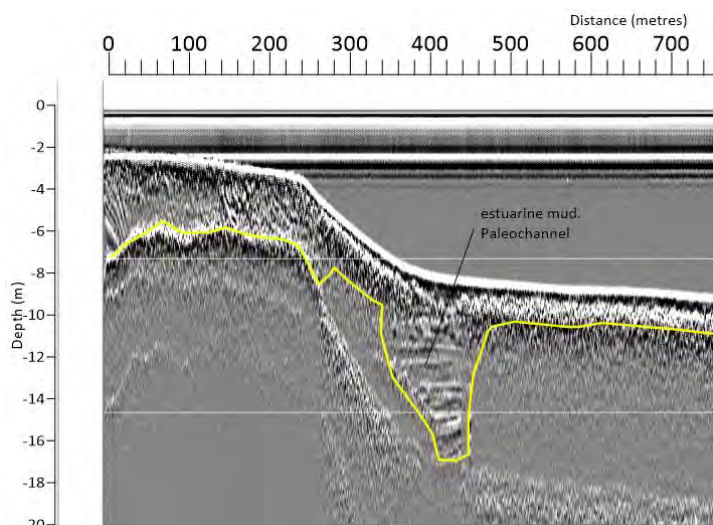
The site geology (GNS QMAP, Kaitaia) indicates alluvial mud deposits overlying moderately indurated mudstone / sandstone (bedrock) of the Mangakahia Complex, which is part of the Northland Allochthon.

The indurated mudstone / sandstone generally provides a strong reflection for the SBP signal, and the top of this formation has been interpreted. Where the reflector is not clearly visible, signal attenuation levels have been used to infer the transition into bedrock. The interpretation of the depth to bedrock is presented as contour maps and 3D surfaces (Figures 5,6).

The estimated thickness of sediment lying above the bedrock is shown as Figures 7,8. Thickness is highly variable over this site, and ranges from with a maximum of approximately 8m alluvial sediment thickness observed in some areas, to zero sediment (ie. exposed bedrock interpreted) due to tidal scouring.

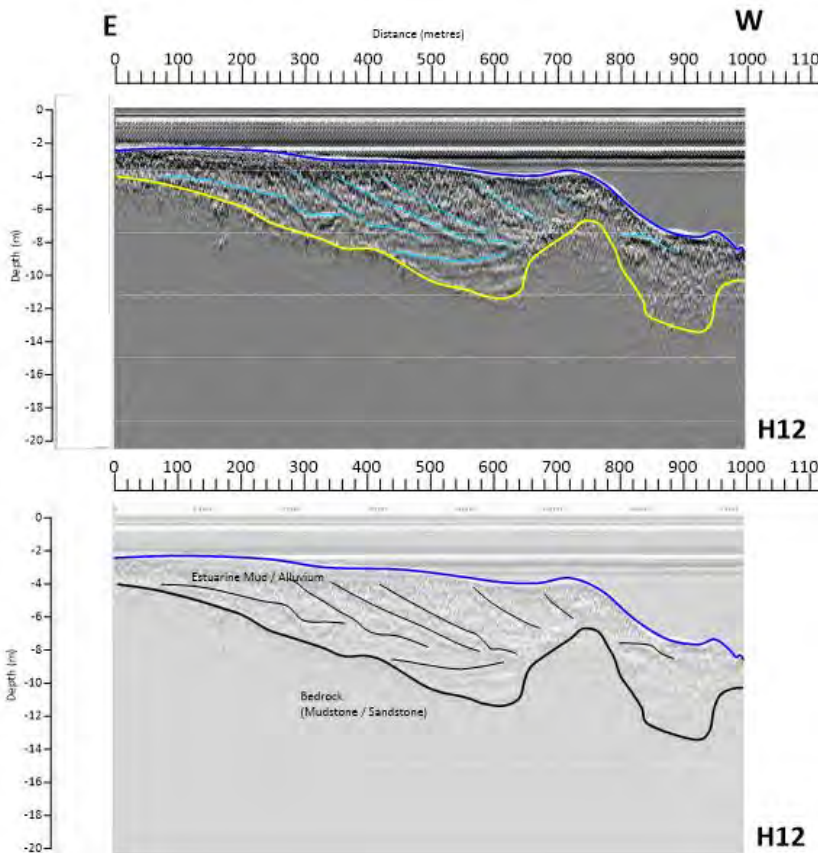
Examples of the SBP lines are indicated as Figure 9,10,11,12. Note that these are vertically exaggerated. The locations of these SBP lines are shown on Figure 5 as the red lines.

Paleochannels are observed which indicate the former positions of stream channels within this part of the Hokianga Harbour. Sedimentary structure (horizontal bedding) is visible within these channels. (see below).



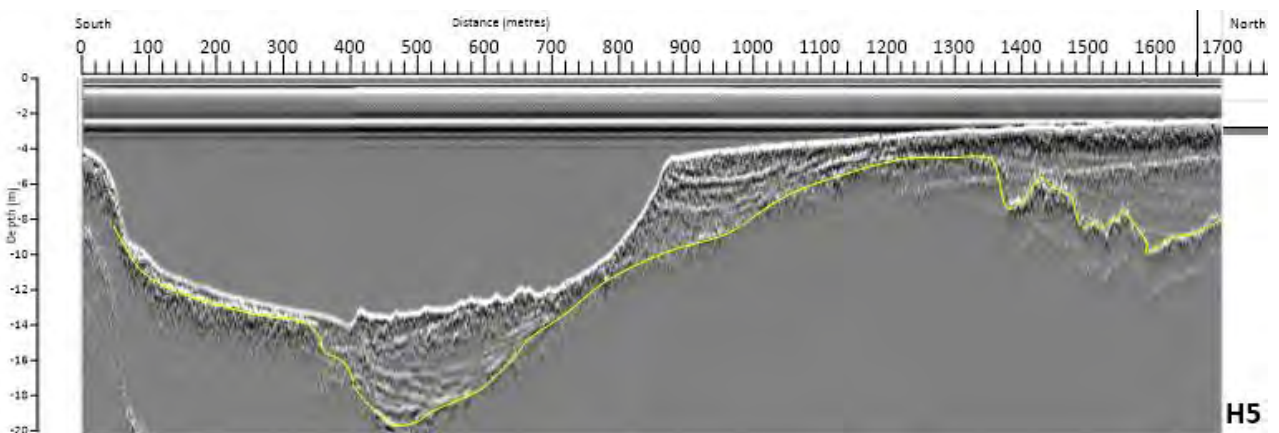
(above) section of SBP Line H10

Sedimentary structure is visible on the edges harbour showing the depositional sequences of alluvial sediment.



(above) SBP Line H12 showing depositional sedimentary structure at edge of harbour.

The degree of erosion of the bedrock varies considerably across this site. For example, profile H5 (below) shows that top of the bedrock as a smooth, highly eroded surface (south side of H5 profile) to very rough, undulating surface (north side of profile)



(above) SBP Line H5 showing variation in bedrock topography.

It is recommended that all SBP data interpretation is validated using boreholes.
Please contact the author directly if you have any questions relating to this survey data.

Matt Watson
Geophysicist
ScanTec Ltd
matt@scantec.co.nz
ph 021-376-644

APPENDIX



Figure 1 - Hokianga Harbour SBP (Sub-bottom Profile) Survey Area

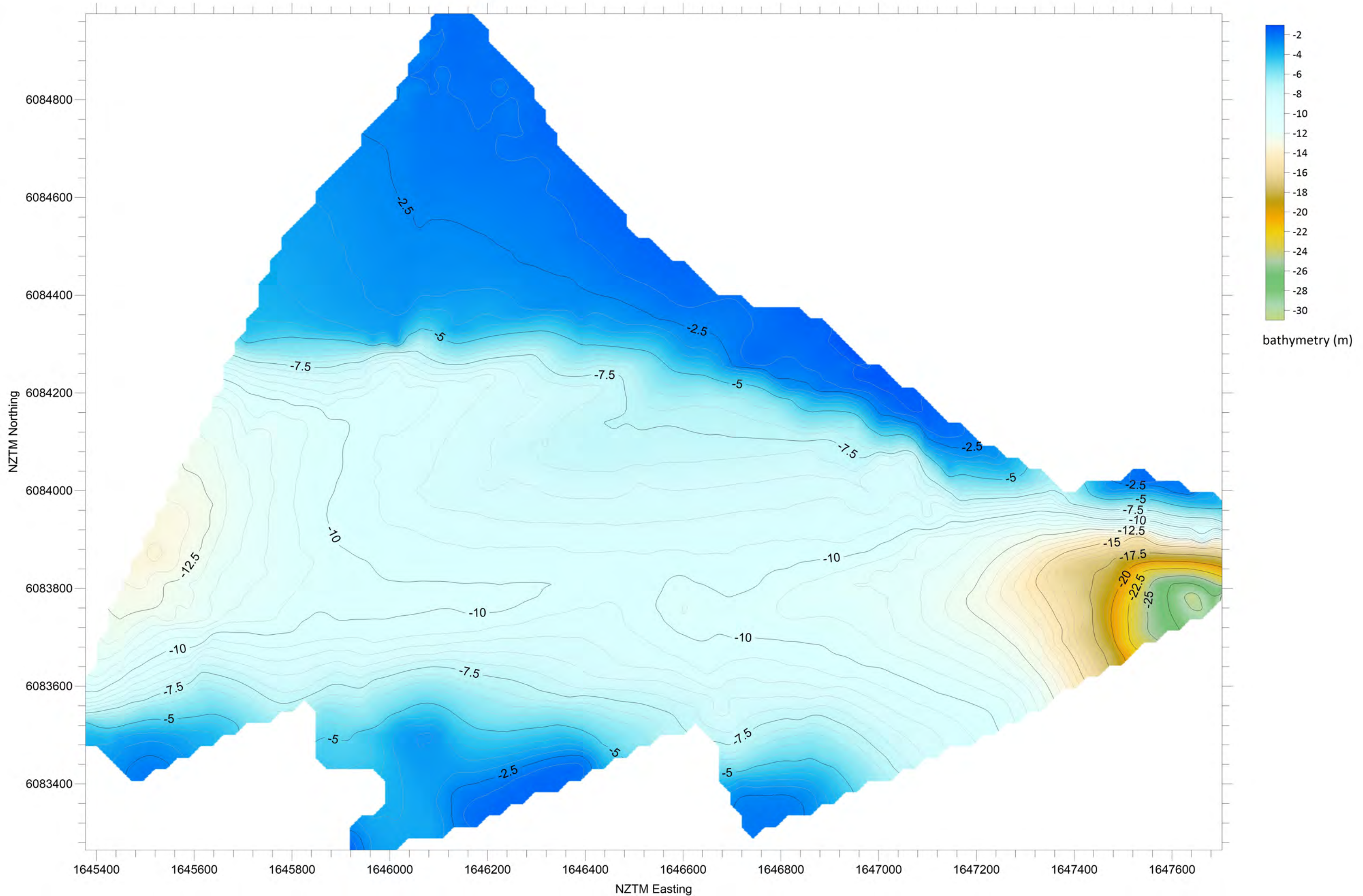
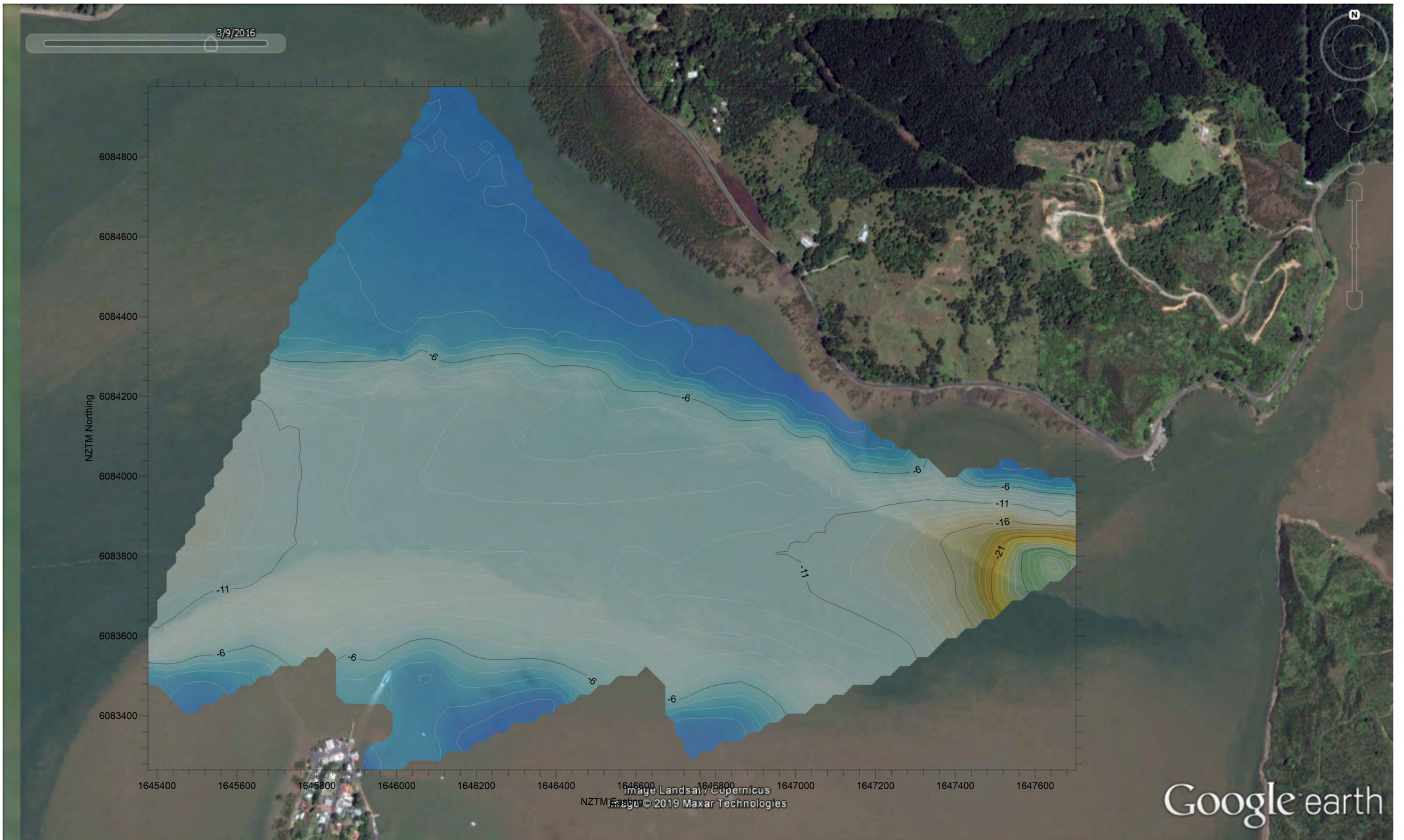


Figure 2 - Bathymetry 200kHz



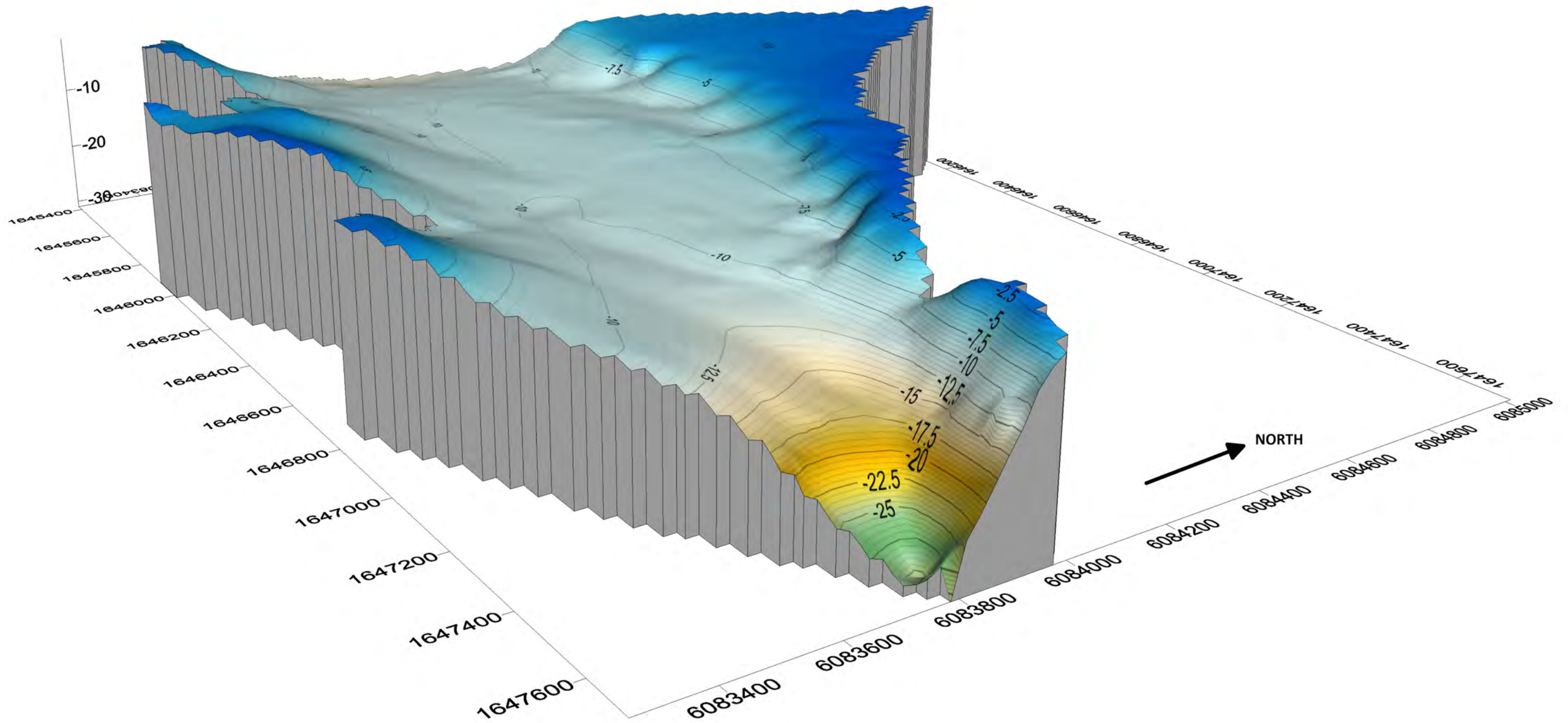


Figure 4 - Bathymetry - 3D projection

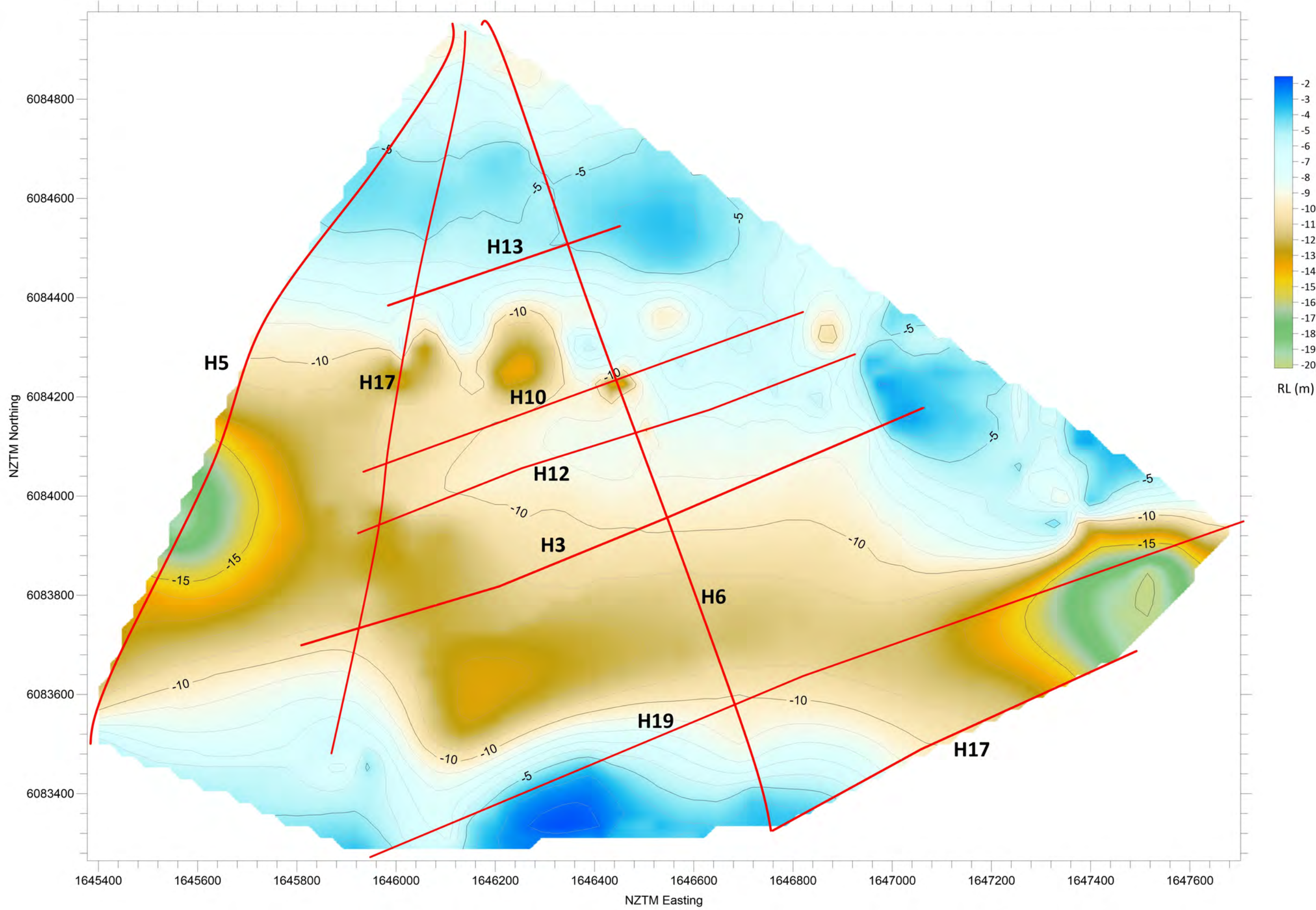
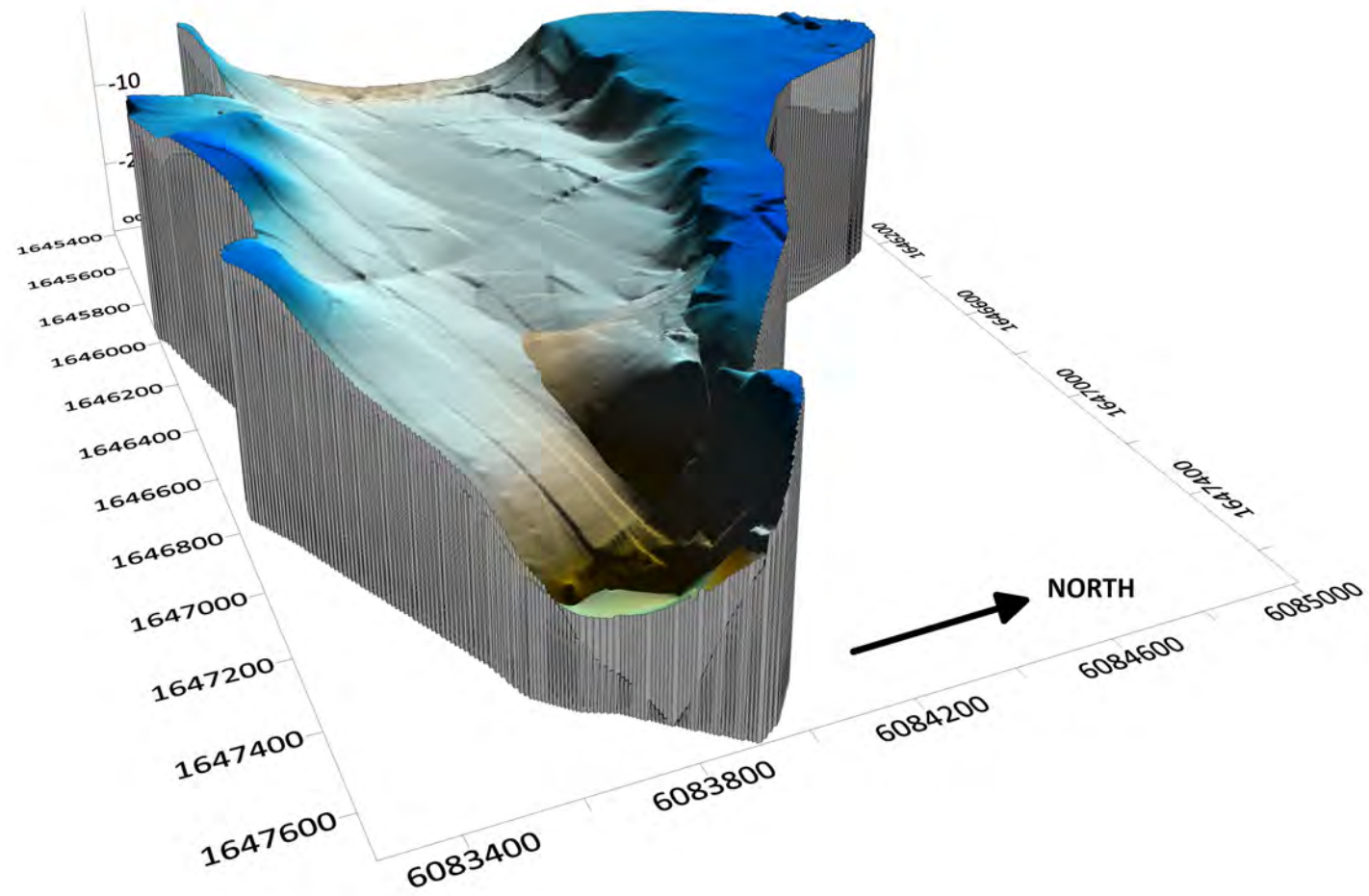
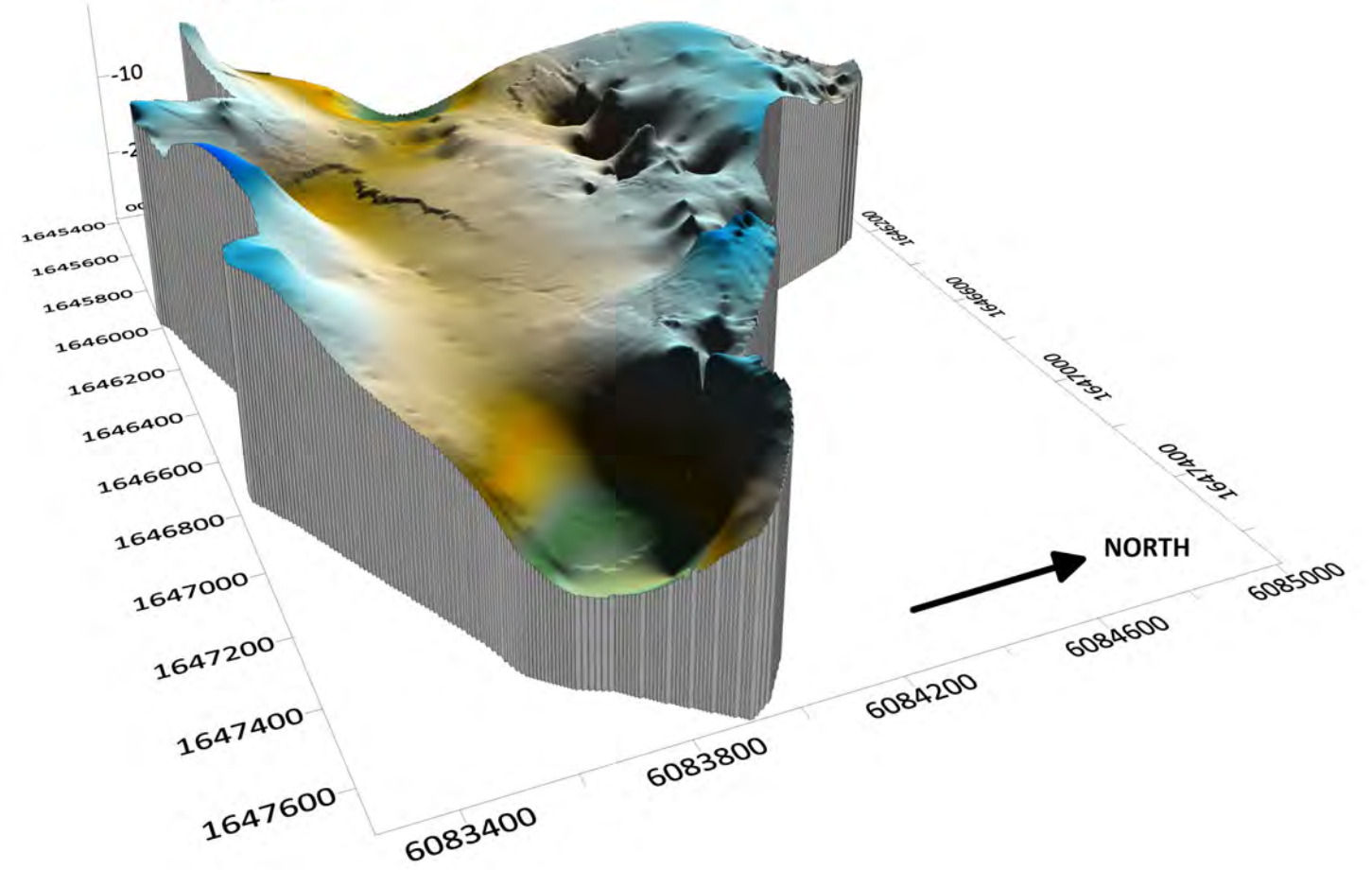


Figure 5 - Interpretation of depth to bedrock (SBP)

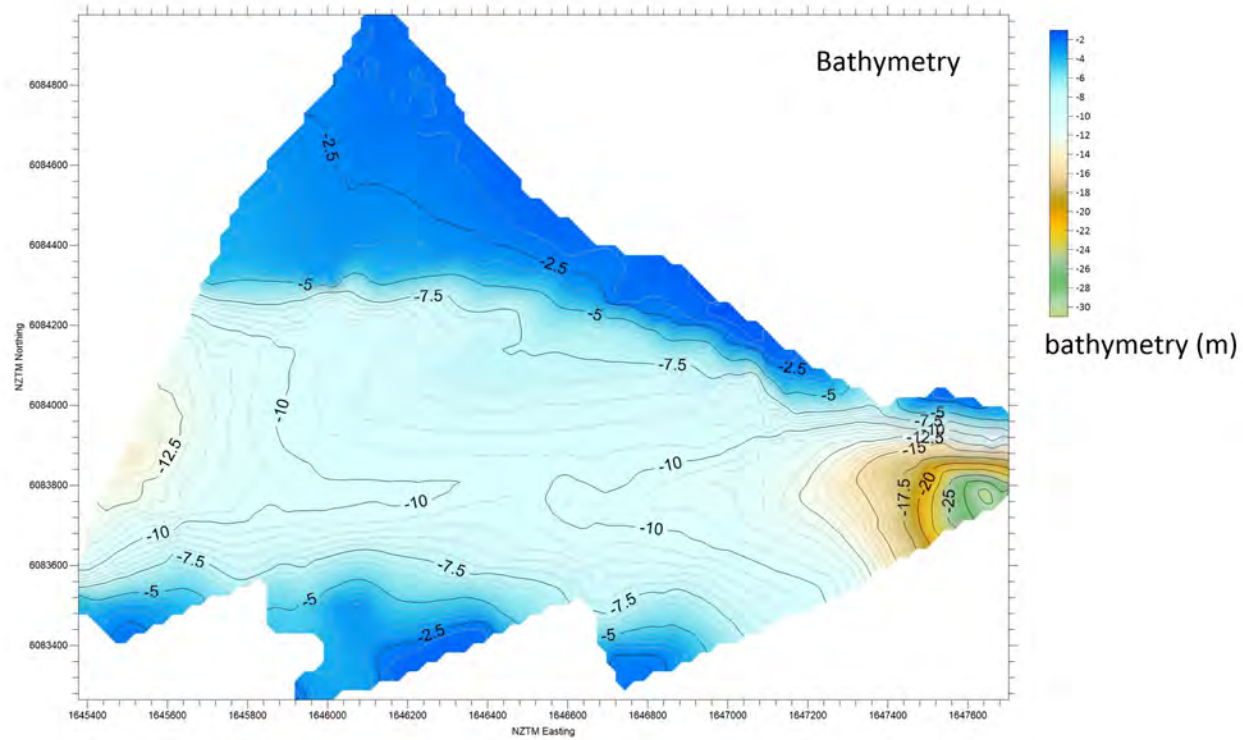
Bathymetry



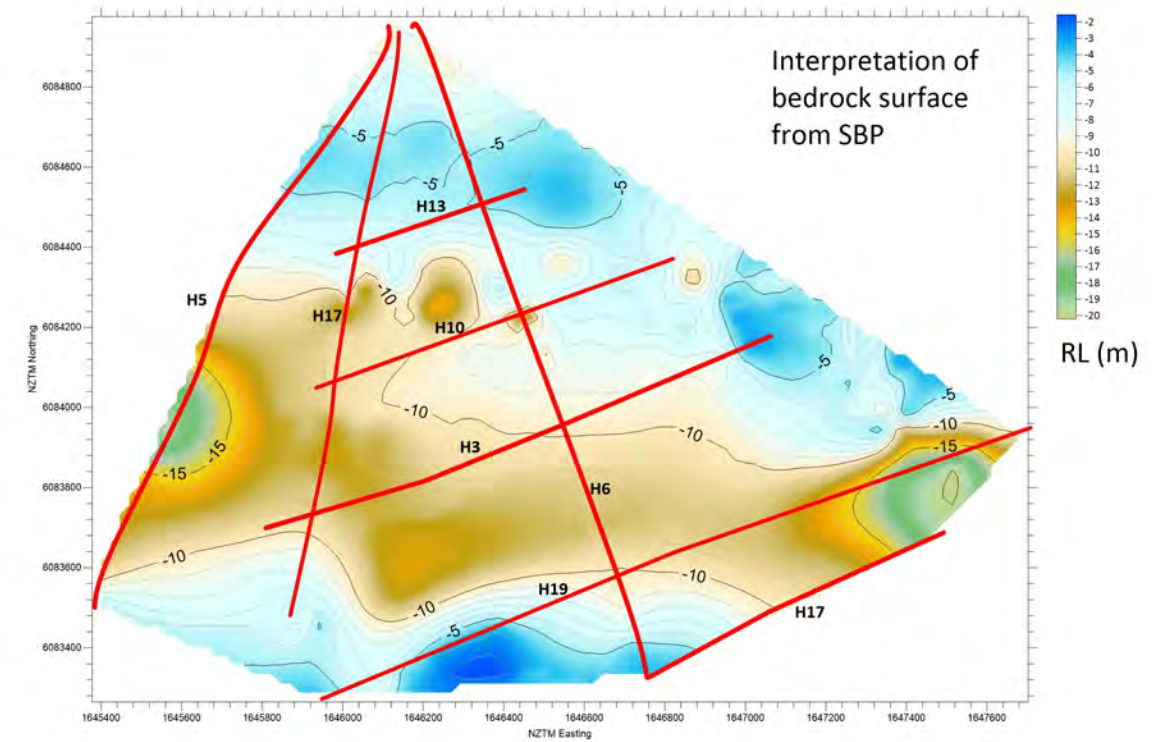
Interpretation of bedrock surface from SBP



Bathymetry



Interpretation of bedrock surface from SBP



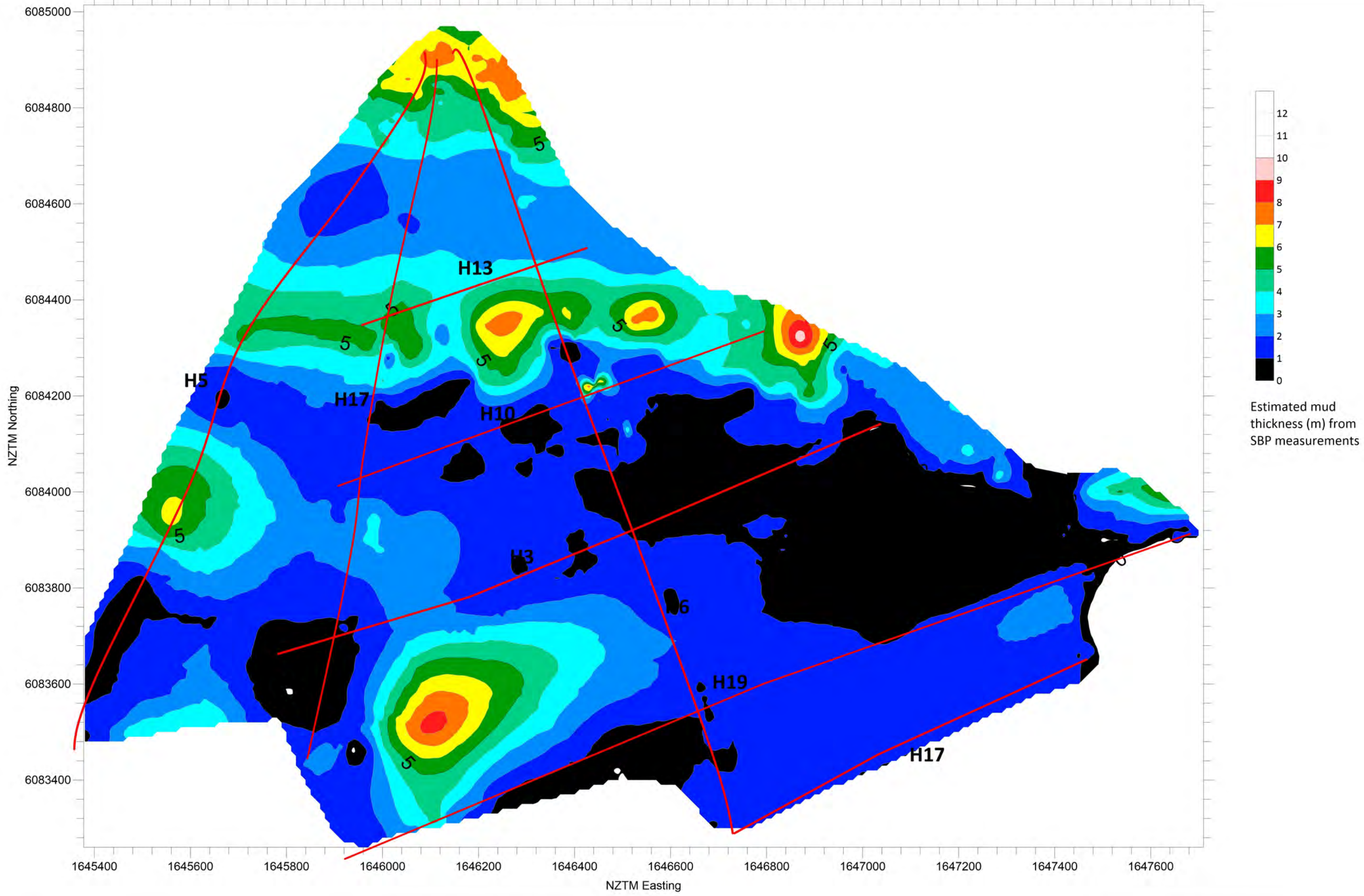


Figure 7 - Estimate of estuarine mud thickness (SBP)



